Technische Universität München

Wissenschaftszentrum Weihenstephan für Ernährung, Landnutzung und Umwelt

Professur Biotechnologie gartenbaulicher Kulturen

Plant acyltransferases involved in brassinosteroid and scopolin modification

Gan Sufu

Vollständiger Abdruck der von der Fakultät Wissenschaftszentrum Weihenstephan für Ernährung, Landnutzung und Umwelt der Technischen Universität München zur Erlangung des akademischen Grades eines

Doktors der Naturwissenschaften

genehmigten Dissertation.

Vorsitzender: Prof. Dr. Wolfgang Liebl

Prüfer der Dissertation:

1. Prof. Dr. Brigitte Poppenberger-Sieberer

2. Prof. Dr. Wilfried Schwab

Die Dissertation wurde am 06.05.2020 bei der Technischen Universität München eingereicht und durch die Fakultät Wissenschaftszentrum Weihenstephan für Ernährung, Landnutzung und Umwelt am 31.07.2020 angenommen.

Contents

Abstract

Plant acyltransferases catalyze conjugation of many plant secondary metabolites with organic acid residues to alter their function and thereby impact chemotypic and phenotypic outcomes. Studies with *Arabidopsis thaliana* allowed the identification and functional characterization of some of them. However, the majority of the acyltransferases remains poorly studied and improving this will enhance our understanding of plant metabolic systems.

In the first part of this thesis, the BAHD acyltransferase PMAT1 was identified as being able to malonylate a glucosylated version of the brassinosteroid (BR) brassinolide (BL). BRs are steroid hormones that are essential for growth control and stress responses in plants. *PMAT1* knock out mutants exposed to BL were unable to form BL-23-*O*-malonylglucoside (BL-23MalGlc). Overexpression of *PMAT1* in a background in which the UDP-glucosyltransferase *UGT73C6* is overexpressed, and thus BR-glucoside formation is increased, enhanced the BR-deficient phenotypes of *UGT73C6oe* plants. In line, BR signaling capacities were decreased by *PMAT1* overexpression in an *UGT73C6oe* background, as evidenced by increased expression of BR biosynthesis genes, which are feedback repressed by BR.

In the second part of this thesis, evidence is provided that in addition to BR-glucosides PMAT1 and its closest homologue PMAT2 can also catalyze the malonylation of scopolin, a hydroxy-coumarin that is important for plant defenses. A *PMAT1* knock out mutant failed to produce malonylscopolin. Overexpression of *PMAT1* and *PMAT2* caused hyper-accumulation of malonylscopolin and increased resistance against externally applied scopoletin, the scopolin aglycone.

In the third part of this thesis, the acyltransferase BIA1 was characterized, which had previously been implicated in BR homeostasis, since *BIA1* overexpression gave strong BR-deficient phenotypes. However, the substrates of BIA1 had remained unknown. It is shown that BIA1 acetylates CS (castasterone) and CS variants using acetyl-CoA as a donor substrate *in vitro*. Feeding experiment with *BIA1* overexpression lines revealed that monoacetylated and diacylated versions of CS were formed in increased amounts in the overexpression lines as compared to wild type. These products were absent in a *bia1* knock out mutant confirming that BIA1 is required for CS-acetylation.

In summary, this work characterizes the activity of several acyltransferases involved in the catabolism of BRs and shows that additional substrates including scopolin are acceptors. How these multiple enzymatic activities may be coordinated is discussed.

Zusammenfassung

Pflanzliche Acyltransferasen katalysieren die Modifikation Von Sekundär metaboliten mit Resten organischer Säuren, um so ihre Funktion zu verändern, mit daraus resultierenden chemotypischen und phänotypischen Auswirkungen. Studien mit *Arabidopsis thaliana* ermöglichten die Identifizierung und funktionale Charakterisierung einiger dieser Enzyme. Jedoch ist die Mehrzahl an der Acyltransferasen noch immer nicht gut erforscht, weshalb Fortschritte auf diesem Gebiet unser Verständnis des pflanzlichen Sekundärmetabolismus erweitern werden.

Im ersten Teil dieser Dissertation wird gezeigt, dass die BAHD Acyltransferase PMAT1 die Fähigkeit besitzt, eine glukosilierte Version des Brassinosteroids (BR) Brassinolid (BL) zu malonylieren. BRs sind Steroidhormone, welche essentiell für die Wachstumskontrolle und Stressantwort von Pflanzen sind. *PMAT1* knock-out Mutanten, die mit BL behandelt wurden, konnten kein BL-23-*O*-Malonylglukosid (BL-23MalGlc) mehr bilden. Eine Überexpression von *PMAT1* in einer Linie, in der die UDP-Glukosyltransferase *UGT73C6* überexprimiert und somit die Bildung von BR-Glukosid erhöht ist, verstärkte den BR-Mangel-Phänotyp von *UGT73C6oe* Pflanzen. In Übereinstimmung damit war die Kapazität an BR Signalübertragung durch die *PMAT1* Überexpression in *UGT73C6oe* Linien verringert, was sich dadurch äußerte, dass BR Biosynthese-Gene induziert waren, welche durch BR Feedbackregulation unterdrückt werden.

Im zweiten Teil der Dissertation werden Ergebnisse vorgestellt welche nahelegen dass PMAT1 und sein nächster Verwandter PMAT2 zusätzlich zu BR-Glukosiden auch Scopolin, ein Hydroxycumarin, welches für Abwehr-Reaktionen von Pflanzen wichtig ist, malonylieren können. Eine *PMAT1* knock-out Mutante konnte kein Malonylscopolin mehr produzieren. Überexpression von *PMAT1* und *PMAT2* verursachte dagegen eine Überakkumulation von Malonylscopolin und erhöhte Resistenz gegenüber extern appliziertem Scopoletin, das Aglykon von Scopolin.

Im dritten Teil der Dissertation wurde die Acyltransferase BIA1 charakterisiert, von welcher vermutet wurde, an der BR Homöostase beteiligt zu sein, da *BIA1* Überexpression zu starken BR-Mangel Phänotypen führte. Jedoch waren die Substrate von BIA1 bis zur Beginn der Arbeit unbekannt geblieben. Es wird gezeigt, dass BIA1 castasterone (CS) und CS Varianten unter Verwendung von Acetyl-CoA als Donor-Substrat acetyliert. Fütterungsversuche mit BIA1 Überexpressionslinien offenbaren, dass mono- und di-acetylierte Formen von CS in den Überexpressionslinien in

verstärktem Maße gebildet wurden. Diese Produkte waren in einer *bia1* Knock-out Mutante nicht vorhanden, was bestätigt, dass BIA1 für die CS-Acetylierung benötigt wird.

Zusammenfassend charakterisiert diese Arbeit die Aktivität von mehreren Acyltransferasen, welche am Katabolismus von BRs beteiligt sind und zeigt, dass zusätzliche Substrate wie Scopolin Akzeptoren sind. Es wird diskutiert auf welche Weise diese zahlreichen enzymatischen Aktivitäten koordiniert sein könnten.

Abbreviations

ACN	Acetonitrile
BAHD	BEAT, AHCT, HCBT, and DAT
BL	Brassinolide
BR	Brassinosteroid
CBB	Coomassie Brilliant Blue
CR	Campesterol
CS	Castasterone
CTAB	Cetyl trimethylammonium bromide
DTT	Dithiothreitol
EtAc	Ethyl acetate
HPLC-QTOF	High performance liquid chromatography-quadrupole time-of-flight mass spectrometry
qPCR	Quantitative polymerase chain reaction
MS	Murashige and Skoog
NASC	Nottingham Arabidopsis Stock Center
SAAT	Strawberry alcohol acyltransferase
SD	Standard deviation
SDS	Sodium dodecyl sulfate
SE	Standard error
TLC	Thin layer chromatography
wt	Wild type
YFP	Yellow fluorescent protein

1 Introduction

1.1 Plant acyltransferase

Plants produce a large variety of secondary metabolites with a wide range of functions. At present, an estimated 200,000 distinct plant secondary metabolites have been isolated and identified (Wurtzel and Kutchan, 2016; Kessler and Kalske, 2018; Pyne et al., 2019). Although many plant natural products are present at very low levels, these chemical compounds not only play vital roles in growth and development but are also necessary for a plant's ability to interact with its' environment and thereby survive. In addition, humans benefit from plant secondary metabolites when present in food and utilize them for non-food purposes including medical and industrial applications.

Plant secondary metabolites exhibit great chemical diversity (Bourgaud et al., 2001). The structural and stereochemical diversity of these compounds is largely achieved by decoration of the basic skeletons or side chains with moieties such as sugars, organic acids, methyl, hydroxyl and prenyl residues by modifying enzymes (Negre et al., 2003; Dudareva et al., 2004; Tholl et al., 2005; Wang et al., 2019). From the genomic annotation of the first sequenced flowering plant *Arabidopsis. thaliana* (*A. thaliana*), it had been estimated that approximately 4,000 enzymes may participate in metabolism (Initiative, 2000; Mueller et al., 2003). Among them, two classes of enzymes can catalyze acylation of small molecules in plants: BAHD (**B**EAT, **A**HCT, **H**CBT, and **D**AT) acyltransferases and serine carboxypeptidase-like acyltransferases (Milkowski and Strack, 2004; D'Auria, 2006). Serine carboxypeptidase-like acyltransferases use 1-*O*-β-glucose esters as acyl donors, while BAHD acyltransferases utilize CoA thioesters and contribute to the formation of diverse groups of plant metabolites including small volatile esters, modified anthocyanins, as well as constitutive defense compounds and phytoalexins (D'Auria, 2006; Bontpart et al., 2015).

The BAHD acyltransferase superfamily was named after the first four biochemically characterized enzymes: **B**EAT, **A**HCT, **H**CBT, and **D**AT (St-Pierre and De Luca, 2000). **B**EAT, benzylalcohol *O*-acetyltransferase, catalyzes the formation of the floral scent volatile ester benzylacetate from the California wildflower *Clarkia breweri* (Dudareva et al., 1998). **A**HCT, anthocyanin *O*-hydroxycinnamoyltransferase, are related enzymes from *Gentiana triflora* or *Perilla frutescens* that

catalyze acylation of anthocyanin with residues of aromatic acids (Fujiwara et al., 1997; Fujiwara et al., 1998a; Fujiwara et al., 1998b). **H**CBT, anthranilate hydroxycinnamoyl/benzoyl-transferase, catalyzes the first committed reaction of phytoalexin biosynthesis in carnation (*Dianthus caryophyllus* L.) (Yang et al., 1997). **D**AT, deacetylvindoline 4-*O*-acetyltransferase, is involved in the biosynthesis of the alkaloid vindoline from *Catharanthus roseus* (St-Pierre et al., 1998).

1.1.1 Specifications of BAHD acyltransferase superfamily

Sequencing of the *A. thaliana* genome revealed that plant BAHD acyltransferases constitute a large gene family with approximately 50-60 members (D'Auria, 2006; Yu et al., 2009). The average length of a BAHD protein is approximately 445 amino acids with a molecular mass ranging from 48 to 55 kDa. BAHD acyltransferases display an overall low sequence identity and typically function as monomers (Ma et al., 2005). Sequence alignment of BAHD family members allow for the identification of two conserved motifs: a HxxxD motif and the less conserved DFGWG motif (St-Pierre and De Luca, 2000; D'Auria, 2006). An additional conserved YFGNC motif serves as a signature sequence for the members responsible for acylating anthocyanins/flavonoids (Nakayama et al., 2003b). Structural and mutational studies of anthocyanin malonyltransferases indicated that the HxxxD motif is involved in substrate binding while the DFGWG motif probably plays a structural role (Unno et al., 2007).

1.1.2 Catalytic mechanism of BAHD family members

Crystal structural studies on vinorine synthase, the first representative of the BAHD superfamily to be characterized, provide insight into the catalytic mechanism and the importance of the motifs (Ma et al., 2005). Vinorine synthase contains 14 β-strands and 13 α-helices and consists of two domains with nearly equal size connected with a large crossover loop. A solvent channel is formed at the interface between the two domains. The HxxxD sequence motif is located at the interface between the two domains, and the catalytic histidine residue is accessible from both sides of the channel. The histidine residue in the HxxxD motif plays a key role in the proposed catalytic mechanism. This basic residue deprotonates the oxygen or nitrogen atom on the acceptor substrate, which initiates

nucleophilic attack of the carbonyl carbon of the CoA thioester. This results in formation of a tetrahedral intermediate between the CoA thioester and the acceptor substrate. Finally, the acetylated substrate and free CoASH are formed. The DFGWG motif is located away from the active site of the enzyme and this conserved sequence seems to have a structural role by maintaining the conformational integrity of the enzyme structure (Ma et al., 2005; Unno et al., 2007).

1.1.3 Catalytic versatility of BAHD enzymes

Enzyme activities can be associated with amino acid sequences. However, predication of enzymatic functions based on sequence similarity alone has regularly proven to be problematic and this is also the case for the BAHD acyltransferases. For example, a sequence comparison of SAAT (strawberry alcohol acyltransferase) from the cultivated strawberry (*Fragaria* x *ananassa*) and VAAT (wild strawberry alcohol acyltransferase) from wild strawberry (*Fragaria vesca* L.) showed 86% sequence identity between the two enzymes. Nevertheless, they utilized different types of aliphatic alcohols as acceptors (Aharoni et al., 2000; Beekwilder et al., 2004). Another example is the two malonyl-CoA anthocyanin transferases from *Salvia splendens* which, although they did not share high overall sequence homology, exhibited similar substrate specificities, with one transferring a malonyl group to the 6' position of cyanidin 5-*O*-glucoside, and the other transferring a malonyl group to the 4' position of the same acceptor (Suzuki et al., 2001; Suzuki et al., 2004b).

In some cases, phylogenetically related BAHD acyltransferases did display substrate similarities. For instance, the three malonyltransferases (At1g03940, At1g03495 and At3g29590) that use anthocyanins as acceptors are members of one subgroup (Luo et al., 2007; Yu et al., 2009). Moreover, the hydroxycinnamoyl transferase At2g19070 belongs to a subclade including two other enzymes, At5g48930 and At5g57840, that have been shown to transfer aromatic acyl groups to various acceptors (D'Auria et al., 2007a; Grienenberger et al., 2009). Until now, over 13 different BAHD acyltransferases from *A. thaliana* have been characterized by genetic and/ or biochemical studies, and donors and/ or acceptors are known; the results of which are briefly summarized in **Table 1**.

Table 1: Characterized BAHD acyltransferases of *A. thaliana*.

Name	TAIR ID	Known donor	Known acceptor	Reference(s)
At3AT1	At1g03940	Caffeoyl-CoA	Anthocyanins	(Luo et al., 2007)
At3AT2	At1g03495	Caffeoyl-CoA	Anthocyanins	(Luo et al., 2007)
At5MAT	At3g29590	Malonyl-CoA	Anthocyanins	(D'Auria et al., 2007b)
AtHCT	At5g48930	Coumaroyl-CoA	Shikimate and quinate	(Hoffmann et al., 2005)
AtHHT	At5g41040	Feruloyl-CoA	Suberin aromatics	(Gou et al., 2009)
CHAT	At3g03480	Acetyl-CoA	(*Z*)-3-hexen-1-ol	(D'Auria et al., 2007a)
COSY	At1g28680	Hydroxycinnamoyl-CoA	Coumarins	(Vanholme et al., 2019)
DCR	At5g23940	Unknown	Cutin	(Panikashvili et al., 2009)
FACT	At5g63560	Caffeoyl-CoA	Fatty alcohol	(Kosma et al., 2012)
PMAT1	At5g39050	Malonyl-CoA	Naphthol malonylglucoside	(Taguchi et al., 2010)
PMAT2	At3g29670	Malonyl-CoA	Phenol malonylglucoside	(Taguchi et al., 2010)
PIZ	At4g31910	Lauroyl-CoA	BRs	(Schneider et al., 2012)
SHT	At2g19070	Feruloyl-CoA	Spermidine	(Grienenberger et al., 2009)

1.1.4 Classification of BAHD enzymes

In *A. thaliana*, four clades of BAHD acyltransferases have been defined based on phylogenetic analysis (Yu et al., 2009). Clade I BAHD acyltransferases comprise the alcoholic acyltransferases and polyamine hydroxycinnamoyl transferases. Clade II contains members characterized as anthocyanin/flavonoid malonyltransferases and hydroxycinnamoyl transferases. Clade III genes encode four protein sequences with unknown functions and a petunia coniferyl alcohol acetyltransferase (PhCFAT). Lastly, Clade IV encompasses several sequences encoding alcohol- and alkaloid-acetyltransferases.

1.1.5 Acylation and malonylation catalyzed by BAHD enzymes

Acylation is the process of transferring an acyl group via an activated donor to an acceptor molecule. BAHD acyltransferase use acyl-CoA thioesters as donors. The acceptors range from low molecular weight chemicals such as choline and L-malate to large compounds such as anthocyanins and

triterpenoid glycosides (Lehfeldt et al., 2000; Shirley et al., 2001; Fraser et al., 2007; Mugford et al., 2013). Acylation has a wide range of functions in plants. Acylation of anthocyanins affects the solubility, stability, transportation, vacuolar uptake, storage and color properties of the compounds (Nakayama et al., 2003a; Gomez et al., 2009; Zhao and Dixon, 2010). In oat, acylation of avenacins contributes to plant disease resistance (Mugford et al., 2009).

Malonylation is a common modification of secondary metabolites. In their conversion, the malonyl group is mainly transferred from malonyl-CoA to the glycosyl moiety of glucoconjugates (Taguchi et al., 2005; Khan et al., 2016). Malonylation is thought to increase structural diversity, change stability and solubility of metabolites and provide a means of detoxification. For example, xenobiotic phenolic glucosides are also often modified by malonylation and stored as malonylated glucosides in the cell vacuoles (Schmitt and Sandermann, 1982; Sandermann et al., 1991; Taguchi et al., 2010). Malonylation of anthocyanins increases pigment stability at the pH of the intracellular milieus and enhances resistance to β-glucosidase degradation (Suzuki et al., 2002). In addition, malonylation increases both the affinity and transport efficiency of flavonoid glucosides (Zhao et al., 2011). Malonylation of diterpene glycosides may play a critical role in defense against herbivores and influence stylar development of *Nicotiana attenuate* (Heiling et al., 2010; Li et al., 2018).

1.2 Acylated and malonylated plant metabolites

Acylated and malonylated compounds are conjugates of plant metabolites, which can be roughly classified into three large families: phenolics, terpenes and steroids, and alkaloids (Bourgaud et al., 2001). Phenolic compounds in plants are synthesized from shikimate and pentose phosphate via the phenylpropanoid pathway and are often modified by conjugation with small molecules. For example, flavonoids are one of the most important phenolic compounds, with substitutions including glycosyl, acyl or malonyl groups (Harborne and Williams, 2000). Scopolin, the predominant coumarin glucoside occurring in *A. thaliana*, is also malonylated to some extent (Matsuda et al., 2010).

1.2.1 Phenolic compounds

Phenolic compounds comprise an aromatic ring bearing one or more hydroxyl groups and range from simple phenolic molecules to complex high-molecular weight polymers (Bravo, 1998; Balasundram et al., 2006). These molecules are involved in structural support (lignin), antioxidants (flavonoids and carotenoids), biotic stress signaling (salicylic acid and flavonoids) and defense responses (tannins and phytoalexins) (Lin et al., 2016).

1.2.1.1 Scopoletin and scopolin biosynthesis

Scopoletin and scopolin, which are major coumarin compounds, occur in many plants (Bertolucci et al., 2013). Their biosynthesis was shown to depend on CYP98A3 (Kai et al., 2006), a cytochrome P450 that catalyzes 3′-hydroxylation of p-coumarate to produce caffeoyl-CoA (Schoch et al., 2001). Caffeoyl-CoA is then converted to feruloyl-CoA by a caffeoyl CoA 3'-O-methyltransferase encoded by gene the *CCoAOMT1* (Kai et al., 2008). The first committed step in scopoletin biosynthesis is, hydroxylation of feruloyl-CoA to 6-hydroxyferuloyl-CoA by F6′H1, an iron (Fe) II and 2-oxoglutarate-dependent dioxygenase (2OGD) (Kai et al., 2008). Hydroxyferuloyl-CoA is further subjected to trans/cis isomerization of the side chain and lactonization by COSY to form scopoletin (Kai et al., 2008; Vanholme et al., 2019). Sugar moieties are transferred to scopoletin by one or several UDP-glucosyltransferases to produce glucosylated scopoletin, which is called scopolin that is formed in the cytoplasm and then transferred into the vacuole (Taguchi et al., 2000; Chong et al., 2002; Lim et al., 2003; Gachon et al., 2004). This reaction appears to be reversible since as at least three β-glucosidases (BGLU21, BGLU22 and BGLU23) are able to hydrolyze scopolin and can thereby free the aglycon scopoletin (Ahn et al., 2010).

1.2.1.2 Scopoletin and scopolin modification

Natural variation of scopoletin and scopolin accumulation between various *Arabidopsis* accessions were revealed and new loci for their biosynthesis in *Arabidopsis* were identified (Siwinska et al., 2014). Interestingly, among candidates possibly involved in scopoletin and scopolin accumulation, multiple loci encoding putative enzymes were detected, indicating that further modifications might

be involved in scopoletin and scopolin accumulation. Recently, scopoletin 8-hydroxylase (S8H) was reported to convert scopoletin into fraxetin, via hydroxylation at the C-8 position. Fraxetin is glucosylated by unknown enzymes to generate fraxin (Siwinska et al., 2018; Tsai et al., 2018). A CYP P450 enzyme (CYP82C4) further oxidizes fraxetin to produce sideretin, which can be glucosylated by unknown enzymes to generate sideretin glucoside (Rajniak et al., 2018). These phenolics have been widely recognized as critical components in iron acquisition of plants (Schmidt, 2019). Multiple scopoletin-derived compounds including various combinations of scopoletin and sideretin conjugated with moieties such as pentose, hexose, acetylhexose, sulfate and malonate were identified, evidence for a high diversity of compounds in this class of coumarins (Vanholme et al., 2019).

1.2.2 Brassinosteroids

Brassinosteroids (BRs) are steroid hormones of plants that can be modified by acylation (Tong, 2013; Hillier and Lathe, 2019). Known acyl substituents include lauric and myristic acid moieties (Asakawa et al., 1996; Schneider et al., 2012). Malonic acid moiety attached to BL and CS glucosides were also identified (Husar et al., 2011).

BRs are phytohormones that are essential for multiple physiological and cellular processes, including cell elongation and division, photomorphogenesis, generative and reproductive development, and stress responses (Sasse, 2003; Clouse, 2011b; Lozano-Elena and Cano-Delgado, 2019; Nolan et al., 2019). Brassinolide (BL) is the biologically most active BR in many plant species. It was first isolated from organic extracts of *Brassica napus* pollen using its' growth-promoting effects as a readout and was named "brassin" (Mitchell et al., 1970). The chemical structure of brassin was elucidated by extracting 4 mg of pure substance from 227 kg of bee-collected *B. napus* pollen and structure elucidation using single crystal X-ray analysis (Grove et al., 1979; Steffens, 1991). The compound was found to be a steroidal lactone and renamed brassinolide [2α, 3α, 22α, 23α-tetrahydroxy-24α-methyl-β-homo-7-oxa-5α-cholestan-6-one]. Soon thereafter chemical syntheses of 24-epiBL, a biologically active analogue of BL, was achieved, and promoted BR research (Thompson et al., 1979).

Today more than 60 BRs and several derivates are known. They are widely distributed in the plant kingdom and endogenous BRs levels vary between plant tissue types (Fujioka, 1999; Bajguz, 2011). According to the structure-activity relationship from natural BRs and numerous synthetic analogues, cis-vicinal hydroxyls at C-2 and C-3 in ring A, a lactone function at C-6/C-7, cis geometry for hydroxyls at C-22 and C-23 and a methyl substitution at C-24 are regarded as indispensable requirements for BRs to elicit activity (Mandava, 1988).

1.2.2.1 Brassinosteroid biosynthesis

Feeding cell suspension cultures of *Catharanthus roseus* with deuterated and tritiated BR intermediates and screening for sterol biosynthetic mutants have advanced our understanding of the BR biosynthesis pathway and enabled the identification of key enzymes such as DWARF1 (DWF1), CYP90A1/CPD, DDWF1, DWF4 (DWARF4), CYP90C1/ROT3, BR6OX1 and BR6OX2 (Fujioka and Yokota, 2003; Bishop, 2007; Clouse, 2011b; Zhao and Li, 2012; Rozhon et al., 2019).

Campesterol (CR) is the main precursor of BRs biosynthesis. It is modified by hydroxylation, epimerization and oxidation reactions to form the final products, castasterone (CS) and BL. DWF1 catalyzes the conversion of 24-methylenecholesterol to CR in *Arabidopsis* (Choe et al., 1999). CPD catalyzes C-3 oxidation of the early BR intermediates (*22S*)-22-hydroxyCR and (*22R*,*23R*)-22,23-dihydroxyCR, as well as of 6-deoxocathasterone (6-deoxoCT) and 6-deoxoteasterone (6-deoxoTE) (Ohnishi et al., 2012). DDWF1, a cytochrome P450 hydroxylase from pea, catalyzes the conversion from typhasterol (TY) and 6-deoxoTY to castasterone (CS) and 6-deoxoCS, respectively, via C-2 hydroxylation (Kang et al., 2001). While direct biochemical evidence for DWF4 being a C-22 hydroxylase is still lacking, feeding studies demonstrated that 22α-hydroxylated BR intermediates can rescue the *dwf4* phenotype (Choe et al., 1998). For ROT3 and CYP90D1 of *A. thaliana* direct evidence for enzymatic activities exists. Their recombinant proteins proved to catalyze C-23 hydroxylation of various 22-hydroxylated BRs *in vitro*, including the conversion of 6-deoxoCT to 6-deoxoTE and CT to TE (Ohnishi et al., 2006). Consistent with results from biochemical analysis, a double *cyp90c1/cyp90d1* mutant displayed typical BR deficiency phenotypes, which could be rescued exclusively with C-23 hydroxylated BR intermediates. Functional expression of *AtBR6OX1* (CYP85A1) in yeast confirmed that it acts as C-6 oxidase, catalyzing multiple steps in BRs

biosynthesis: 6-deoxoTE to TE, 6-deoxoTY to TY and 6-deoxoCS to CS (Bishop et al., 1999; Shimada et al., 2001). AtBR6OX2 (CYP85A2), like AtBR6OX1, possesses C-6 oxidation activity by mediating a Baeyer-Villiger oxidation step converting CS to BL (Kim et al., 2005). Tomato CYP85A3, which is preferentially expressed in tomato fruits, catalyzes the conversion of 6-deoxoCS into BL via the formation of CS (Nomura et al., 2005).

1.2.2.2 Brassinosteroid signaling

BR signaling is well defined today (Kim and Wang, 2010; Clouse, 2011a). BRs are perceived by a subfamily of membrane-bound receptors, the best studied being BRI1, which was identified in a screen of an EMS-mutagenized population, for *A. thaliana* plants with enhanced resistance against 24-epiBL. This identified the first BR-insensitive mutant allele, *bri1-1* (*brassinosteroid-insensitive 1-1*) (Clouse et al., 1993; Clouse et al., 1996). Positional cloning of *bri1-1* revealed that BRI1 is a leucine-rich repeat receptor-like kinase (Li and Chory, 1997). Direct evidence for BR binding came from binding studies using a biotin-tagged photoaffinity derivative of CS (BPCS), as well as from interaction studies using ^{3}H-labelled BL and recombinant BRI1 fragments. This showed that BRI1 binds BR via the 94 amino acids comprising ID-LRR22 in the extracellular domain (Kinoshita et al., 2005). X-ray diffraction experiments showed that the island domain create a surface pocket for binding of BL and initiating BR signaling (Hothorn et al., 2011; She et al., 2011). Close homologues of BRI1 are BRL1 and BRL3, which are considered to be involved in BR perception in specialized tissues, in particular in the vasculature (Cano-Delgado et al., 2004; Zhou et al., 2004).

Once BR is bound, BRI1 auto-phosphorylates its intracellular kinase domain and thereby autoactivates (Wang et al., 2001; Wang et al., 2005). Activated BRI1 then phosphorylates BKI1 and directs BKI1 release from the membrane, thus facilitating BRI1 association with BAK1 or its homologs BKK1 and SERK1 (Li et al., 2002; Nam and Li, 2002; Karlova et al., 2006; Wang and Chory, 2006; He et al., 2007; Jaillais et al., 2011). BRI1/BAK1 trans-phosphorylation fully activates the kinase activity of BRI1, leading to phosphorylation and release of the membrane-anchored cytoplasmic kinases BSK1 and CDG1 from the receptor complex (Tang et al., 2008; Wang et al., 2008; Kim et al., 2011; Sreeramulu et al., 2013). Subsequently, BSK1 interacts with and activates the phosphatase BSU1, which dephosphorylates and inactivates GLYCOGEN SYNTHASE

KINASE 3 (GSK3)-like kinases, including BIN2 (Mora-Garcia et al., 2004; Yan et al., 2009; Rozhon et al., 2010). Through an independent route, CDG1 phosphorylates BSU1 and enhances BSU1– BIN2 binding, thus enabling BIN2 dephosphorylation and inactivation (Kim et al., 2011). In addition to dephosphorylation, several other mechanisms also regulate BIN2 activity, such as ubiquitination, deacetylation, oxidation and sequestration (Truernit et al., 2012; Anne et al., 2015; Hao et al., 2016; Zhu et al., 2017; Houbaert et al., 2018; Song et al., 2019).

BIN2 and its functional homologues are major repressors of BR responses. They have many targets, including transcription factors that control BR responsive gene expression. Besides bHLH proteins, like the CES/BEE subfamily and certain PIFs such as PIF4 (Poppenberger et al., 2011; Bernardo-Garcia et al., 2014), the small subfamily of BES1/BZR1-type transcription factors are important BIN2 targets. BIN2 phosphorylates specific residues in BZR1 and BES1, which leads to an inhibition of their DNA-binding activity, their retention in the cytoplasm by 14-3-3 proteins, and their degradation (He et al., 2002; Li and Nam, 2002; Wang et al., 2002; Yin et al., 2002; He et al., 2005; Yin et al., 2005; Vert and Chory, 2006; Gampala et al., 2007; Ryu et al., 2007). After BIN2 inactivation, BZR1 and BES1 undergo dephosphorylation by a cytoplasmic protein phosphatase 2A (PP2A) and accumulate in the nucleus (Tang et al., 2011). BES1, BZR1, and the homologs BEH1-BEH4 act redundantly (Wang et al., 2002; Yin et al., 2002; Yin et al., 2005; Chen et al., 2019a; Chen et al., 2019b) to regulate BR-responsive gene expression (Sun et al., 2010; Yu et al., 2011; Oh et al., 2012; Guo et al., 2013).

1.2.2.3 Regulation of brassinosteroid synthesis

To ensure optimal BR signaling outputs, plants utilize precise biosynthetic and metabolic systems to maintain an intracellular homeostasis of bioactive BRs. For example, the transcription of the BR biosynthetic genes, *DWF1*, *DWF4*, *CPD*, *CYP90C1*, *CYP90D1*, and *CYP85A2,* is feedback repressed by BL (Mathur et al., 1998; Bancos et al., 2002; Youn et al., 2018). Active BES1/BZR1 has been shown to bind to the promoters of BR biosynthetic genes including *CPD*, *DWF4*, *ROT3* and *BR6OX* and participate in the feedback repression (He et al., 2005; Youn et al., 2018). Also a number of transcription factors stimulating BR biosynthesis have been identified. TCP1 and CES positively regulate the expression of *DWF4* and *CPD* by directly binding to their promoters,

respectively (Guo et al., 2010; Poppenberger et al., 2011). COG1, PIF4 and PIF5 cooperate to modulate BR biosynthesis by promoting the expression of *DWF4* and *BR6OX2* (Wei et al., 2017). HBI1 positively regulates BR biosynthesis by stimulating the expression of the BR biosynthetic genes *CPD*, *DWF4*, and *BR6OX1* (Bai et al., 2012; Fan et al., 2014).

1.2.2.4 Inactivation of brassinosteroids

Multiple catabolic processes have been reported to inactive bioactive BRs or their biosynthetic precursors in plants and include sulfatation, hydroxylation, glucosylation and acylation.

A sulfotransferase from *Brassica napus* was shown to display activity specifically against the hydroxyl group at position C-22 of BRs. 24-epiBL sulfatation caused a loss of its biological activity in the bean second internode elongation bioassay (Rouleau et al., 1999). A sulfotransferase from *A. thaliana*, encoded by *AtST4a*, sulfated BRs including 24-epiBRs and the naturally occurring (*22R*,*23R*)-28-homoBRs. A second sulfotransferase from *A. thaliana*, encoded by *AtST1*, exhibited a substrate preference for the metabolic precursor 24-epicathasterone and additional catalytic activity for hydroxysteroids and estrogens (Marsolais et al., 2007). However, plants overexpressing sulfotransferases failed to produce BR deficiency phenotypes (Marsolais et al., 2007).

Hydroxylation is catalyzed by the cytochrome P450s BAS1 (*phyB* activation-tagged suppressor1-dominant)/CYP72B1 (Neff et al., 1999). An activation-tagging screen for suppressors of the long hypocotyl phenotype of the *phyB-4* mutant, which is defective in the phytochrome B photoreceptor identified the *bas1-D* mutant. Endogenous levels of BRs were greatly reduced in *bas1-D phyB-4*. Moreover, overexpression of BAS1 in *A. thaliana* and tobacco plants resulted in BR-deficient phenotypes, which correlated with enhanced production of 26-hydroxycastasterone (26-OHCS) and 26-hydroxybrassinolide (26-OHBL) (Neff et al., 1999; Turk et al., 2003). The closest homologue of BAS1, SOB7 may also regulate endogenous BL levels, since in *A. thaliana* binding studies showed that SOB7 bind with BR precursors (Nakamura et al., 2005; Takahashi et al., 2005; Turk et al., 2005; Thornton et al., 2010). However, the *in planta* substrates of SOB7 remain elusive.

Glucosylation is another means of BR inactivation. Two UDP-glycosyltransferases (UGTs) termed UGT73C5 and UGT73C6, were found to be involved in the glucosylation of BRs at the C-23 position

(Poppenberger et al., 2005; Husar et al., 2011). Plants overexpressing *UGT73C5* or *UGT73C6* displayed typical BR deficiency phenotypes, which could be rescued by external application of BR (Poppenberger et al., 2005; Husar et al., 2011). Consistent with the morphological changes indicating BR deficiency, the contents of the BR intermediates, typhasterol, 6-deoxocastasterone, and CS were reduced in *UGT73C5oe* plants. Feeding experiments with BL showed a strong increase in BL-23-*O*-glucoside (BL-23Glc) formation in *UGT73C5oe* plants, whereas knocking-down expression of the gene by RNAi abolished BL-23Glc formation capacities (Poppenberger et al., 2005). When using a LC-HRMS method to analyze BR-glucoside formation in BR-treated *UGT73C5oe* and *UGT73C6oe* lines in a time-course manner, it was found that, while BR-glucoside contents declined over time, amounts of novel BR catabolites increased. Based on their predicted molecular masses, these novel products were considered to be CS-23-*O*-malonylglucoside (CS-23MalGlc) and BL-23-*O*-malonylglucoside (BL-23MalGlc) (Husar et al., 2011). However, the biological significance of the conversion of BR-glucosides to malonylated products and the enzyme(s) catalyzing these reactions have remained elusive.

Another mode of BR catabolism is acylation. The acyltransferase PIZ (also referred to DRL1 and BAT1) modulates endogenous BR levels in *A. thaliana* by converting BL, CS and TY to the corresponding lauroyl esters (Schneider et al., 2012; Choi et al., 2013; Zhu et al., 2013). This conjugation is in agreement with previous reports that BRs can be modified by conjugation with fatty acids including lauric, myristic and palmitic acid (Asakawa et al., 1994; Kolbe et al., 1995; Soeno et al., 2000). A novel BAHD family acyltransferase, BIA1/ABS1, was proposed to inactivate BRs probably by acylation (Roh et al., 2012; Wang et al., 2012), which was supported by several lines of evidence: 1) the dominant *bia1-1D* mutant, which was identified in a screen of an activation tagging *A. thaliana* population, exhibited a dwarf phenotype with dark-green, small and round leaves, that strongly resembles BR-deficient mutants; 2) endogenous levels of 6-deoxoteasterone, 3-dehydro-6-deoxoteasterone, 6-deoxotyphasterol, 6-deoxocastasterone, TE, TY, and CS were reduced in *bia1-1D*; 3) the dwarfism of *bia1-1D* could be rescued with BL application (Roh et al., 2012). However, direct evidences for a role of BIA1 in BR catabolism is still lacking, since its enzymatic activity has not been elucidated yet.

1.3 Objectives

Since previous work in the Poppenberger group had provided evidence that BR-glucoside can be malonylated, the objectives of this thesis were 1) to identify malonyltransferase(s) responsible for BR-glucoside malonylation, to study their enzymatic properties in detail and to investigate their function in plant growth and development; and 2) to characterize the enzymatic properties of BIA1 and its homologue BIA2, acyltransferases that had previously been implicated in the control of BR homeostasis.

2 Materials and Methods

2.1 Plant growth conditions

Arabidopsis thaliana (L.) Heynh. ecotype Columbia (Col-0) was used as the wild type. The T-DNA insertion lines, *at5mat-2* (SM_3_35619), *pmat1-2* (SALK_007564, stock number N507564), *pmat2-1* (WiscDsLox508E02, stock number CS859395), and *bia1-3* (WiscDsLox474E11, stock number CS857512) were obtained from NASC. The *bia1-1D* mutant was obtained from Hyungmin Roh. To generate *pmat1 at5mat* double knock out mutant, *at5mat-2* and *pmat1-2* single mutant plants were crossed. To generate *pmat1 pmat2* double knock out mutant, *pmat1-2* and *pmat2-1* single mutant plants were crossed. To generate *PMAT1* and *UGT73C6* double overexpression plants, *35S:PMAT1oe-8* and *35S::UGT73C6:YFP-30* overexpression plants were crossed. To generate *At5MAT* and *UGT73C6* double overexpression plants, *35S:At5MAToe-10.5* and *35S::UGT73C6:YFP-30* overexpression plants were crossed. F1, F2 and F3 progenies were analyzed by PCR or phenotype analysis. F2, F3 and F4 seeds were obtained by self-pollination. Plants were grown in growth chambers (CLF) under (16 h white light, 80 µmol·m^{-2}·s^{-1}/8 h dark) at 21 °C, relative humidity 50-60%. Primers used for genotyping are listed in **Table 2**.

Seeds were sterilized with 70% ethanol containing 0.05% Triton X-100 for 15 min and washed with 99% ethanol. Surface sterilized seeds were sown on 1/2 strength Murashige and Skoog (MS) medium plates containing 1% sucrose and subsequently stratified for two days in the dark at 4 °C. Then the plates were transferred to growth incubators CLF,16 h white light, 80 µmol·m^{-2}·s^{-1}/8 h dark, relative humidity 50-60% at 21 °C for most of the experiments or under 16 h white light, 20 µmol·m^{-2}·s^{-1}/8 h dark, relative humidity 50-60% at 21 °C for low light condition experiments. For dark grown experiments, plates were wrapped with aluminium foil.

Seeds were filled in 2 mL tubes and the tubes were placed in a plastic box. Four gram of sodium bromate was wrapped in filter paper and placed into a glass beaker containing 50 mL of 25% (w/v) hydrochloric acid. The seeds were sterilized in the chlorine gas for two to three hours. Afterwards, the box was opened and kept in the fume hood for 20 min, prior transferring the tubes to a laminar flow hood for plating. Seeds were sown on 1/2 MS medium plates containing 1% sucrose and subsequently stratified for two days in the dark at 4 °C. Then the plates were incubated in growth

incubators (CLF) under (16 h white light, 80 μmol·m^{-2}·s^{-1}/8 h dark) at 21 °C, relative humidity 50-60%.

2.2 DNA extraction from *Arabidopsis*

DNA was extracted from leaf tissues. Briefly, one leaf was frozen in liquid nitrogen and ground to a fine powder using a MM400 Resch mill. Then 500 μL CTAB (20 mM EDTA, 1.4 M NaCl, 100 mM TRIS/HCl pH=8.0) extraction buffer was added and incubated for 10-30 min at 65 °C. 500 μL chloroform was added and mixed thoroughly by vortex. The mixture was centrifuged for 5 min at 13000 rpm. The supernatant was transferred into a new tube and an equal volume of isopropanol was added and mixed. DNA was precipitated by centrifugation (13000 rpm, room temperature) for five minutes. The pellet was washed with 70% ethanol, dried completely and resuspended in 50-100 μL water.

2.3 Plasmid DNA isolation from *E. coli*

Plasmids were isolated from *E. coli* cultures using E.Z.N.A Plasmid DNA Mini Kit (Omega Bio-tec, USA). Briefly, overnight grown culture from a single colony of *E. coli* containing desired plasmids were transferred to a 2 mL tube. Bacterial cells were centrifuged at 13000 rpm for 30 s at room temperature. Culture media were discarded and cell pellets were resuspended in 250 μL Solution I/RNase A. Subsequently, 250 μL Solution II was added. The tubes were gently rotated several times and incubated 2-3 min to obtain a clear lysate. 350 μL Solution III was added, mixed and centrifuged (13000 rpm, room temperature) for 10 min. Clear supernatants were transferred to a HiBind DNA Mini Column and centrifuged at 13000 rpm for 60 s at room temperature. Filtrates were discarded and the HiBind DNA Mini Column were washed with HB buffer and DNA Wash buffer. After washing, the HiBind DNA Mini Column were centrifuged for 2 min at maximum speed to dry the column matrix. Plasmids were eluted using 50 μL Elution buffer.

2.4 Plant RNA extraction and cDNA synthesis

RNA was isolated from plant materials using the E.Z.N.A. Plant RNA Kit (Omega Bio-tec, USA) according to the instruction manual. DNA residues were removed by DNase I treatment (Thermo Scientific, Waltham, MA, USA). First strand cDNA was synthesized according to the Revert Aid First Strand cDNA Synthesis Kit (Thermo Scientific, Waltham, MA, USA). The generated cDNA was diluted 1:10 in nuclease free water and stored at -20 °C for PCR or qPCR analysis.

2.5 PCR and qPCR

For PCR amplification of a specific DNA fragments, either GoTaq G2 DNA Polymerase (Promega, Madison, USA) or Phusion High-Fidelity DNA Polymerase (Thermo Scientific, Waltham, MA, USA) was used according to the supplier's manual. Primers are listed in **Table 2**.

qPCR analysis was performed with a Mastercycler Realplex (Eppendorf, Hamburg, Germany). The reactions included 10 µL 2 x qPCRBIO SyGreen qPCR master mix (Bioline, London, UK), 0.8 µL primer mix (5 µM forward and 5 µM reverse primer) and 2 µL of each cDNA sample in a total volume of 20 µL. For quantification eight standards (cloned cDNAs) in the range of 3×10^2 to 1×10^6 copies/µL were included. The amplification program started with initial denaturation at 95 °C for 2 min. Next, 40 cycles of 95 °C for 10 s and 60 °C for 20 s were applied for amplification. A melting curve was recorded by increasing the temperature linearly from 60 °C to 95 °C within 20 min. The amplification curves were linear ($r^2 > 0.99$) and the primer pairs showed high efficiency (E = 95-105%). Melting curves confirmed absence of unspecific by-products. Expression levels were normalized to the internal standard *GAPC2* and measured in three to four technical replicates. Primers used for qPCR are listed in **Table 2**.

Table 2: Oligonucleotides used in this thesis.

Primer name	Sequence (enzyme sites are underlined)	Purpose
PMAT1 ko fwd	TCTCATAACACATCATGGTGAACGA	Genotyping/ RT-PCR
PMAT1 ko rev	TCCGCAAAAGAAATCGCTTCA	Genotyping/ RT-PCR
SalkLBb1	GCGTGGACCGCTTGCTGCAACT	Genotyping
At5MAT ko fwd	TTAAACCCTCCGTTACCGCCGAC	Genotyping/ RT-PCR

At5MAT ko rev	GGTCAAAGTCTCCACCGCCG	Genotyping/ RT-PCR
dSpm LB	TACGAATAAGAGCGTCCATTTTAGAGT	Genotyping
PMAT2 ko fwd	CTGGCCACATCACTTGGGAG	Genotyping/ RT-PCR
PMAT2 ko rev	CGAAAGTGTCCGCAATGGTCT	Genotyping/ RT-PCR
WiscDsLOx LT6	AATAGCCTTTACTTGAGTTGGCGTAAAAG	Genotyping
bia1-3 15400F1	CGAACCTTCTAAGATTGCTG	Genotyping
bia1-3 WiscLB	TAGCTCTTGCTAAGCTCCTC	Genotyping
bia1-3 15400WR	GGATCTTCATGTTGTGCATC	Genotyping
At5g39090 fwd	CATG<u>CCATGG</u>ATCCATCACTAAACTTCATC	Cloning of At5g39090
At5g39090 rev	ATAAGAAT<u>GCGGCCGC</u>TTTTTATCCCCTTGTGTAGCAAA	Cloning of At5g39090
BIA2 fwd	CG<u>GGATCC</u>ATGGACACCATGAAGGTAGAAACTA	Cloning of BIA2
BIA2 rev	CCG<u>CTCGAG</u>TTAGATCAATACACTTGGATTTGGG	Cloning of BIA2
PMAT1 fwd	TTTACGGGTTGGATTTTGGGTG	qPCR
PMAT1 rev	TCCGCAAAAGAAATCGCTTCA	qPCR
At5MAT fwd	TAGGGATTTACGGGTCTGATTT	qPCR
At5MAT rev	GAAACCGAAGCATCCTTATCAA	qPCR
PMAT2 fwd	ACACTTTCGTGGAAGGATTTAG	qPCR
PMAT2 rev	CCACCCGAAATCCGCCTC	qPCR
BIA1 fwd 901	GCGGAGAGCGAGTTTGAGAT	qPCR
BIA1 rev 1041	TGACACAGTTTCCGCCATCA	qPCR
GAPC2 fwd	TTGGTGACAACAGGTCAAGCA	qPCR/ RT-PCR
GAPC2 rev	AAACTTGTCGCTCAATGCAATC	qPCR/ RT-PCR
CPD-1	CTTGCTCAACTCAAGGAAGAG	qPCR
CPD-2	CTCGTAGCGTCTCATTAACCAC	qPCR
BR6ox2-1	AGCTTGTTGTGGGAACTCTATCGG	qPCR
BR6ox2-2	CGATGTTGTTTCTTGCTTGGACTC	qPCR
ROT3-3	CTTGTAACCCGGTACAGTTGC	qPCR
ROT3-4	TCCGCTTCATCTTCACAGTC	qPCR
UGT73C6-fwd	GTAAGTGCCGAGGTTAAAGAGG	qPCR
UGT73C6q-rev	TCTCCAAGCTCTTTGGCTCT	qPCR

The restriction sites used for cloning are underlined.

2.6 Generation of various constructs

Cloning was performed using standard methods. Restriction enzymes and T4 DNA ligase used for cloning were obtained from Thermo Scientific (Thermo Fisher Scientific, Braunschweig, Germany). PCR products or digested DNA products were purified from agarose gels using the E.Z.N.A. Gel

Extraction Kit (Omega Bio-tec, USA) according to the manufacturer's protocol. *E. coli* strain DH5a was used for amplification of the plasmids. Antibiotics (kanamycin 30 µg/mL, ampicillin 100 µg/mL) for bacterial selection were used. All constructs were confirmed by DNA sequencing.

2.6.1 Generation of pTNTSP6 series malonyltransferase constructs

Coding sequences of *At5g39080* (PciI/NotI), *At3g29635* (PciI/NotI) and *At5g61160* (PciI/NotI) were released from pGEM-T easy vector by the enzymes indicated. Coding sequences of *PMAT1/At5g39050*, *At5MAT/At3g29590*, *PMAT2/At3g29670* and *At3g29680* were released by NcoI/NotI digestion from pGEX-4T2 vector. *At5g39090* was amplified by PCR (primers used for cloning are listed in **Table 2**) and digested with NcoI/NotI. All digested inserts were ligated with T4 DNA ligase into pTNTSP6 vector.

2.6.2 Generation of pGEX-4T2-BIA2 construct

BIA2 was amplified by PCR from Col-0 genomic DNA (primers are listed in **Table 2**). The amplicon was digested and ligated into pGEX-4T2 by using the BamHI/XhoI restriction sites.

2.6.3 Generation of pGWR8-PMAT2 construct

The *PMAT2* open reading frame was released by NcoI/NotI digestion from pGEX-4T2 vector and cloned into the plant expression vector pGWR8 (Rozhon et al., 2010).

2.7 Plant transformation and selection

The constructs were electroporated into *Agrobacterium tumefaciens* GV3101/pSOUP component cells. Positive clones were selected on MLB solid medium containing kanamycin (30 µg/mL) at 28 °C for two to three days. A single colony was used to inoculate 50 mL of MLB medium containing kanamycin (30 µg/mL) which was incubated (28 °C, 110 rpm) for two days. The culture was inoculated to 300 mL MLB to an OD_{600} of 0.3. The culture was grown (28 °C, 110 rpm) until the OD_{600} reached 0.8. Subsequently, the bacterial cells were collected (4000 rpm, 15 min) and the bacterial pellet was resuspended in 300 mL 5% sucrose. The bacteria suspension was transferred to a beaker and Sylvet L-77 (final concentration: 0.05%) was added. The inflorescences of 4-5 weeks old plants were dipped in the suspension for about 30 s. The plants were covered with plastic

bags to maintain high humidity in the dark for one night. The dipped plants were grown as usual until the seeds were harvested. For the selection of transformants, seeds were surface sterilized using chlorine gas and plated on 1/2 MS media supplemented with kanamycin (30 µg/mL) at standard incubator conditions for 12-14 days. Antibiotic-resistant seedlings producing green leaves and well-developed roots were transferred to soil until the seeds were harvested for further confirmation.

2.8 Wheat germ protein expression

Proteins were synthesized using TNT SP6 High-Yield Wheat Germ Protein Expression System according to the instruction (Promega, Cat.L3261). Briefly, TNT SP6 High-Yield Wheat Germ Master Mix was removed from -80 ºC and the master mix rapidly thawed on ice. Reactions were carried out in 1.5 mL microcentrifuge tubes containing 15 µL master mix, 2 µg plasmid DNA and water in a final volume of 25 µL. The tubes were incubated at 25 °C for 2 h. Translation were analyzed by Western blot analysis (see section 2.10).

2.9 Recombinant protein purification

Correct pGEX-4T2-UGT73C5, PMAT1, At5MAT, PMAT2, BIA1 and BIA2 constructs were transformed into *E. coli* BL21. GST-fusion proteins were expressed using a previously described protocol (Unterholzner et al., 2017) and purified according to manufactures instructions (GE Healthcare) with slight modification. In brief, the bacterial pellet was suspended in 10 mL ice cold 1 x PBS (8 g/L NaCl, 0.2 g/L KCl, 1.44 g/L Na_2HPO_4, 0.24 g/L KH_2PO_4, pH 7.4) containing 50 µL 400 mM PMSF (dissolved in DMSO) and 50 µL 1 M DTT by shaking until no cell clumps remained. Resuspended bacteria were transferred to a 30 mL centrifugation tube and 200 µL of a freshly prepared solution of lysozyme (100 mg/mL in water) was added. The mixture was kept on ice for 10 min and 500 µL 20% Triton x-100 was added. Cells were mixed by inverting the tube several times and sonicated four times for ten seconds at an output power of 30% using a Sonoplus HD2070 equipped with a UW 2070 probe (Bandelin, Berlin, Germany). Cells were centrifuged (15000 rpm, 4 °C) for ten minutes and the clear supernatant was transferred to a new tube and

again centrifuged (15000 rpm, 4 °C) for 10 min. The supernatant was transferred to a 15 mL tube containing 200 µL GSH beads (the GSH beads were washed with 10 mL 1 x PBS containing 5 mM DTT prior use) and incubated for 1 h at 4 °C on a shaker. The beads were precipitated by centrifugation at 1000 rpm for 1 min. The supernatant was dumped and the beads were washed with 50 mL of 1 x PBS containing 5 mM DTT at 4 °C on a shaker for in total 5 times (5 min interval). After the last wash, the beads were resuspended with 1.5 mL 1 x PBS containing 5 mM DTT and transferred to a 2 mL reaction tube. The beads were centrifuged at 1000 rpm for 1 min and the supernatant was removed completely. Proteins were eluted by adding 500 µL elution buffer (150 mM NaCl, 5 mM DTT, 20 mM glutathione reduced form, 50 mM TRIS/HCl, pH 8.0) and incubation at 4 °C on a shaker for 30 min. Eluates were collected by centrifugation and glycerol was added to a final concentration of 50% and the protein stored at -20 °C.

2.10 SDS-PAGE and Protein immunoblotting

SDS-polyacrylamide-gel electrophoresis (SDS-PAGE) was performed using PerfectBlue™ System (Peqlab Biotechnology, Erlangen, Germany). To obtain optimal resolution of proteins, either 10% (v/v) or 15% (v/v) separation gel were casted. For electrophoresis, electrode buffer 1x (14.4 g glycine, 3 g TRIS base, 1 g SDS sodium salt were dissolved in 1 L water) was used and a protein ladder (Thermo Scientific, Waltham, MA, USA) was loaded as a size marker. Gels were either stained directly or used for western blot analysis.

Proteins produced using the wheat germ expression system were mixed with 2 x loading buffer containing 100 mM TRIS/HCl (pH 6.8), 200 mM DTT, 4% (w/v) SDS, 20% (v/v) glycerol, 0.025% (w/v) bromophenol blue and heated for 3 min. Samples were separated by 15% SDS-PAGE gel and transferred onto a PVDF membrane (Merck Millipore, Burlington, MA, USA). The membrane was blocked with 5% milk, and then incubated with anti-cMyc-HRP (1:5000, Santa Cruz Biotechnology, Santa Cruz, CA, USA) antibody. The signal was revealed by ECL (GE Healthcare).

To confirm expression of the BIA1 transgene, 8-day-old seedlings grown on 1/2 MS plates were frozen, ground and extracted by adding one volume/fresh weight of 2 x SDS buffer containing 100 mM TRIS/HCl (pH 6.8), 200 mM DTT, 4% (w/v) SDS, 20% (v/v) glycerol, 0.025% (w/v) bromophenol

blue and heating the homogenate (95 °C, 5 min). Protein extracts equivalent to 10 mg seedlings were resolved on a 10% SDS-PAGE gel and transferred onto a PVDF membrane. After blocking with 5% blocking buffer, the membrane was incubated with anti-GFP-HRP antibody overnight (1:10000, Miltenyi Biotec, Bergisch Gladbach, Germany). Detection was done with ECL reagent (GE Healthcare). The membrane was stained with the Coomassie Brilliant Blue R250 to confirm loading.

To probe BES1 phosphorylation, total proteins were extracted from opened flowers from adult plants. Samples were frozen and ground. Proteins were extracted with two volumes/fresh weight of 2 x SDS buffer containing 125 mM TRIS/HCl (pH 6.8), 4% (w/v) SDS, 20% (v/v) glycerol, 20 mM DTT, 0.02% (w/v) bromophenol blue by heating the homogenate (95 °C, 5 min). Extracts were resolved on 15% SDS-PAGE gel and transferred onto a PVDF membrane. After blocking with 5% milk powder for 60 min, the membrane was incubated with BES1 antibody (1:2000, kindly provided by Yanhai Yin, Iowa State University, USA) overnight and then the HRP-conjugated anti-rabbit antibody (1:10000) was added. The signal was developed by ECL (GE Healthcare).

2.11 Synthetic procedures

Synthesis of 24-epiBL-23Glc: The synthetic scheme used to generate 24-epiBL-23Glc from 24-epiBL is based on the results that UDP-glycosyltransferase UGT73C5 from *A. thaliana* catalyzes 23-*O*-glucosylation of BRs (Poppenberger et al., 2005). GST-UGT73C5 recombinant proteins were purified (see section 2.9) and glucosylation reactions performed in assay buffer (50 mM TRIS/HCl, pH 8.0, 10 mM UDP-glucose, 0.5 mM ATP, 50 mM $MgCl_2$, 10 mM DTT and 0.5 mM 24-epiBL) and incubated at 30 °C for overnight. Reaction products were subjected to preparative HPLC for further separation. A Shimadzu system, which fitted with a column (Luna, C18(2), 100A, 5 µL, 100 x 21 mm; Phenomenex) was used for preparative HPLC. Elution was carried out using mobile phases A (10% acetonitrile) and B (100% acetonitrile). The gradient protocol was as follows: 100% A, 0% B for 0 min, linear gradient to 20% A, 80% B for 120 min, at a constant flow rate of 2 mL/min. Fractions were collected and aliquots were analyzed by TLC (see section 2.13). Fractions containing 24-epiBL-23Glc were evaporated to dryness using a vacuum concentrator. 24-epiBL-23Glc were dissolved in DMSO for enzyme assays.

Synthesis of BL-23Glc and d₃BL-23Glc: The synthetic scheme and separation method were identical to synthesis of 24-epiBL-23Glc.

Synthesis of BL-23MalGlc and d₃BL-23MalGlc: The newly identified malonyltransferase (PMAT1) was used. GST-PMAT1 recombinant proteins were purified (see section 2.9) and reactions performed in assay buffer (50 mM diethanolamine, 1.25 mM malonyl-CoA, 10 mM DTT and substrates) and incubated at 30 °C for overnight. Reaction products were separated by preparative HPLC for further separation. The same system as stated above was used. Elution was carried out using mobile phases A (10% acetonitrile plus 10 mM formic acid) and B (100% acetonitrile). The gradient protocol was as follows: 100% A, 0% B for 0 min, linear gradient to 50% A, 50% B for 120 min, at a constant flow rate of 2 mL/min. Fractions were collected and aliquots were analyzed by TLC (see section 2.13). Fractions containing BL-23MalGlc and d₃BL-23MalGlc were dried using a vacuum concentrator.

Quantification of BL-23Glc and BL-23MalGlc: 200 µL BL-23Glc (in ethyl acetate) or BL-23MalGlc (in acetonitrile) were dried using a vacuum concentrator. Samples were dissolved in ethyl acetate and loaded on TLC plate with BL standards alongside. Plate was separated (see section 2.13) and quantified using Image J software.

2.12 Enzyme assays

2.12.1 Enzyme assay for BL-23Glc malonylation

To screen the potential BR malonyltransferases, enzyme assays were performed with 5 µL protein produced by wheat germ system (see section 2.8), 50 mM diethanolamine (pH 9.0), 1.25 mM malonyl-CoA, 10 mM DTT and 2 µL 24-epiBL-23Glc (see section 2.11). Assays were performed in a final volume of 20 µL and incubated at 30 °C overnight. Ethyl acetate extracts of the enzyme assays were analyzed by TLC (see section 2.13). To test for BR malonyltransferases activity, different amounts (3, 1.5, 0.75, 0.375, 0.18, 0.09, 0.045, 0.0225, 0.01, 0.005 µg in 5 µL) of purified GST-PMAT1 or GST-At5MAT proteins (see section 2.9) were used. Assay conditions and detection were identical to BR malonyltransferases screening. To test for BR malonyltransferases activity, different buffer pH levels (50 mM diethanolamine, pH 6-10.5) were used. Enzyme assays were

carried out with 180 ng GST-PMAT1 or 750 ng GST-At5MAT proteins (see section 2.9). Assay conditions and detection were identical to BR malonyltransferases screening.

2.12.2 Enzyme assay for BIA1 acylation

Substrates for enzyme assays (CS, 24-epiBL, 24-epiCS, 6-deoxo-24-epiCS, tris-epiCS, and 3,24-diepiCS) were purchased from Olchemim (Olomouc, Czech Republic). The co-enzymes malonyl-CoA and myristoyl-CoA were purchased from Sigma-Aldrich (St. Louis, MO, USA) and caffeoyl-CoA and coumaroyl-CoA were obtained from (TransMIT GmbH, Marburg, Germany). For initial experiments (Figure 11), enzyme assays were performed in a final volume of 20 µL containing 3 µg GST-BIA1 protein (see section 2.9), 100 mM sodium phosphate buffer (pH 8), 5 mM DTT, 1 mM substrate and 10 mM acetyl-CoA (BioChemica, Darmstadt, Germany) or 2.5 mM of the other CoA-thioesters. The reactions were incubated at 25 °C overnight. Products were analyzed by TLC (see section 2.13).

For optimizing enzymatic reaction conditions assays were performed as described above except that 25 mM diethanolamine buffer set with phosphoric acid to the desired pH was used (Figure 13 A) and different reaction times (Figure 13 B) and temperatures (Figure 13 C) were tested. The reaction products were analyzed by HPLC using a Nucleodur 100-5 C18ec (125 x 4.6 mm, Macherey-Nagel) column for separation. A LC-10A high performance liquid chromatography system (Shimadzu, Kyoto, Japan) was used for analysis. The HPLC system consisted of a SCL-10A system controller, a FCV-10AL valve for eluent selection, a LC-10AT pump equipped with DGU-14A inline degasser, a SIL-10A autosampler, a CTO-10ASvp column oven, a SPD-10A UV detector and a RF-10AXL fluorescence detector. Elution started with 70% solvent A (10% acetonitrile in water) and 30% solvent B (pure acetonitrile). The concentration of B was then raised linearly to 100% B in 20 min before reducing it to the initial conditions within 1 min. Finally, the column was equilibrated for 7 min before injection of the next sample. The absorbance was recorded at 210 nm. The obtained chromatograms were analyzed with the Clarity software package (DataApex, Prague, Czech Republic).

For enzyme kinetics (Figure 13 D) reactions were performed in a total volume of 100 µL and contained 25 mM diethanolamine buffer set with phosphoric acid to pH 9.0, 2 mM DTT, 2 mM acetyl-CoA, 160 ng GST-BIA1 and 0 to 75 µM CS as a substrate. The reactions were incubated at 30 °C for 60 min prior addition of 25 nmol testosterone as an internal standard. The samples were extracted twice with ethyl acetate as described above. Dried residues were derivatized by addition of 50 µL dansylhydrazine (2 mg/ml in acetonitrile) and 50 µL trifluoroacetic acid (1 M in acetonitrile) and incubation at 50 °C for 90 min. Samples were analyzed by HPLC using the system described above except that elution started with 55.6% A and 44.4% B. The concentration of B was then raised linearly to 77.8% B in 20 min before reducing it to the initial conditions within 1 min. Finally, the column was equilibrated for 7 min before injection of the next sample. Fluorescence was recorded at an excitation wavelength of 355 nm and an emission wavelength of 512 nm. *Km* and *Vmax* were calculated using non-liner regression analysis based on the Michaelis-Menten model. Calculations were performed in Excel using the solver add in.

2.12.3 Enzyme assay for scopolin malonylation

Proteins produced using the wheat germ expression system (see section 2.8) were assayed in assay buffer (2 µL protein, 50 mM diethanolamine, 1.25 mM malonyl-CoA, 10 mM DTT, 0.5 mM scopolin) and incubated at 30 °C. Assays were incubated for 1 h and stopped by adding formic acid to final 80 mM and the reaction mixture was subjected to HPLC analysis. For *in vitro* enzymatic assays detection, samples were analyzed with a Nucleosil C18HD 100-5 250 x 4.6 mm column using 92.2% acetonitrile plus 1 mM formic acid (mobile phases A) and 7.8% acetonitrile (mobile phase C). The flow rate was 0.8 mL/min at an oven temperature of 25 °C. The fluorescence detector was set to a wavelength of 345/430 nm. Recombinant proteins were assayed with different incubation times, buffers and substrate concentrations (see above). Enzyme activity assays (20 µL) with purified proteins contained either 120 ng GST-PMAT1 or 400 ng GST-PMAT2 (see section 2.9). Reaction conditions were as follows: 50 mM diethanolamine pH 7.5 (GST-PMAT1) or pH 8.5 (GST-PMAT2), 10 mM DTT, 1.25 mM malonyl-CoA, and different scopolin concentrations. Reactions were incubated for 15 min at 30 °C and stopped by adding formic acid to final 80 mM and analyzed.

2.13 Detection of BRs and their conjugates by TLC

This method is designed for analysis of samples from: enzyme assays for BR malonyltransferases (see section 2.12.1) and substrates screening for BIA1 acylation (see section 2.12.2). Water was added to the *in vitro* reaction to a final volume of 100 µL. 10 µL 10% TCA is added as BL-23MalGlc analyzed. 100 µL EtAc was added and the tube was shaken vigorously. Subsequently, the tube was centrifuged for 1 min at 13000 rpm. The upper aqueous phase was transferred into a new tube and the residue extracted with 100 µL EtAc. After centrifugation, both organic extracts were pooled and evaporated in the vacuum. The residue was dissolved in EtAc for loading. Samples were loaded on a silica 60 TLC plate and dried for 10 min in the fume hood. Plates were developed in solvent A (CHCl$_3$/EtAc/MeOH/HCOOH/H$_2$O = 30/10/4/0.5/0.5) for analysis of free BRs and acetylated BRs or in solvent B (CHCl$_3$/EtAc/MeOH/HCOOH/H$_2$O = 10/10/5/2/1) for detection of glycosylated or malonyl-glycosylated BRs. When the solvent had traveled almost to the top of the plate, the plates were removed and dried for 10 min in the fume hood. To visualize the spots, the plates were sprayed with enough methanolic 1% H$_2$SO$_4$ and heated at 110 °C for 10 min. The BRs and their conjugates were visualized with UV of 366 nm and pictures were recorded with Cannon digital camera.

2.14 Plant feeding and sample extraction

2.14.1 BL feeding

For quantification experiments in Figure 4, around 30-35 eleven days old seedlings of Col-0, *at5mat-2*, *pmat1-2*, *pmat1-2 at5mat-2*, *35S:At5MAToe*, *35S::At5MAT:cMyc oe*, *35S:PMAT1oe* and *35S::PMAT1:cMyc oe*, grown on 1/2 MS plates, were transferred to sterile flasks containing 30 mL liquid 1/2 MS media. BL was added to a final concentration of 1 µg/mL. Plant materials were incubated on a shaker (60 rpm) placed in an incubator for 48 h. Plant material was harvested, ground in liquid nitrogen and stored at -80 °C freezer until extraction. 10-20 mg plant material was extracted twice with 100 µL of aqueous methanol (50+50, v+v) and deuterium-labeled internal standard was added. Quantification of BRs was performed by Prof. Franz Berthiller (Universität für Bodenkultur, Vienna, Austria).

2.14.2 CS feeding

30-35 eleven days old seedlings of Col-0, *bia1-3*, *bia1-1D* and *35S::BIA:YFP*#4.2, grown on 1/2 MS plates, were transferred to sterile flasks containing 30 mL liquid 1/2 MS medium. CS was added to an end concentration of 1 µg/mL. Seedlings were incubated on a shaker (60 rpm) in incubator for 24 h. Plant material was harvested, ground in liquid nitrogen and stored in -80°C freezer until extraction. Approximately 100 mg plant material was extracted twice with 800 µL of methanol. Measurement of CS conjugates was performed by Prof. Franz Berthiller (Universität für Bodenkultur, Vienna, Austria).

2.15 Quantification of scopolin and malonylscopolin

For metabolites detection, approximately 100 mg plant materials were ground to a fine powder and extracted using 1 mL 10% acetonitrile supplemented with 10 µL acetic acid by shaking for 10 min in a Thermo mixer at full speed (1400 rpm). Samples were centrifuged and filtered using syringe filter (13 mm, Nylon 66, 0.22 µm). HPLC was performed with a Nucleosil C18HD 100-5 250 x 4.6 mm column using the mobile phase A (10% acetonitrile containing 1 mM formic acid) and B (100% acetonitrile). The flow rate was 0.8 mL/min and the column oven temperature was set to 25 °C. The fluorescence detector was set to excitation and emission wavelength of 345 and 430 nm, respectively.

3 Results

3.1 PMAT1 catalyzes malonylation of BL-23Glc *in planta*

3.1.1 Phylogenic analysis identifies eight candidates for BR-MalGlc formation

To identify proteins involved in BR-Glc malonylation a candidate gene approach was chosen. For this purpose, BLASTP searches using PMAT1 against the Araport11 protein sequence database were conducted and identified 71 loci with high similarity. Manual curation was done to exclude either loci that lack a conserved motif (HxxxD or DFGWG) or loci that are redundant. A final list of 55 unique putative *A. thaliana* BAHD acyltransferases was obtained (**Figure 1** A), which is consistent with the results of others (Tuominen et al., 2011).
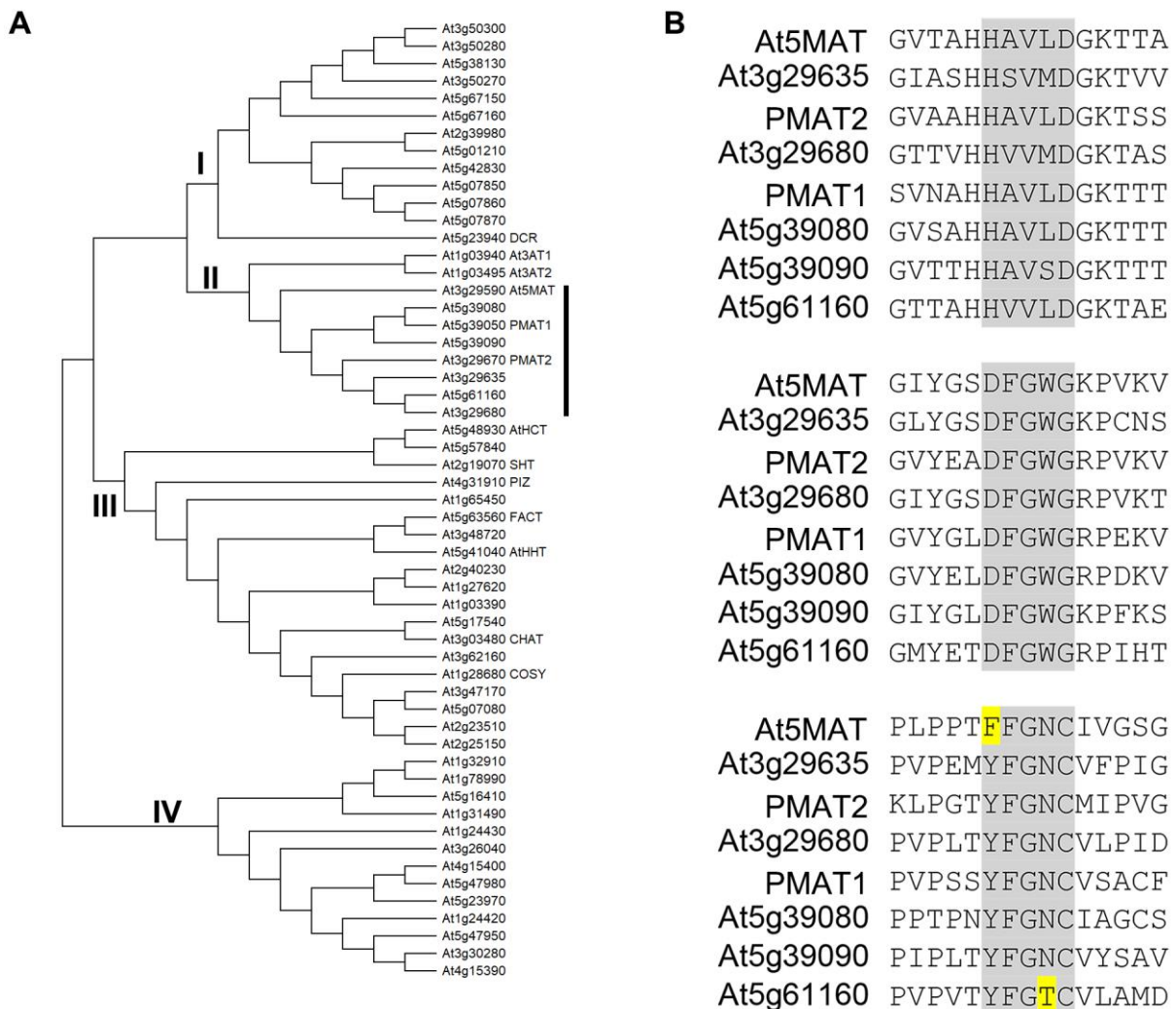

Figure 1: Phylogenetic analysis of *A. thaliana* BAHD acyltransferases. (**A**) Phylogeny tree of 55 *A. thaliana* BAHD acyltransferases. (**B**) Conserved domains in members of clade II.

A phylogenetic tree was assembled with the 55 acyltransferases and showed that the enzymes sorted into four major groups, again being consistent with previous reports (D'Auria, 2006; Yu et al., 2009). Members from clade II were selected as the most promising candidates for BR-Glc malonylation, since some of them had already been shown to use malonyl-CoA as donor substrate (Luo et al., 2007; Taguchi et al., 2010; Khan et al., 2016). Motif analysis revealed the presence of the conserved HxxxD, DFGWG and YFGNC motifs in those candidates (**Figure 1** B), providing further support to the notion that they may utilize the common donor malonyl-CoA.

3.1.2 PMAT1 and At5MAT catalyze the formation of BL-23MalGlc *in vitro*

To test, if the candidates can catalyze BR-MalGlc formation, enzymatic activity assays with recombinant proteins were carried out. Since previous results had shown that expression as GST-fusion proteins in *Escherichia coli* (*E. coli*) failed for some of the selected malonyltransferases, a wheat germ extract-based *in vitro* protein translation system was used for protein production. The coding regions of the eight malonyltransferases were cloned from available pGEX or pGEM vectors into the pTNTSP6 vector which incorporates barley yellow dwarf virus sequences flanking the protein-coding region and cMyc tag sequences at the C-terminus (**Figure 2** A). Proteins were translated and expression was analyzed by Western blot analysis using an anti-cMyc antibody. This showed that all proteins were successfully expressed, however, efficiencies varied (**Figure 2** B).

The enzymes were incubated with malonyl-CoA as a donor and 24-epiBL-23-*O*-Glc (24-epiBL-23Glc) as an acceptor substrate (see synthetic procedures in 2.11). Reaction products were separated by thin-layer-chromatography (TLC) and visualized with UV of 365 nm after spraying with sulfuric acid. The results showed that an additional band was obtained in the reactions with cMyc-tagged PMAT1 and also with At5MAT, albeit at a lower level for the latter (**Figure 2** C). No products were produced with any of the other enzymes. To verify the catalytic activities of PMAT1 and At5MAT and investigate the enzymes *in vitro* activities in more detail, both proteins were expressed in *E. coli* BL21. The activity assays with 24-epiBL-23Glc and malonyl-CoA were then repeated and different buffer pH conditions and input protein amounts were tested.
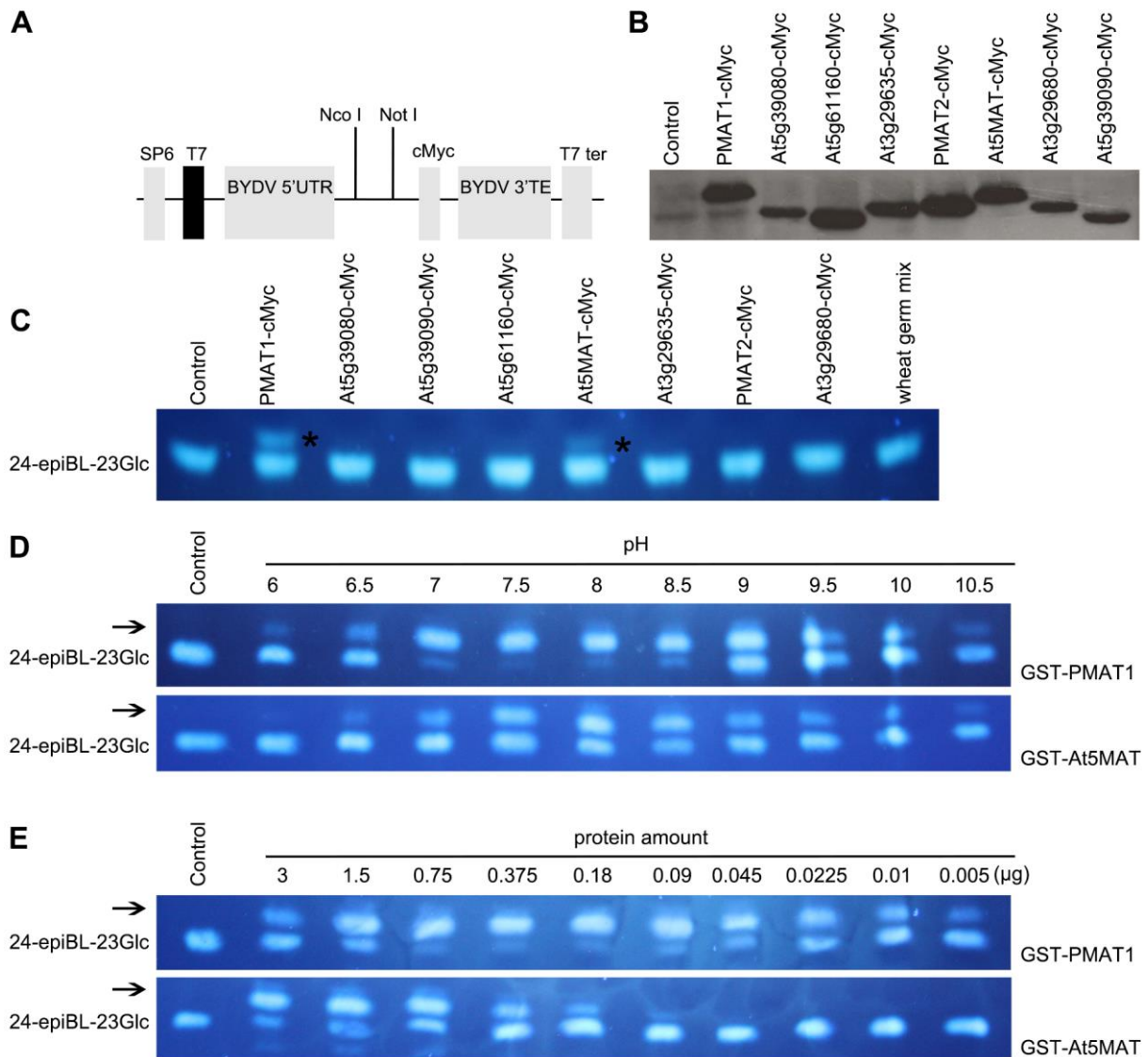
Figure 2: PMAT1 and At5MAT showed malonyltransferase activity against 24-epiBL-23Glc. (**A**) Illustration of the pTNTSP6 vector. SP6: SP6 promoter, T7: T7 promoter, BYDV 5'UTR: barley yellow dwarf virus 5'untranslated region, cMyc: cMyc tag, BYDV 3'TE: barley yellow dwarf virus 3' translation element, T7 ter: T7 terminator sequence. (**B**) Western blot analysis of translated products using an anti-cMyc antibody. (**C**) Activity of the expressed malonyltransferases toward 24-epiBL-23Glc. Reaction products were separated by TLC. Positions of malonylated products are indicated by asterisks. (**D**) 24-epiBL-23Glc were incubated with 180 ng GST-PMAT1 or 750 ng GST-At5MAT under pH levels as indicated. (**E**) 24-epiBL-23Glc were incubated with different amounts of GST-PMAT1 or GST-At5MAT as indicated. Samples were extracted and run on TLC. Positions of 24-epiBL-23Glc are indicated. Malonylated products in (**D**, **E**) are indicated by arrows on left side.

This showed that both enzymes preferred neutral to slight alkaline conditions, with best conversion rates at pH 7.5 to pH 8.0 (**Figure 2** D). For input protein amounts, PMAT1 activity clearly increased, when the protein amount was dropped from 3 to 0.18 µg. In contrast, At5MAT activity decreased by reducing input protein concentrations (**Figure 2** E). In summary, there is evidence that both PMAT1

and At5MAT catalyzed the transfer of a malonyl moiety from malonyl-CoA to 24-epiBL-23Glc *in vitro*, but PMAT1 had higher catalytic activity than At5MAT.

3.1.3 *PMAT1* and *At5MAT* knock out and overexpression plants do not show obvious developmental defects

To investigate the function of the two malonyltransferases *in planta*, T-DNA-insertion lines with predicated insertions in the open reading frames of the genes were ordered from NASC and the T-DNA insertion sites were identified by PCR and sequencing. Line SALK_007564 was previously characterized as *pmat1-2* (Khan et al., 2016). In line with the previously published work, the T-DNA was found to be integrated at position 538 bp of the *PMAT1* open reading frame (**Figure 3** A). Line SM_3_35619 harbors a T-DNA in the *At5MAT* gene at position 929 bp (**Figure 3** A). Since one *at5mat* knock out allele has already been published, but is not the same line (D'Auria et al., 2007b), this new allele was named *at5mat-2*. Double *pmat1-2 at5mat-2* mutants were generated by crossing and homozygosity of the offspring was analyzed by RT-PCR in the F3 generation (**Figure 3** B).

In addition to generate knock out mutants in a single and higher order setting, overexpression lines were characterized. Wild type Col-0 plants transformed with *35S:PMAT1* or *35S:At5MAT* constructs had previously been generated in the Poppenberger lab and were obtained in the T2 generation. Homozygous lines from independent transgenic individuals were selected and transgene expression was determined by qPCR. This showed that *35S:PMAT1oe* line -3, -6 and -8 (*35S:PMAT1oe*-3, -6, -8) and *35S:At5MAToe* line -1.2, -5.4 and -10.5 (*35S:At5MAToe*-1.2, -5.4, -10.5) had high levels of transgene expression (**Figure 3** C, D). These lines were selected for further experiments.

Both knock out and overexpression lines were phenotyped and it was found that under standard growth conditions, they did not exhibit obvious morphological differences in the adult growth stage (**Figure 3** E). Also in term of seedling hypocotyl and root elongation, as well as cotyledon areas there were no significant differences to wild type under low light conditions (**Figure 3** F, G, H). To assess if BR responsive growth might be altered, the effect of externally applied 24-epiBL on

hypocotyl elongation in the dark was studied. Again, no significant differences to wild type responses were observed (**Figure 3** I).
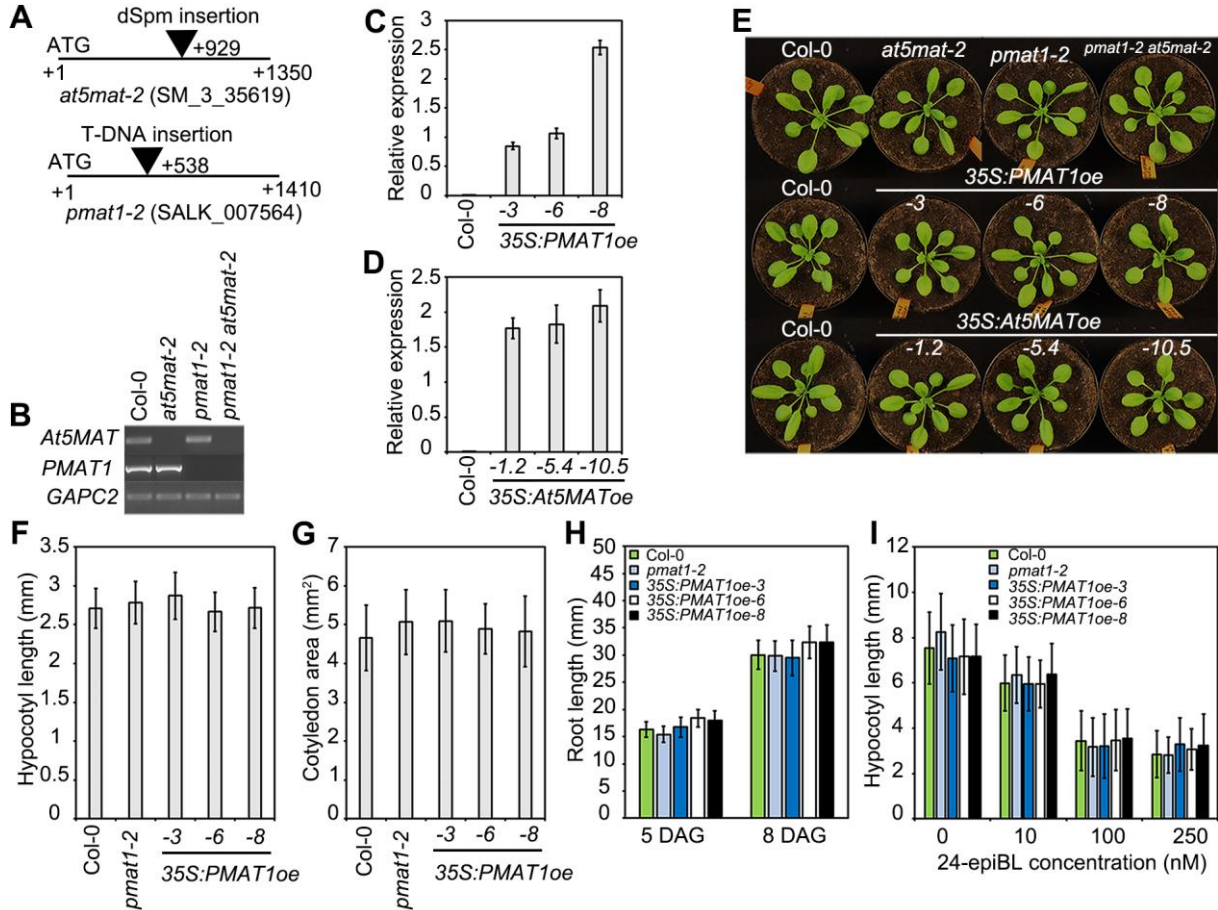

Figure 3: A loss or gain of PMAT1 and At5MAT function did not yield obvious morphological phenotypes. (**A**) Illustration of the T-DNA insertions sites in the two genes. The insertion position is marked by triangles with the respective nucleotide number counted from the start codon. (**B**) *PMAT1* and *At5MAT* gene expression in wild type, single- and double insertion mutants were determined by RT-PCR analysis. Expression of *GAPC2* is shown as a reference. (**C**, **D**) Expression levels of the *PMAT1* or *At5MAT* in wild type and overexpression lines relative to *GAPC2*. (**E**) Representative pictures of 3-week-old plants of the indicated genotypes. (**F**) Hypocotyl length of plants with altered *PMAT1* expression grown for 5 DAG (days after germination) on 1/2 MS medium under low light conditions (16 h white light, 20 µmol·m^{-2}·s^{-1}/8 h dark). (**G**) Cotyledon area of plants grown under low light conditions for 8 DAG. (**H**) Root length of 5 or 8 DAG seedlings grown under low light conditions. (**I**) 24-epiBL sensitivity test of *35S:PMAT1oe* and *pmat1-2* knock out plants. Seedlings were grown on 1/2 MS medium supplied with 10, 100, 250 nM 24-epiBL in the dark for 3 days. Plates supplemented with the pure solvent (DMSO) served as control. The columns and bars represent the average and SD of three replicates in (**C**, **D**) and at least 25 individuals in (**F-I**).

3.1.4 A loss of PMAT1 function abolishes BL-23MalGlc formation capacities

The generated knock out and overexpression lines were used to test whether altering *PMAT1* or *At5MAT* expression may impact the BR-Glc malonylation capacities of plants. For this purpose, feeding experiments were performed with BL, since it is known that this can increase BR-Glc concentrations to detectable amounts (endogenous levels are below the detection limit (Poppenberger et al., 2005; Husar et al., 2011)). For the feeding experiment standards had to be generated, since BL-23Glc and BL-23MalGlc are not commercially available. They were generated using an enzyme catalyzed approach. First UDP-glycosyltransferase UGT73C5 from *A. thaliana* was used to catalyze the formation of BL-23Glc from BL and UDP-glucose (Poppenberger et al., 2005). Then PMAT1 was used to generate BL-23MalGlc from BL-23Glc. Synthesized BL-23Glc and BL-23MalGlc were quantified by TLC analysis using BL as a standard (**Figure 4** A).

In addition to the untagged lines also cMyc-tagged lines were used in the feeding studies. Wild type Col-0 plants transformed with *35S::PMAT1:cMyc* or *35S::At5MAT:cMyc* constructs had previously been generated in the Poppenberger lab and were obtained in the T2 generation. Homozygous lines from independent transgenic individuals were selected and transgene expression was determined by Western blot analysis. This showed that *35S::PMAT1:cMyc oe* line -15, -38, -43 and *35S::At5MAT:cMyc oe* line -3.1, -6.3, -7.2 had high levels of transgene expression (**Figure 4** B). For the feeding experiments, 11-day-old seedlings of all lines and wild type were incubated in liquid 1/2 MS medium supplemented with 1 µg/mL BL for 48 hours. Following methanol extraction, the samples were analyzed by HPLC-QTOF using BL-23Glc and BL-23MalGlc as standards, which was carried out by Prof. Franz Berthiller at the Universität für Bodenkultur, Vienna, Austria. The results showed that while in the *at5mat-2* mutant, BL-23MalGlc levels were comparable to wild type, BL-23MalGlc was undetectable in the *pmat1-2* single and the *pmat1-2 at5mat-2* double mutant (**Figure 4** C), providing evidence that PMAT1 is required for its formation while At5MAT is of minor importance. In the *pmat1-2* single and *pmat1-2 at5mat-2* double mutants increased amounts of the substrate, BL-23Glc, were observed (**Figure 4** D), indicating that the decreased conversion to BL-23MalGlc enriched BL-23Glc in that plants. In the PMAT1 and At5MAT overexpression lines, similar amounts of BL-23Glc and BL-23MalGlc were detected like in wild type (**Figure 4** C, D).
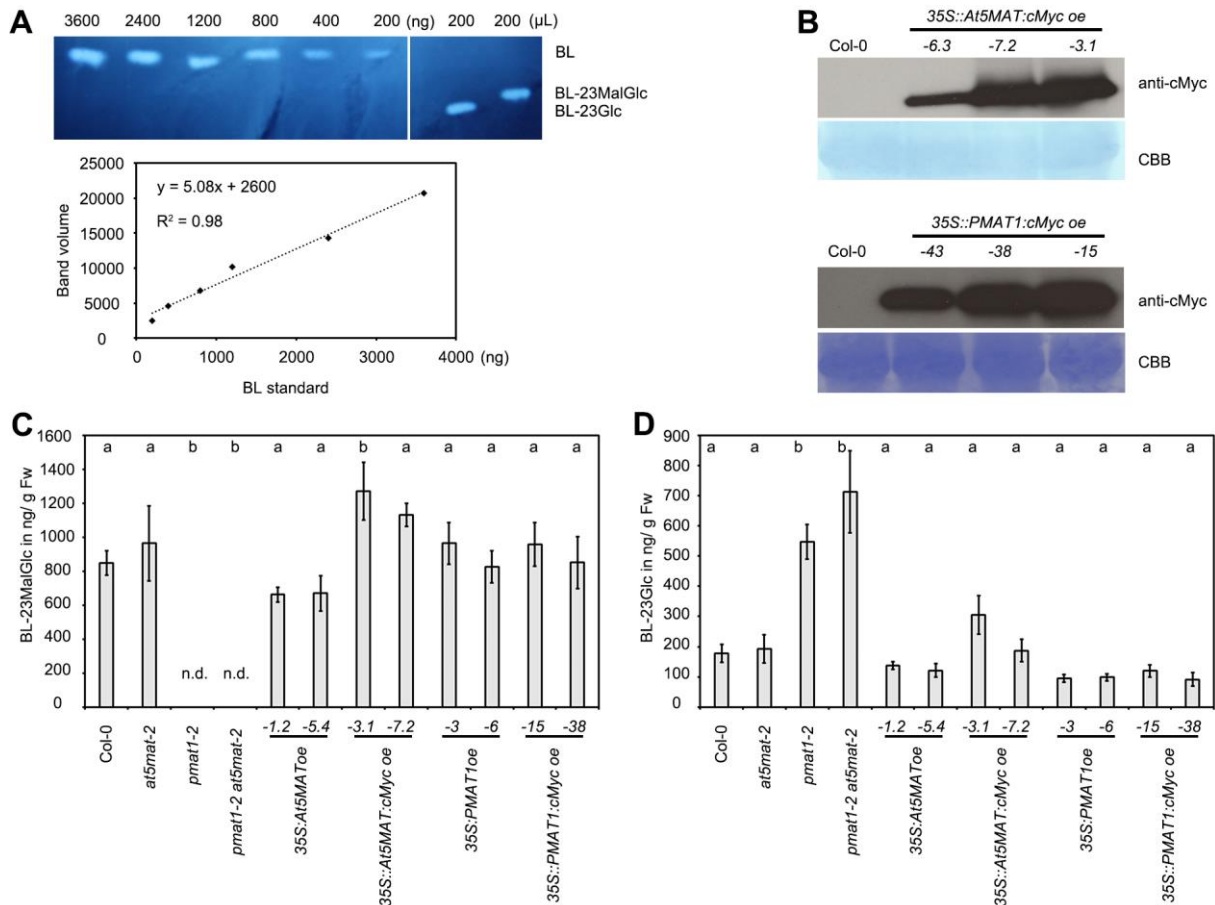
Figure 4: BL-23MalGlc formation capacities were lost in *pmat1-2* mutants. (**A**) Quantification of the synthesized BL-23Glc and BL-23MalGlc by TLC. Upper panel: synthesized products and BL standards were loaded and separated by TLC. Lower panel: band intensities (band volumes) were measured by Image J software and plotted with known BL standards. (**B**) Expressions of *At5MAT:cMyc* and *PMAT1:cMyc* in overexpression plants were confirmed by Western blot. Wild type Col-0 plants served as negative control. BL-23MalGlc (**C**) and BL-23Glc (**D**) levels in BL treated seedlings of the indicated lines. 11-day-old seedlings were treated with 1 µg/mL BL for 48 hours and following extraction the samples were analyzed by HPLC-QTOF. Quantification was performed by Prof. Franz Berthiller, Universität für Bodenkultur, Vienna, Austria. Values are the means ± SD of three to four replicates; n.d., not detected. Different letters indicate significantly different values at $p < 0.05$ (one way ANOVA, Tukey post hoc test) to wild type.

3.1.5 PMAT1 overexpression enhances BR deficiency in plants with increased BR-glucoside accumulation

While PMAT1 efficiently catalyzed malonylation of BR-Glc *in vitro*, and a loss of PMAT1 function abolished BL-23MalGlc formation *in planta*, *PMAT1oe* plants did not show increased BL-23MalGlc levels. Several reasons may account for this fact, one being insufficient BL-23Glc acceptor availability in these lines. To test the hypothesis that BL-23Glc substrate is the limiting factor, *PMAT1oe-8* was introduced into the *UGT73C6* overexpression line *UGT73C6:YFP-30* (Husar et al.,

2011) by crossing. *UGT73C6oe* plants accumulated large amounts of BL-23Glc and showed dwarfism and other typical symptoms of BR-deficiency (Husar et al., 2011). In addition, also *At5MAToe-10.5* was crossed with *UGT73C6:YFP-30* and F3 progeny homozygous for the transgenes was selected. Since all used overexpression constructs are driven by the *35S* promoter, qPCR analysis was used to assess whether cosuppression of the transgenes occurred. When seedlings from agarose plates were used as sample, qPCR analysis showed that no *At5MAT* co-repression occurred in line *At5MAToe-10.5 x UGT73C6:YFP-30* (**Figure 5** A). Only *PMAT1* co-repression occurred to some extent, yielding approximately 30% reduction of *PMAT1* mRNA as compared to the parent line in the double over-expressor *PMAT1oe-8 x UGT73C6:YFP-30* (**Figure 5** B). *UGT73C6* expression was not cosuppressed, neither in line *PMAT1oe-8 x UGT73C6:YFP-30* nor in line *At5MAToe-10.5 x UGT73C6:YFP-30* (**Figure 5** C). Seedlings were then transferred to soil and grown for longer time. Under soil conditions, plants in line *At5MAToe-10.5 x UGT73C6:YFP-30* did not show any cosuppression effects, while plants in line *PMAT1oe-8 x UGT73C6:YFP-30* exhibited varied cosuppression phenotypes. Moreover, the cosuppressed plants in the double over-expressor *PMAT1oe-8 x UGT73C6:YFP-30* can be clearly differentiated and removed in following analysis. When opened flowers of non-cosuppression plants in line *PMAT1oe-8 x UGT73C6:YFP-30* from soil were used as sample, qPCR analysis revealed that both *PMAT1* and *UGT73C6* in the double over-expressor *PMAT1oe-8 x UGT73C6:YFP-30* did not show co-repression as compared to the parent lines (**Figure 5** D, E).

To investigate the impact of introducing PMAT1 and At5MAT into the *UGT73C6:YFP* background, several growth parameters were investigated in the F3 progeny of the crosses and compared to the parental lines and wild type. At 32 days post germination it was apparent that the characteristic BR-deficient phenotype of the *UGT73C6:YFP* line was intensified by overexpression of *PMAT1* in *PMAT1oe-8 x UGT73C6:YFP-30*, since rosette size was significantly reduced (**Figure 5** F, G). This effect was not seen in the *At5MAToe-10.5 x UGT73C6:YFP-30* line (**Figure 5** F, G). At 8 weeks post germination the enhanced BR-deficient phenotype of *PMAT1oe-8 x UGT73C6:YFP-30* became even more obvious: plant height and fertility were strongly compromised and senescence was further delayed as compared to the *UGT73C6:YFP-30* parent (**Figure 5** H, I).
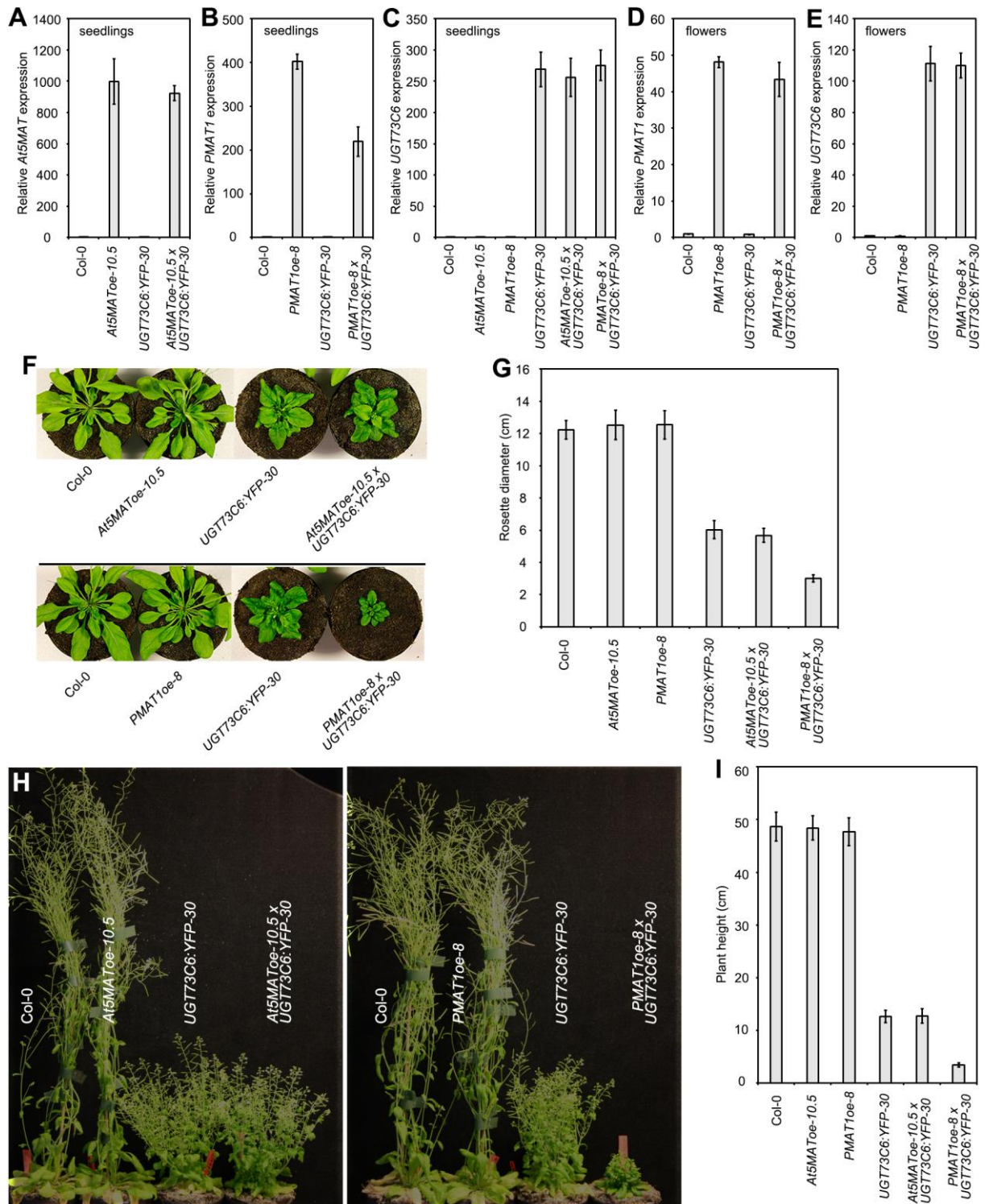
Figure 5: PMAT1 overexpression enhanced the BR-deficient phenotypes of *UGT73C6oe* plants. (**A-E**) Expression levels of *At5MAT* (**A**), *PMAT1* (**B**, **D**) and *UGT73C6* (**C**, **E**) in the seedlings or the opened flowers of wild type, single- and double overexpressing plants were analyzed by qPCR. *GAPC2* was used as a reference. The columns and bars indicate the average and SD of four to eight biological replicates. (**F**) Representative plants of the double over-expressors, parental lines and wild type. The plants were grown on agar medium for 11 days and then grown in soil for 21 days. (**G**) Rosette diameters of plants shown in (**F**). (**H**) Representative plants of the indicated lines grown for 8 weeks in soil. (**I**) Plant height of the plants shown in (**H**). Values are means ± SD of at least 12 plants in (**G**, **I**).

To investigate if the enhanced BR-deficient phenotype of *PMAT1oe-8 x UGT73C6:YFP-30* is due to decreased BR activity in this line, two types of readouts for BR signaling capacity were measured. On the one hand, the expression of the BR biosynthetic genes *CPD*, *ROT3* and *BR6OX2*, which are feedback-induced by BR deficiency (Bancos et al., 2002; Tanaka et al., 2005), was analyzed by qPCRs. One the other hand the phosphorylation state of BES1 was determined by Western blot analysis, using a BES1-specific antibody (Yin et al., 2002). This showed that, when compared to the parental lines and wild type, the expression of all analyzed BR biosynthetic genes was elevated in the double over-expressor *PMAT1oe-8 x UGT73C6:YFP-30* (**Figure 6** A-C). This was correlated with decreased levels of BES1 proteins (**Figure 6** D), providing clear evidence that BR signaling capacities are reduced in this line.
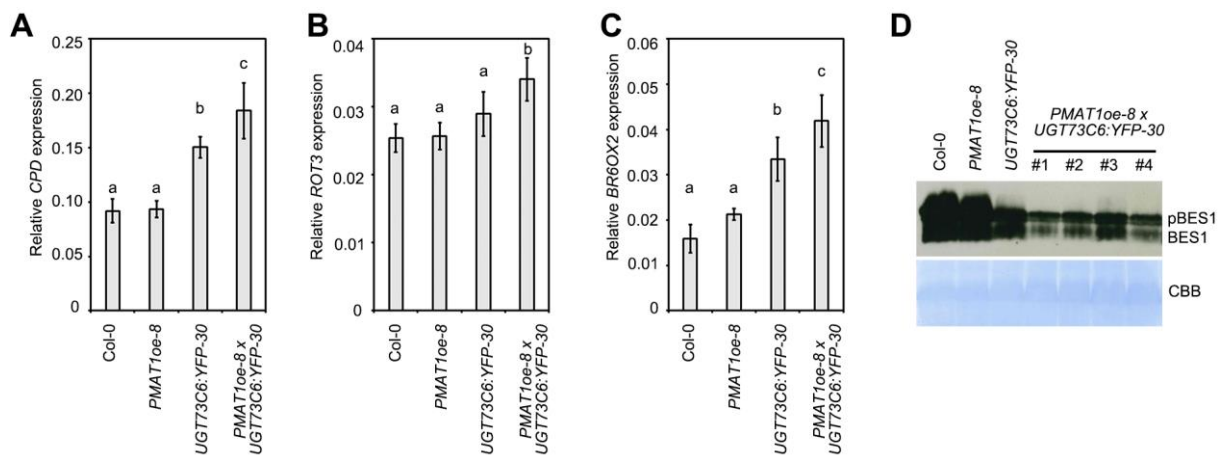
Figure 6: Combined overexpression of *PMAT1* and *UGT73C6* increased the expression of BR biosynthesis genes and decreased BES1 protein levels. (**A-C**) The relative expression levels of the BR marker genes of *CPD*, *ROT3* and *BR6OX2* in the Col-0 wild type, parental and double overexpression lines were measured. *GAPC2* was used as a reference. Opened flowers were used for analysis. The columns and bars indicate the average and SD of four to eight biological replicates. Different letters indicate significantly different values at $p < 0.05$ (one way ANOVA, Tukey post hoc test). (**D**) The phosphorylation status of BES1 in the wild type, parental and double overexpression lines. Opened flowers were used for analysis.

3.1.6 Response of *PMAT1* expression to BR-treatment and coregulation with *UGT73C6*

Several genes encoding BR catabolizing enzymes are induced by BR (Roh et al., 2012; Schneider et al., 2012; Wang et al., 2012; Choi et al., 2013; Zhu et al., 2013), which allows for BR signaling to increase their expression when BR levels become too high. To investigate whether *PMAT1* and/ or *At5MAT* are BR-regulated, 10-day-old wild type seedlings were treated with 24-epiBL for 24 hours

and transcript levels determined by qPCR. Expression of both genes was significantly increased by BR-treatment (**Figure 7** A, B). To test if the BR-induction requires BR signaling the analysis was repeated with the *bri1-1* mutant, which is a null allele of BRI1 in which BR signaling is severely compromised (Li and Chory, 1997). In *bri1-1* both genes were down-regulated constitutively and their expression was not responsive to external 24-epiBL (**Figure 7** A, B). Thus, in summary there is evidence that BR signaling positively regulates the expression of both *PMAT1* and *At5MAT.*
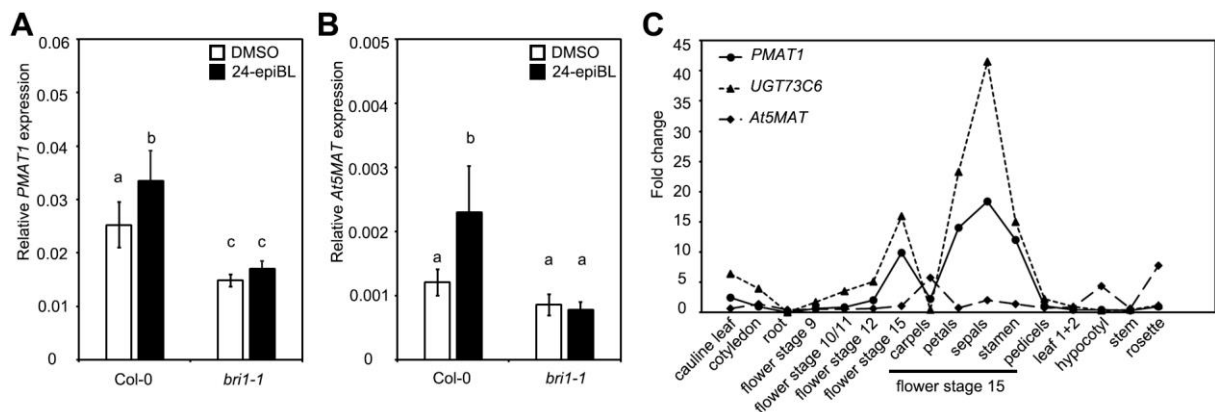
Figure 7: *PMAT1* is induced by BL and coregulates with *UGT73C6*. Impact of BR-treatment on *PMAT1* (**A**) and *At5MAT* (**B**) expression. Wild type (Col-0) and *bri1-1* plants were grown on 1/2 MS plates for 10 days and then transferred to liquid 1/2 MS medium supplemented with 1 µM 24-epiBL for 24 hours. Liquid 1/2 MS medium supplemented with DMSO was control. Expression of *GAPC2* was used for normalization. Values are means ± SD of four biological replicates. Different letters indicate significantly different values at p < 0.05 (one way ANOVA, Tukey post hoc test). (**C**) Coexpression analysis using public transcriptome data from TAIR.

Catabolizing enzymes that cooperate in the conversion of secondary metabolites and act in consecutive manners are often co-regulated. This is essential in particular in metabolite biosynthesis processes, where a first catabolizing step, often glucosylation, can produce a more reactive product that requires by a second modification, for example malonylation (D'Auria et al., 2007b; Heiling et al., 2010; Irmisch et al., 2018; Chen et al., 2020). To assess if expression of *UGT73C6* and *PMAT1* may be coordinately regulated, the publicly available transcriptome database of the University of Toronto at http://bar.utoronto.ca/efp/cgi-bin/efpWeb.cgi was consulted. This showed that *PMAT1* was the top co-expressed gene of *UGT73C6*, having a Pearson correlation coefficient (r = 0.76). In terms of developmental regulation *PMAT1* was mainly expressed in the sepals, petals and stamen of flower at stage 15, which highly overlaps with the expression pattern of *UGT73C6* (**Figure 7** C). *At5MAT* expression, in constitutive settings, is very

low in these tissues, an indication that PMAT1 is of higher relevance for the conversion of products of UGT73C6 activity.

3.2 PMAT1 catalyzes malonylation of scopolin *in planta*

3.2.1 PMAT1 and PMAT2 catalyze malonylation of scopolin *in vitro*

PMAT1 and its close homologue PMAT2 have previously been shown to be able to convert the coumarin scopolin, a secondary metabolite that is thought to be of relevance for defense reactions of plants (Stringlis et al., 2019) into its malonylated product (Taguchi et al., 2010). To expand the PMAT1 work into additional acceptor substance groups, scopolin was used as an acceptor and *in vitro* malonylation assays were carried out. All cloned malonyltransferases were included (**Figure 2** B), to compare activities among PMAT1 relatives. The results showed that whereas the other tested malonyltransferases displayed only marginal activity, both PMAT1 and PMAT2 were able to catalyze formation of malonylscopolin (**Figure 8** A, B). As compared to the control reaction, PMAT1 produced 3.3 nmol malonylscopolin per hour, and PMAT2 formed 0.7 nmol malonylscopolin per hour (**Figure 8** A, B).
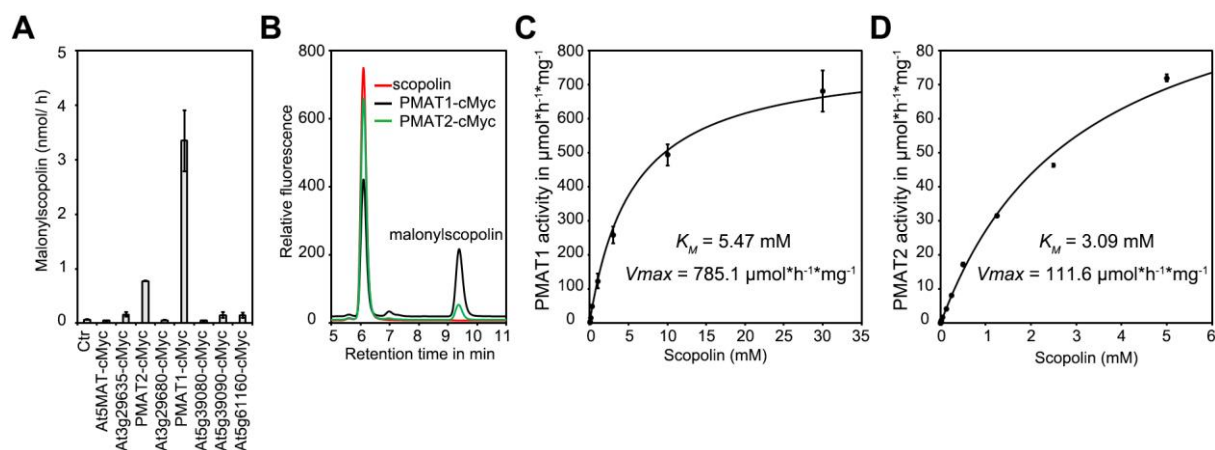
Figure 8: PMAT1 and PMAT2 showed malonyltransferase activities toward scopolin. (**A**) Eight malonyltransferases were incubated with scopolin and malonyl-CoA. At the end of the incubation, reaction products were subjected to HPLC analysis. Values are means ± SD of two biological replicates, each of which contains two technical replicates. (**B**) HPLC profiles obtained from reactions in (**A**). (**C**, **D**) Kinetics of PMAT1 (**C**) and PMAT2 (**D**) with scopolin as acceptor substrates. Plot according to the Michaelis-Menten equation is represented as solid lines. Values are means ± SE of three replicates.

To further characterize the enzymes catalytic properties *in vitro*, the coding region of PMAT1 and PMAT2 were fused with an N-terminal GST tag and purified from *E. coli* BL21 using GST-beads. Following optimization of the reaction conditions, enzyme kinetics were established and showed that the calculated *Km* value of PMAT1 on scopolin was approximately 5.5 mM, which is comparable to the *Km* of PMAT2 (3 mM). However, PMAT1 displayed a much higher specific catalytic velocity efficiency of approximately 785 μmol*h^{-1}*mg^{-1}, as compared to PMAT2 with a specific activity of approximately 111 μmol*h^{-1}*mg^{-1} (**Figure 8** C, D).

3.2.2 PMAT1 catalyzes scopolin malonylation *in planta*

Since both PMAT1 and PMAT2 could catalyze scopolin malonylation *in vitro*, it was decided to generate double mutants affected in the expression of both enzymes, for investigating their functions *in planta.* A *PMAT2* mutant was ordered from NASC (WiscDsLox508E02) with a predicted insertion at position 521 bp of the *PMAT2* open reading frame. In this line PMAT2 expression was not detectable (**Figure 9** A, B). It was named *pmat2-1*, since it is the first allele to be described. *pmat2-1* was crossed with *pmat1-2*, homozygous lines for both insertions were selected and RT-PCRs confirmed that the expression of both genes was below the detection limits in the *pmat1-2 pmat2-1* double mutant (**Figure 9** B). To complement the loss-of-function analyses, PMAT2 overexpression lines were generated. For this purpose, wild type Col-0 plants transformed with *35S:PMAT2* construct were generated. Homozygous lines from independent transgenic individuals were selected and transgene expression was determined by qPCRs (**Figure 9** C). No obvious phenotypic changes were observed under standard growing conditions in these overexpression lines.

To investigate if in plants with altered PMAT1 and/or PMAT2 abundance scopolin homeostasis was altered, scopolin and malonylscopolin quantities were determined in aerial tissues of 11-day-old seedlings of the knock-out lines by HPLC. This showed that whereas in the *pmat2-1* mutant similar amounts of malonylscopolin were detected like in wild type, *pmat1-2* was unable to form malonylated scopolin in the tissues assessed (**Figure 9** D). Correspondingly, also in the *pmat1-2 pmat2-1* double mutant malonylscopolin formation was defective (**Figure 9** D). While the

differences in malonylscopolin abundance were clear, the abundance of the substrate scopolin was not altered in neither of the analyzed lines (**Figure 9** D). In addition to the knockout lines, also the PMAT1 and PMAT2 overexpression lines were included in the analyses. This showed that malonylscopolin abundance was strongly increased by almost 10-fold and scopolin level was depleted by about 4-5 folds in the *PMAT1oe* and *PMAT2oe* lines (**Figure 9** D). Thus in summary, there is clear evidence that PMAT1 acts in the malonylation of scopolin and that this activity can reduce levels of scopolin in plants.
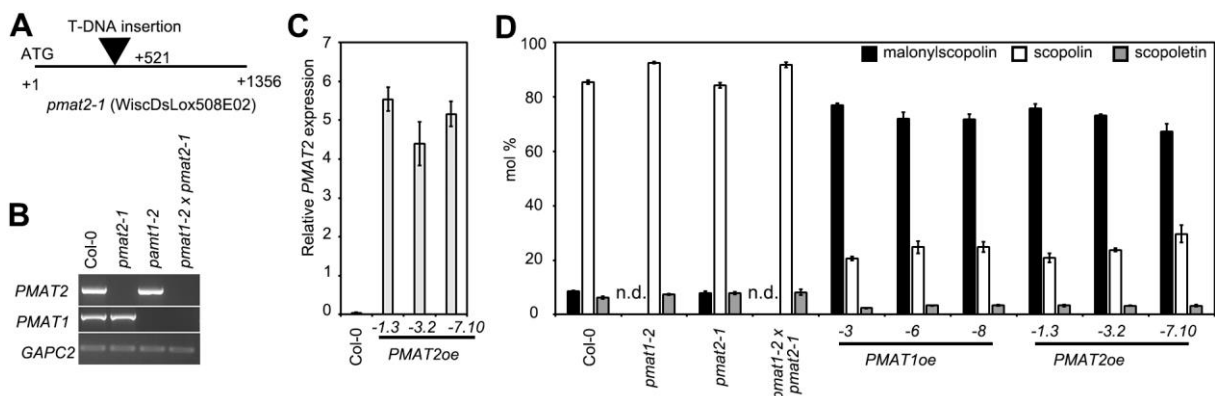
Figure 9: PMAT1 and PMAT2 can malonylate scopolin *in planta*. (**A**) Illustration of the T-DNA insertion in the *PMAT2* gene. The insertion position is marked by a triangle with the respective nucleotide number counted from the start codon. (**B**) *PMAT1* and *PMAT2* gene expressions in wild type (Col-0), single- and double insertion mutant were determined by RT-PCR analysis. Expression of *GAPC2* is shown as reference. (**C**) Expression levels of *PMAT2* in wild type and overexpression lines relative to *GAPC2*. (**D**) Levels of malonylscopolin, scopolin and scopoletin in wild type (Col-0), knock out mutants and overexpression lines as indicated. Plants were grown on 1/2 MS plates for 11 days under standard conditions. Approximately 100 mg aerial plant material was harvested, extracted and measured. Values are the means of five replicates ± SE; n.d., not detected.

3.2.3 *PMAT1* and *PMAT2* overexpression increases scopoletin tolerance

Scopoletin, the aglycon of scopolin, has phytotoxic activity in plants, which is well-documented for *A. thaliana* (Grana et al., 2017). To address whether altered scopolin malonylation capacities may impact the phytotoxic potential of scopoletin in plants, the *PMAT1* and *PMAT2* knock out and overexpression lines were plated on scopoletin-containing media and the effects on primary root elongation and over-all seedling development were evaluated. The root elongation of wild type seedlings was inhibited by scopoletin in a dose-dependent manner, with an inhibition of close to 50% for 5 µg/mL and close to 80% for 10 µg/mL scopoletin (**Figure 10** A , B). While the single and

double *pmat1* and *pmat2* mutants showed the same response like wild type, the overexpression lines were clearly resistant to scopoletin. In particular the *PMAT1oe* lines showed a high level of scopoletin tolerance, with essentially no repression of primary root elongation even at 10 µg/mL (**Figure 10** A, B) and a clearly reduced repression of over-all development at 30 µg/mL post germination as compared to all other lines (**Figure 10** C, D).
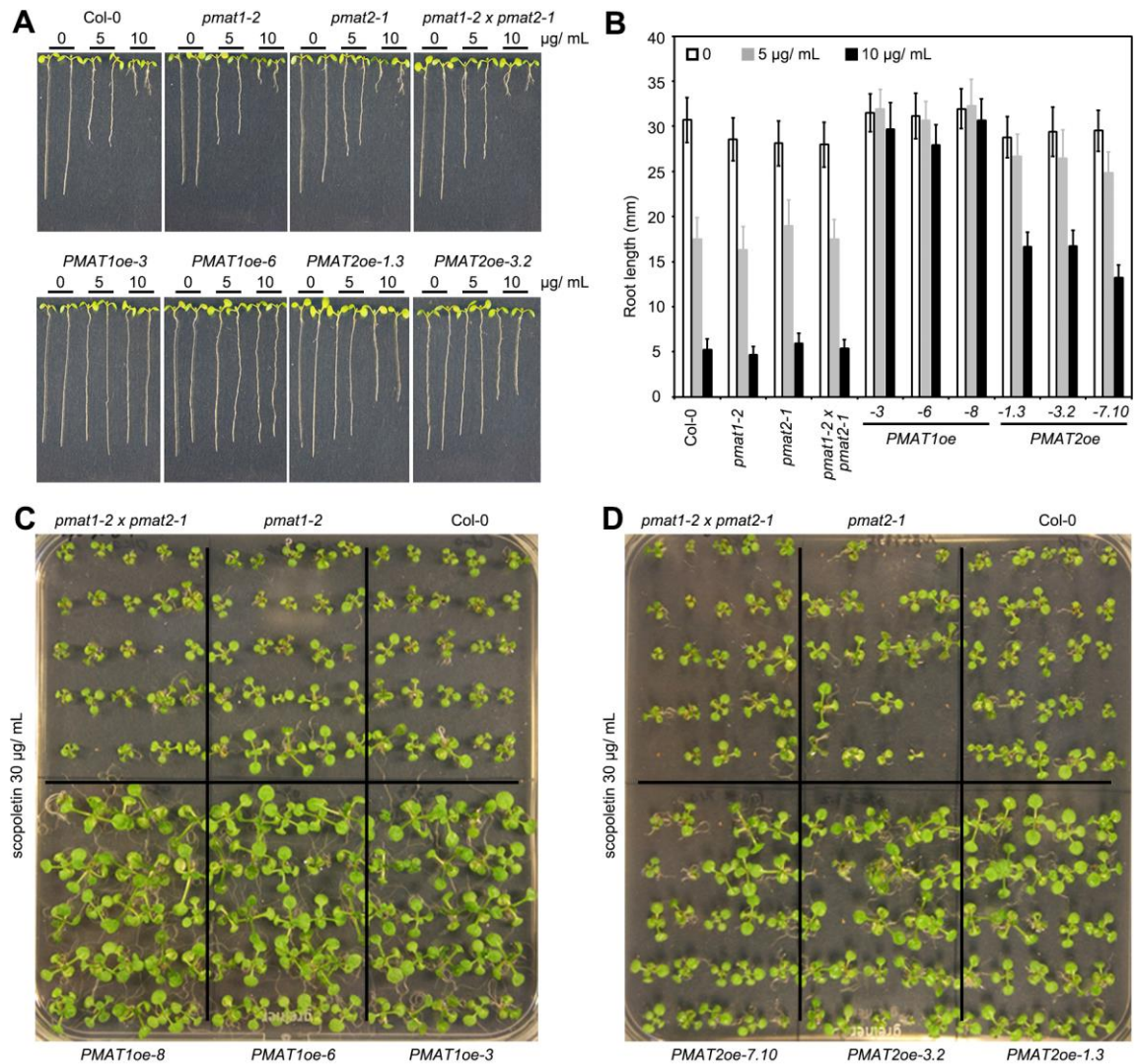
Figure 10: Effect of scopoletin on root elongation and growth of different *A. thaliana* genotypes. (**A**) Representative seedlings of Col-0 wild type, *pmat1-2* or *pmat2-1* single mutant, *pmat1-2 pmat2-1* double mutant, *PMAT1oe* and *PMAT2oe* lines. Plants were vertically grown on 1/2 MS medium for 7 d. Scopoletin concentrations were 5 or 10 µg/mL. Pure solvent (DMSO) was used as a control. (**B**) Quantification of the root length of the plants shown in (**A**). Values are means ± SD of at least 33 individuals. (**C**, **D**) Images of representative 12-day-old seedling of the indicated genotypes. Plants were grown on 1/2 MS medium containing scopoletin (30 µg/mL).

3.3 BIA1 inactivates CS by acylation

3.3.1 BIA1 acylates CS and CS variants

BIA1 is an acyltransferase that had previously been implicated in the control of BR homeostasis. However, its enzymatic activity had remained elusive. The BR profiles of the dominant *bia1-1D* mutant indicated that BIA1 might acylate BR intermediates, probably including the bioactive BR (Roh et al., 2012; Wang et al., 2012). To test this, BIA1 was expressed as GST-tagged fusion protein in *E. coli* BL21 and purified by affinity chromatography. As potential substrates CS and 24-epiBL were selected. As the most promising CoA-thioester, myristoyl-CoA was tested since all BR-acyl conjugates described so far contains lauric acid, myristic acid or palmitic acid as acyl components (Asakawa et al., 1994; Kolbe et al., 1995; Soeno et al., 2000; Schneider et al., 2012). In addition, acetyl-CoA, caffeoyl-CoA, coumaroyl-CoA and malonyl-CoA served as controls. Enzymatic reaction conditions were adapted from Schneider and collaborators, and the reaction products were extracted and analyzed by TLC (Augustin et al., 2012; Schneider et al., 2012). Surprisingly, a modified band was observed for the BIA1-catalyzed reaction of acetyl-CoA with CS, while no activity was seen for the other CoA donors (**Figure 11** A). For the reaction of 24-epiBL with acetyl-CoA, activity was observed albeit at a low level as indicated by the weak band of the product (**Figure 11** B). Analysis of the reaction products by HPLC-QTOF (carried out by Prof. Franz Berthiller, Universität für Bodenkultur, Vienna, Austria) revealed that for both reactions mainly the diacetylation products were obtained while only minor amounts of the monoacetylation products were detected (**Table 3**).

Table 3: Analysis of acetylation products of CS and CS variants by HPLC-QTOF (carried out by Prof. Franz Berthiller, Universität für Bodenkultur, Vienna, Austria).

	C-2 OH	C-3 OH	C-22 OH	C-23 OH	C-24 CH_3	Monoacetylation product (Area%)	Diacetylation product (Area%)
Castasterone (CS)	α	α	R	R	S	1.3	98.7
24-epibrassinolide (24-epiBL)	α	α	R	R	R	3.9	96.1
24-epicastasterone (24-epiCS)	α	α	R	R	R	8.5	91.5
6-deoxo-24-epicastasterone (6-oxo-24-epiCS)	α	α	R	R	R	3.8	96.2
tris-epicastasterone (tris-epiCS)	α	α	S	S	R	46.9	53.1
3,24-diepicastasterone (3,24-diepiCS)	α	β	R	R	R	100.0	0.0
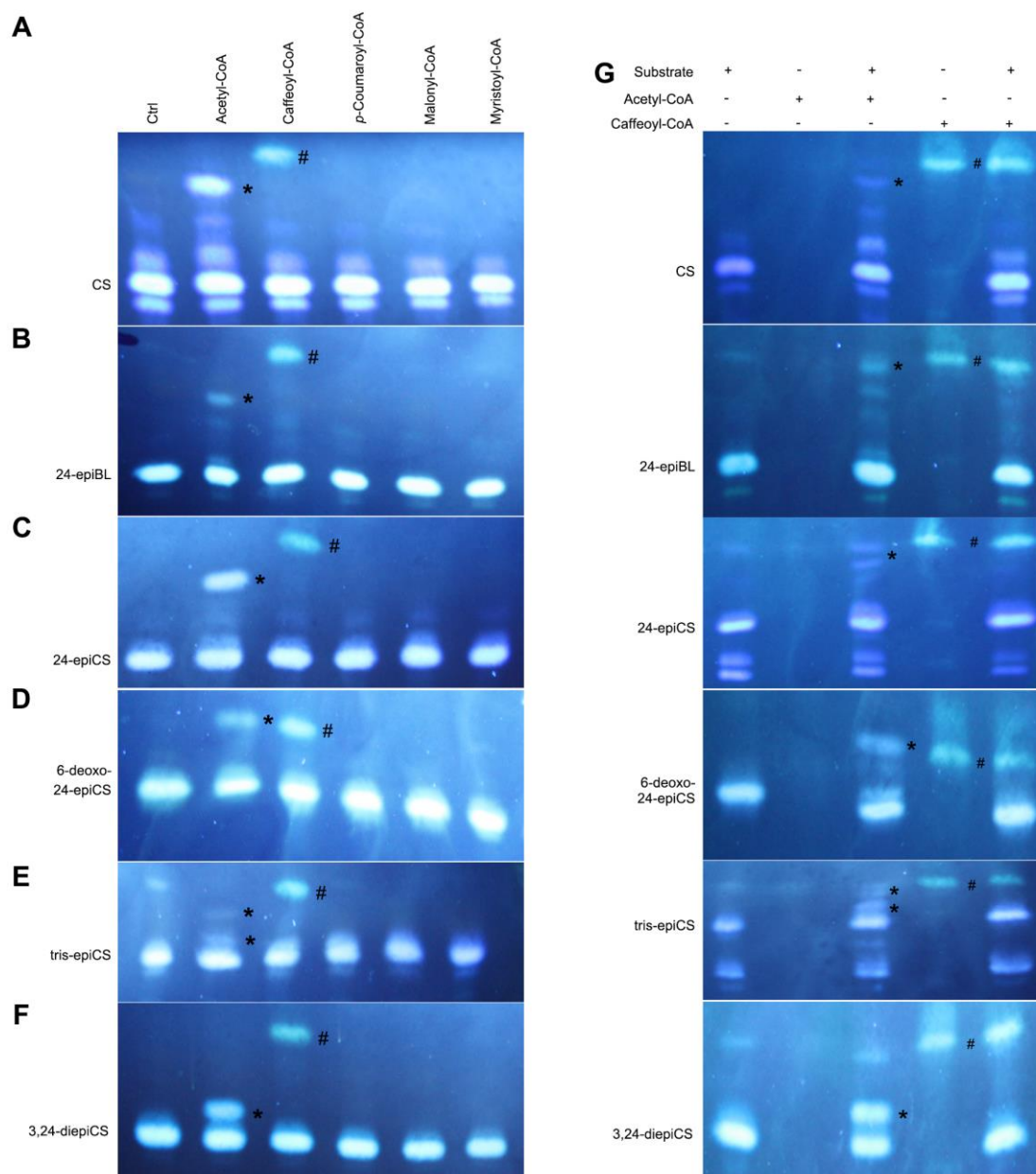
Figure 11: Activity of the purified BIA1 proteins toward CS variants. (**A-F**) Enzyme assays contained 3 µg of recombinant BIA1 in a total volume of 20 µL and 1 mM CS (**A**), 24-epiBL (**B**), 24-epiCS (**C**), 6-deoxo-24-epiCS (**D**), tris-epiCS (**E**), or 3,24-diepiCS (**F**) as acceptor substrates. Lane 1 was substrate control. 10 mM acetyl-CoA (lane 2), 2.5 mM caffeoyl-CoA (lane 3), 2.5 mM coumaroyl-CoA (lane 4), 2.5 mM malonyl-CoA (lane 5) or 2.5 mM myristoyl-CoA (lane 6) were added as donors. (**G**) Caffeoyl-CoA caused a fluorescent band indicated by hashes (lanes 4 and 5). In contrast, acetyl-CoA does not show autofluorescence (lanes 2 and 3). Positions of acetylation reaction products are indicated by asterisks (lane 3). The assays (**A-G**) were incubated at 25 °C for overnight. Samples were extracted and analyzed by TLC. Positions of reaction products are indicated by asterisks. Hashes indicates autofluorescence originating from caffeoyl-CoA.

To investigate the structural properties required for CS acetylation in more detail, the CS variants 24-epiCS, 6-deoxo-24-epiCS, tris-epiCS and 3,24-diepiCS were tested. BIA1 acetylated 24-epiCS efficiently (**Figure 11** C), indicating that the stereochemical pattern of C24 carrying a methyl group

is of minor importance. Similar to CS and 24-epiBL, mainly the diacetylation product was obtained (**Table 3**). A comparable result was also observed for 6-deoxo-24-epiCS (**Figure 11** D, **Table 3**), suggesting that the 6-oxo group is not required for BIA1 activity. When tris-epiCS was used as a substrate, two bands were observed by TLC analysis (**Figure 11** E), one fast migrating and a second slow migrating one. Analysis by HPLC-QTOF (carried out by Prof. Franz Berthiller, Universität für Bodenkultur, Vienna, Austria) revealed that similar amounts of mono and diacetylation products were obtained (**Table 3**). This suggests that the stereochemical properties of C22 and/or C23 carrying OH groups are critical for BIA1-mediated acetylation. Interestingly, for 3,24-diepiCS only a slow migrating band was observed by TLC analysis (**Figure 11** F), indicating that solely the monoacetylation product was formed. This assumption was fully confirmed by HPLC-QTOF analysis (carried out by Prof. Franz Berthiller, Universität für Bodenkultur, Vienna, Austria) (**Table 3**). A fluorescent band was also seen for all reactions when using caffeoyl-CoA as acyl donor. However, control reactions revealed that this band originates from caffeoyl-CoA itself and is not a conjugate (**Figure 11** G). Taken together, these data suggest that CS is mainly diacetylated by BIA1. One acetyl residue seems to be transferred to ring A, most likely to the hydroxy group on C-3, and the second acetyl moiety to the aliphatic side chain, either to the hydroxy group on C-22 or the one on C-23.

Recently, BIA2, a homolog of BIA1 sharing 37% identity at the amino acid level, was reported to induce strong BR-deficiency phenotypes when over-expressed in *A. thaliana* (Zhang and Xu, 2018). To investigate whether this putative BAHD acyltransferase may also acetylate CS and thus act redundantly to BIA1, the corresponding cDNA was cloned and a GST fusion protein produced by heterologous expression in *E. coli*. However, the obtained recombinant protein did not show any activities using different CS variants and 24-epiBL as substrates and acetyl, malonyl, caffeoyl, coumaroyl and myristoyl-CoA as co-substrates (**Figure 12**). These data suggest that either the purified recombinant protein was not active or BIA1 doesn't have acylation activity.
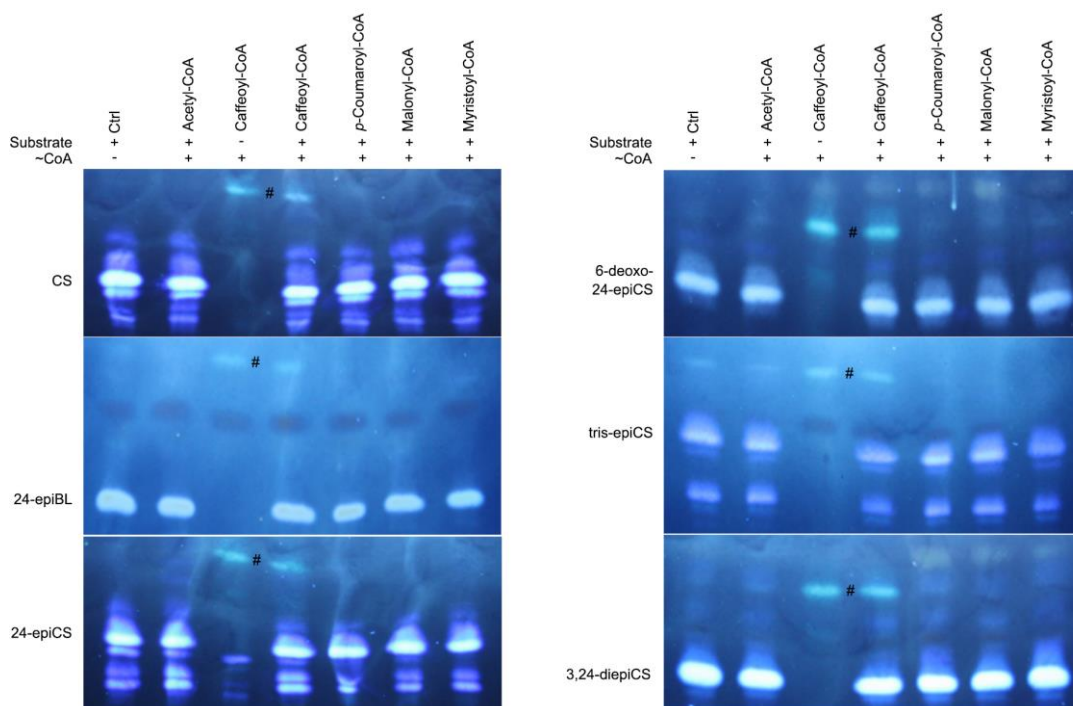
Figure 12: Activity of purified BIA2 proteins toward CS variants. Enzyme assays contained recombinant BIA2 and 1 mM CS, 24-epiBL, 24-epiCS, 6-deoxo-24-epiCS, tris-epiCS, or 3,24-diepiCS as acceptor substrates. In both panels, lane 1 was substrate control. 10 mM acetyl-CoA (lane 2), 2.5 mM caffeoyl-CoA (lane 4), 2.5 mM coumaroyl-CoA (lane 5), 2.5 mM malonyl-CoA (lane 6) or 2.5 mM myristoyl-CoA (lane 7) as donor, lane 3 was caffeoyl-CoA control. Hashes indicates autofluorescence originating from caffeoyl-CoA.

3.3.2 Enzymatic properties of BIA1

To investigate the enzymatic properties of recombinant BIA1 in more detail, the enzymatic activity was tested in different conditions. First the impact of the pH on BIA1 activity was analyzed using a pH range of 6.5 to 10 (**Figure 13** A). BIA1 had higher activity in a slight alkaline environment with an optimum at pH 9. Below pH 7 hardly any activity was observed. Then the liner range for the reaction time was determined, which was seen during the first 8 hours (**Figure 13** B). Next the impact of the reaction temperature on BIA1 activity was explored, testing a temperature range from 10 to 50 °C. This showed that BIA1 activity increased when the temperature was increased from 10 to 40 °C (**Figure 13** C), reaching a peak at 40 °C and then decreasing again. Using the established conditions (25 mM diethanolamine/phosphate buffer pH 9.0, 30 °C reaction temperature and 1 h reaction time), an enzyme kinetic was measured. The reaction product $CSAc_2$ was derivatized with dansylhydrazine to allow quantification of low CS concentrations by HPLC with fluorescence detection (Winter et al., 1999). The results gave a *Km* value for BIA1 on CS of

approximately 25 µM and a maximal reaction velocity *Vmax* of 1.3 µmol*h^{-1}*mg^{-1} (**Figure 13** D). Thus, BIA1 shows high affinity for CS.
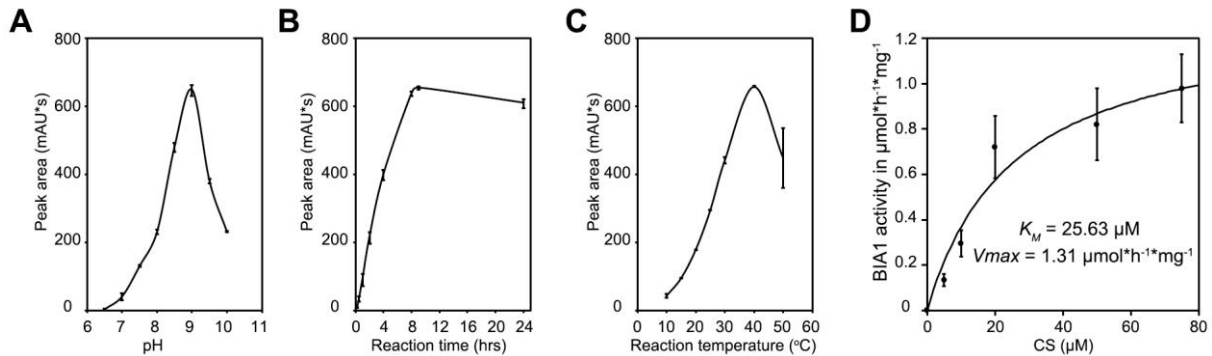
Figure 13: Catalytic properties of BIA1. (**A**) pH. (**B**) Reaction time. (**C**) Temperature, (**D**) Plot according to the Michaelis-Menten equation is represented as solid lines. Values are mean ± SE of two (**A**, **C**) or three (**B**, **D**) replicates.

3.3.3 BIA1 acetylates CS *in planta*

To determine if acylCS and diacylCS are formed also *in planta* and assess if BIA1 is required, the *bia1-3* T-DNA insertional mutant was obtained and characterized. Sequencing revealed that the T-DNA is integrated 49 bp up-stream of the STOP codon and qPCR analysis showed that the transcript abundance in the mutant was reduced to approximately 15% of wild type (**Figure 14** A). In addition, wild type Col-0 plants transformed with *35S::BIA1:YFP* construct had previously been generated in the Poppenberger lab and were obtained in the T2 generation to be included. The strongest symptoms of BR-deficiency were seen in line #4.2 (**Figure 14** B), which also formed most BIA1-YFP protein (**Figure 14** B). BR metabolites are difficult to detect due to their low abundance under normal conditions. However, several studies have shown that novel BRs metabolites can be increased to detectable amounts by externally supplying BRs (Kolbe et al., 1995; Kolbe et al., 1996; Neff et al., 1999; Husar et al., 2011). Thus a feeding experiment was conducted by using wild type seedling, the *bia1-3* knock-out line, dominant *bia1-1D* mutant and the *35S::BIA1-YFP#4.2* overexpression line. For this purpose, seedlings were transferred to 30 mL liquid medium containing CS at a final concentration of 1 µg/mL and incubated for 24 hours. Samples were extracted with methanol and analyzed by HPLC-QTOF (carried out by Prof. Franz Berthiller, Universität für Bodenkultur, Vienna, Austria).
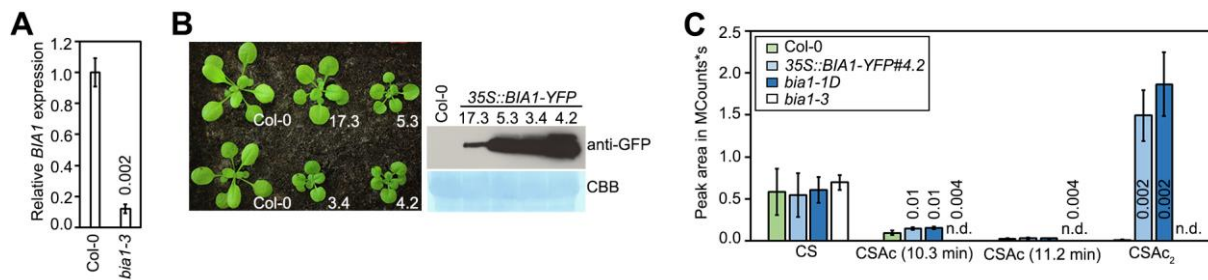
Figure 14: BIA1 acetylates CS *in vivo*. (**A**) *BIA1* transcript levels in wild type plants and the *bia1-3* knock out line. Data were normalized to *GAPC2*. (**B**) Phenotypes of wild type and *BIA1* overexpression plants (left panel). Expression of the transgene was confirmed by Western blot analysis (right panel). (**C**) HPLC-QTOF metabolite analysis of 12 days old *A. thaliana* seedlings. The columns and bars represent the average and SD of three to four biological replicates; n.d., not detected. Numbers are P-values of a two sided t-test with heteroscedastic variance for difference to wild type. Only significant (<0.05) values are shown. Measurement in (**C**) was performed by Prof. Franz Berthiller, Universität für Bodenkultur, Vienna, Austria.

In all samples, unmodified CS was detected at similar levels (**Figure 14** C), which is not surprising given that CS was added in large excess. More interestingly, a metabolite with a mass corresponding to $CSAc_2$ was detected in wild type, *bia1-1D* and *35S::BIA1-YFP*#4.2 plants. This metabolite was 100-times more abundant in *bia1-1D* and *35S::BIA1-YFP*#4.2 plants than in wild type (**Figure 14** C). However, it was undetectable in the *bia1-3* knock out mutants. In addition, peaks with a mass corresponding to monoacetylated CS were detected. Both peaks were present in wild type, *bia1-1D* and *35S::BIA1-YFP*#4.2 plants but absent in the *bia1-3* mutant. These results confirm that CS is acetylated in *A. thaliana* seedlings by BIA1.

4 Discussion

Malonylation, the addition of a malonyl group from malonyl-CoA to the glucosyl moiety of glycosides, is a common modification of plant metabolites. It participates in the detoxification of xenobiotics and re-localization of secondary metabolites to specific cellular compartments. In plants, these functions are largely achieved by BAHD acyltransferases (D'Auria, 2006; Bontpart et al., 2015). Although these enzymes have been studies for a long time, to date only a small number of them have been characterized. By combining phylogenetic analysis of the BAHD acyltransferases and assays of *in vitro* enzymatic activities of eight candidates which sorted into one clade, PMAT1 and At5MAT were identified to catalyze formation of 24-epiBL-23MalGlc, while PMAT1 and PMAT2 were shown to catalyze malonylation of scopolin. In contrast to these enzymes, other members of this clade did not show activities against the two substrates under the tested conditions. Previously, PMAT1 has been implicated in the modification of phenolic glucosides and *N*-lauroylethanolamine glucoside (Taguchi et al., 2010; Khan et al., 2016). Similar to PMAT1, PMAT2 has been shown to exhibit a broad substrate specificity *in vitro* (Taguchi et al., 2010). In contrast, At5MAT showed strong activity towards anthocyanin glucosides (D'Auria et al., 2007b; Luo et al., 2007). It seems that these acyltransferases have specificity for certain acyl-acceptor substrates even though they group into the same clade. This differences in substrate specificities suggests that although acyltransferase sequences can give indications of enzymatic activities, experimental validation is required.

To investigate the biological function of the selected BAHD acyltransferases in more detail, *in planta* studies were performed. The results of feeding experiment with BL revealed that BL-23MalGlc was not detected in seedlings of either *pmat1* mutants or *pmat1 at5mat* double mutants. However, *at5mat* mutants had comparable BL-23MalGlc as wild type. Moreover, the depletion of BL-23MalGlc in either *pmat1* mutants or *pmat1 at5mat* double mutants was accompanied by an increase in the amount of the acceptor substrate BL-23Glc. These results indicate that in seedling tissues PMAT1 is the main enzyme required for catalyzing malonylation of BL-23Glc. This is also supported by the observations that *in vitro* PMAT1 had much higher catalytic activity than At5MAT and that *PMAT1* was more strongly expressed in seedling tissues as compared with *At5MAT*. However, both *At5MAT* and *PMAT1* overexpression lines had comparable levels of BL-23Glc and BL-23MalGlc as wild type plants, indicating that the availability of the BL-23Glc substrate produced by UGT73C5 and

UGT73C6 is a limiting factor. Genetic combination experiments with *UGT73C6oe* also confirmed that PMAT1 but not At5MAT could enhance BR deficiency in a background that hyper-accumulates BR-Glc. Co-expression analysis using publicly available transcriptome data, provided indications that *PMAT1* expression may be co-regulated with *UGT73C6*, suggesting that the capability of PMAT1 to malonylate glucosylated substrates might be dependent on the function of UGT73C6 and/or redundantly acting UGTs. This is supported by the fact that PMAT1 overexpression effects in terms of increased BR inactivation can only be seen in the *UGT73C6oe* background. The observation that the phenotypes of *PMAT1oe-8 x UGT73C6:YFP-30* double transgenic lines are intensified as compared to their parental lines indicates that malonylation might prevent a re-activation of BR glucosides and this will require verification.

The *in planta* studies also expand our knowledge of the functions of PMAT1 in scopolin malonylation. In seedlings, a knock-out of *PMAT1* yielded an absence of malonylscopolin. In contrast, overexpression of *PMAT1* dramatically increased the levels of malonylscopolin. These data indicate that PMAT1 catalyzes malonylscopolin biosynthesis *in planta*. Also *PMAT2* overexpression plants accumulated higher levels of malonylscopolin. However, *pmat2* mutants had comparable concentration of malonylscopolin as wild type plants, suggesting that PMAT1 can complement for a loss of PMAT2 function in seedlings, but not vice versa. This may be due to an absence of *PMAT2* expression in seedling tissues, which would need to be tested.

Scopoletin, the aglycone of scopolin, is a compound with a strong phytotoxic potential (Tal and Robeson, 1986). For instance, Andreae found that high concentrations of scopoletin suppressed root growth of potato plants (Andreae, 1952). This was verified by Grana and co-authors who discovered that scopoletin also compromised root development of *A. thaliana* (Grana et al., 2017). Moreover, scopoletin treatment caused growth retardation in tobacco and sunflower (Einhellig and Kuan, 1971). The phytotoxic effects of scopoletin including retardation of root elongation and seedling growth inhibition were also seen in this thesis. *pamt1* mutant displayed comparable inhibition phenotypes as wild type when grown on scopoletin containing media, indicating that a lack of scopolin malonylation might not be a key process in scopoletin detoxification. However, *PMAT1oe* and *PMAT2oe* plants clearly showed less repression of growth, suggesting that the phytotoxic potential created by scopoletin is alleviated in these overexpression plants. It is possible

that scopoletin is taken up and converted to scopolin for detoxification. Since in this work it is shown that increasing scopolin malonylation through PMAT1 or PMAT2 overexpression causes depletion of scopolin, an increased flux through the scopoletin detoxification pathway may allow for resistance against the phytotoxin.

Scopoletin was shown to possess antifungal activity *in vitro* and *in vivo* and its levels were reported to increase in *Nicotiana attenuata* after *Alternaria alternata* infection (Sun et al., 2014; Li and Wu, 2016). Under normal growth conditions scopolin is stored in the vacuole. However, in response to pathogen exposure, it is rapidly released into the cytosol and hydrolyzed by β-glucosidases to free the bioactive aglycone scopoletin (Ahn et al., 2010). Malonylscopolin might be a storage form of scopolin, since plants need to release their defense compounds rapidly when they encounter pathogens (Valle et al., 1997; Chong et al., 2002; Gachon et al., 2004; Carpinella et al., 2005; Stringlis et al., 2019). Further research efforts are needed to clarify the contribution of malonylscopolin to biotic stress resistance and plant-microbe interactions in a more general sense. In this context it is interesting that plant roots excrete coumarins, such as scopoletin, fraxetin and sideretin to facilitate iron uptake from soil (Schmid et al., 2014; Rajniak et al., 2018; Siwinska et al., 2018; Tsai et al., 2018; Grillet and Schmidt, 2019; Schmidt, 2019) and thereby affect the composition of the root microbiome (Stringlis et al., 2018; Voges et al., 2019). The importance of PMAT1-mediated conversion of scopolin to malonylscopolin for these processes is unclear, but it would be interesting to address, if malonylscopolin can also participate in iron uptake and may thereby impact plant-microbe interactions.

PMAT1 has a rather broad specificity for its acyl acceptor. It has been reported to catalyze the malonylation of xenobiotic substrates such as naphthol glucoside, kaempferol 7-*O*-glucoside, kaempferol 3-*O*-glucoside, hydroxycoumarin glucosides, phenol-glucosides and isoflavone glucoside (Taguchi et al., 2010) as well as *N*-lauroylethanolamine glucoside (Khan et al., 2016). In this thesis, BR-Glc and scopolin are added as two novel acceptors. Since PMAT1 substrates do not share a common core structures, it appears that it is the glucosyl moiety, only that is decisive. Since conjugation of substrates with malonic acid introduces a negative charge, the malonylation of these substrates could facilitate their transport into the vacuole by transporters. For instance, malonylated 1-aminocyclopropane-1-carboxylic acid can be translocated between the cytosol and

the vacuole by tonoplast carriers (Bouzayen et al., 1989). Likewise in parsley cells, flavonoid glycosides are synthesized in the cytoplasm, but their malonylated forms are exclusively located to the vacuoles and transport to this cell organelle depends on the malonylglucose moiety (Matern et al., 1983; Matern et al., 1986). Thus, it is tempting to speculated that BR-MalGlc and malonylscopolin are preferentially stored in the vacuoles, a hypothesis that needs to be addressed in future studies.

For plant secondary metabolites, multiple studies have shown that the malonyl group is typically transferred to the hydroxy group on the *O*-6 position of the glucosyl moiety. For instance, Ss5MaT1 catalyzes the transfer of the malonyl group from malonyl-CoA to the 6'-hydroxyl group of the glucosyl moiety of anthocyanin (Suzuki et al., 2001). Malonic acid is also conjugated at the 6'-hydroxyl group of the glucosyl moiety of *N*-lauroylethanolamine glucoside molecule (Khan et al., 2016). In addition to *O*-6 modification, also other malonylation patterns have been described. Ss5MaT2 transfers the malonyl group to the 4'-hydroxyl group on the sugar of anthocyanin (Suzuki et al., 2004b). Dm3MaT2 catalyzes the consecutive dimalonylation of anthocyanidin 3-*O*-glucoside producing anthocyanidin 3-*O*-3'',6''-*O*-dimalonylglucoside (Suzuki et al., 2004a). Unfortunately, due to the extremely low abundance of BL-23MalGlc and malonylscopolin in plants, it is highly challenging to purify sufficient amounts of the products to determine the exact malonyl group position and the precise structures.

Acylation has been suggested to regulate hormone homeostasis. Acyltransferases such as BIA1, BIA2 and PIZ have been proposed to inactivate BRs through acylation. BIA1 was first identified in mutant screens (Roh et al., 2012; Wang et al., 2012). The dominant, activation-tagged *bia1-1D* and *bia1-2D* mutants showed severe BR-deficient phenotypes, which could be rescued by BR, had significantly reduced amounts of several BRs, including 6-deoxoCS and CS and displayed molecular signatures indicative of BR depletion. In this thesis, the enzymatic activity of BIA1 against CS and CS variants with acetyl-CoA, caffeoyl-CoA, coumaroyl-CoA, malonyl-CoA and myristoyl-CoA as donors was analyzed *in vitro*. Surprisingly, novel conjugates were obtained with acetyl-CoA, while none were formed with the other CoA donors. In comparison, PIZ modified BRs with lauroyl-CoA but not with acetyl-CoA (Schneider et al., 2012), suggesting a donor length preference of the fatty acid chain between the two enzymes. Although BIA1 and PIZ share the HxxxD substrate

binding motif, it is to be expected that other amino acid residues also contribute to the donor binding specificities. In regard to acceptor substrates, BIA1 effectively acylated CS, 24-epiBL, 24-epiCS and 6-deoxo-24-epiCS and mainly the diacetylation products were obtained. When tris-epiCS was used as a substrate, similar amounts of mono and diacetylation products were produced. For 3,24-diepiCS as substrate, solely the monoacetylation product was formed. These data suggest that a methyl group at C-24 and the 6-oxo group of the CS variants do not interfere with the reactions catalyzed by BIA1 and that CS is mainly diacetylated. One acetyl residue seems to be transferred to ring A, most likely to the hydroxy group on C-3, and the second acetyl moiety to the aliphatic side chain, either to the hydroxy group on C-22 or the one on C-23. Since mono- and diacetylated versions of CS were undetectable in BIA1 knock-out plants and were increased in BIA1 over-expressors, there is conclusive evidence now, that BIA1 modifies CS by acylation and, combined with the results of previous studies, that this is an inactivation reaction.

Structure-activity relationship study have revealed that the cis α-oriented hydroxyl groups at C-2 and C-3, and cis hydroxy groups at C-22 and C-23 are required for high activity (Thompson et al., 1982). Accordingly, it has been shown that the C-22 and C-23 hydroxy groups of BL are crucial for interaction with the receptor kinase BRI1, while the C-2 and C-3 hydroxy groups are involved in interaction with the co-receptor BAK1 (Hothorn et al., 2011; She et al., 2011). The fact that the phenotypes of the *bia1-1D* and *bia1-2D* mutants resemble strong *bri1-1* receptor mutants (Li and Chory, 1997), suggests that acetate groups substitution on CS directly decreases its biological activity in plants. Hydroxyl group substitutions are one of the key features of BR catabolism, and clearly affects their biological activities (Zhao and Li, 2012). Hydroxyl groups at C-2, C-3 and C-23 can also be modified by glucosylation, the C-22 group by conjugation with sulfate and probably the C-3 hydroxy acylated conjugation with long chain fatty acids (Poppenberger et al., 2005; Marsolais et al., 2007; Husar et al., 2011; Schneider et al., 2012). How these modifications cooperate or antagonize each other to fine-tune BRs homeostasis at the cellular level and in accordance with developmental and environmental demands are important questions to be addressed in the future.

References

Aharoni, A., Keizer, L.C., Bouwmeester, H.J., Sun, Z., Alvarez-Huerta, M., Verhoeven, H.A., Blaas, J., van Houwelingen, A.M., De Vos, R.C., van der Voet, H., Jansen, R.C., Guis, M., Mol, J., Davis, R.W., Schena, M., van Tunen, A.J., and O'Connell, A.P. (2000). Identification of the *SAAT* gene involved in strawberry flavor biogenesis by use of DNA microarrays. Plant Cell **12**, 647-661.

Ahn, Y.O., Shimizu, B., Sakata, K., Gantulga, D., Zhou, C., Bevan, D.R., and Esen, A. (2010). Scopolin-hydrolyzing beta-glucosidases in roots of Arabidopsis. Plant Cell Physiol **51**, 132-143.

Andreae, W.A. (1952). Effect of Scopoletin on Indoleacetic Acid Metabolism. Nature **170**, 83-84.

Anne, P., Azzopardi, M., Gissot, L., Beaubiat, S., Hematy, K., and Palauqui, J.C. (2015). OCTOPUS negatively regulates BIN2 to control phloem differentiation in *Arabidopsis thaliana*. Curr Biol **25**, 2584-2590.

Asakawa, S., Abe, H., Kyokawa, Y., Nakamura, S., and Natsume, M. (1994). Teasterone 3-Myristate: A New Type of Brassinosteroid Derivative in *Lilium longiflorum* Anthers. Biosci Biotechnol Biochem **58**, 219-220.

Asakawa, S., Abe, H., Nishikawa, N., Natsume, M., and Koshioka, M. (1996). Purification and identification of new acyl-conjugated teasterones in lily pollen. Biosci Biotech Bioch **60**, 1416-1420.

Augustin, J.M., Drok, S., Shinoda, T., Sanmiya, K., Nielsen, J.K., Khakimov, B., Olsen, C.E., Hansen, E.H., Kuzina, V., Ekstrom, C.T., Hauser, T., and Bak, S. (2012). UDP-Glycosyltransferases from the UGT73C Subfamily in *Barbarea vulgaris* Catalyze Sapogenin 3-*O*-Glucosylation in Saponin-Mediated Insect Resistance. Plant Physiology **160**, 1881-1895.

Bai, M.Y., Fan, M., Oh, E., and Wang, Z.Y. (2012). A triple helix-loop-helix/basic helix-loop-helix cascade controls cell elongation downstream of multiple hormonal and environmental signaling pathways in Arabidopsis. Plant Cell **24**, 4917-4929.

Bajguz, A. (2011). Brassinosteroids–occurence and chemical structures in plants. In Brassinosteroids: a class of plant hormone (Springer), pp. 1-27.

Balasundram, N., Sundram, K., and Samman, S. (2006). Phenolic compounds in plants and agri-industrial by-products: Antioxidant activity, occurrence, and potential uses. Food Chemistry **99**, 191-203.

Bancos, S., Nomura, T., Sato, T., Molnar, G., Bishop, G.J., Koncz, C., Yokota, T., Nagy, F., and Szekeres, M. (2002). Regulation of transcript levels of the Arabidopsis cytochrome P450 genes involved in brassinosteroid biosynthesis. Plant Physiology **130**, 504-513.

Beekwilder, J., Alvarez-Huerta, M., Neef, E., Verstappen, F.W., Bouwmeester, H.J., and Aharoni, A. (2004). Functional characterization of enzymes forming volatile esters from strawberry and banana. Plant Physiology **135**, 1865-1878.

Bernardo-Garcia, S., de Lucas, M., Martinez, C., Espinosa-Ruiz, A., Daviere, J.M., and Prat, S. (2014). BR-dependent phosphorylation modulates PIF4 transcriptional activity and shapes diurnal hypocotyl growth. Genes Dev **28**, 1681-1694.

Bertolucci, S.K., Pereira, A.B., Pinto, J.E., Oliveira, A.B., and Braga, F.C. (2013). Seasonal variation on the contents of coumarin and kaurane-type diterpenes in *Mikania laevigata* and *M. glomerata* leaves under different shade levels. Chemistry & Biodiversity **10**, 288-295.

Bishop, G.J. (2007). Refining the plant steroid hormone biosynthesis pathway. Trends Plant Sci **12**, 377-380.

Bishop, G.J., Nomura, T., Yokota, T., Harrison, K., Noguchi, T., Fujioka, S., Takatsuto, S., Jones, J.D.G., and Kamiya, Y. (1999). The tomato DWARF enzyme catalyses C-6 oxidation in brassinosteroid biosynthesis. P Natl Acad Sci USA **96**, 1761-1766.

Bontpart, T., Cheynier, V., Ageorges, A., and Terrier, N. (2015). BAHD or SCPL acyltransferase? What a dilemma for acylation in the world of plant phenolic compounds. New Phytologist **208**, 695-707.

Bourgaud, F., Gravot, A., Milesi, S., and Gontier, E. (2001). Production of plant secondary metabolites: a historical perspective. Plant Sci **161,** 839-851.

Bouzayen, M., Latche, A., Pech, J.C., and Marigo, G. (1989). Carrier-Mediated Uptake of 1-(Malonylamino)cyclopropane-1-Carboxylic Acid in Vacuoles Isolated from Catharanthus roseus Cells. Plant Physiol **91,** 1317-1322.

Bravo, L. (1998). Polyphenols: Chemistry, dietary sources, metabolism, and nutritional significance. Nutr Rev **56,** 317-333.

Cano-Delgado, A., Yin, Y., Yu, C., Vafeados, D., Mora-Garcia, S., Cheng, J.C., Nam, K.H., Li, J., and Chory, J. (2004). BRL1 and BRL3 are novel brassinosteroid receptors that function in vascular differentiation in *Arabidopsis*. Development **131,** 5341-5351.

Carpinella, M.C., Ferrayoli, C.G., and Palacios, S.M. (2005). Antifungal synergistic effect of scopoletin, a hydroxycoumarin isolated from *Melia azedarach* L. fruits. J Agr Food Chem **53,** 2922-2927.

Chen, J., Hu, X., Shi, T., Yin, H., Sun, D., Hao, Y., Xia, X., Luo, J., Fernie, A.R., He, Z., and Chen, W. (2020). Metabolite-based genome-wide association study enables dissection of the flavonoid decoration pathway of wheat kernels. Plant Biotechnol J.

Chen, L.G., Gao, Z., Zhao, Z., Liu, X., Li, Y., Zhang, Y., Liu, X., Sun, Y., and Tang, W. (2019a). BZR1 family transcription factors function redundantly and indispensably in br signaling but exhibit BRI1-independent function in regulating anther development in *Arabidopsis*. Mol Plant **12,** 1408-1415.

Chen, W.Y., Lv, M.H., Wang, Y.Z., Wang, P.A., Cui, Y.W., Li, M.Z., Wang, R.A., Gou, X.P., and Li, J. (2019b). BES1 is activated by EMS1-TPD1-SERK1/2-mediated signaling to control tapetum development in *Arabidopsis thaliana*. Nat Commun **10.**

Choe, S., Dilkes, B.P., Gregory, B.D., Ross, A.S., Yuan, H., Noguchi, T., Fujioka, S., Takatsuto, S., Tanaka, A., Yoshida, S., Tax, F.E., and Feldmann, K.A. (1999). The Arabidopsis *dwarf1* mutant is defective in the conversion of 24-methylenecholesterol to campesterol in brassinosteroid biosynthesis. Plant Physiology **119,** 897-907.

Choe, S.W., Dilkes, B.P., Fujioka, S., Takatsuto, S., Sakurai, A., and Feldmann, K.A. (1998). The *DWF4* gene of Arabidopsis encodes a cytochrome P450 that mediates multiple 22α-hydroxylation steps in brassinosteroid biosynthesis. Plant Cell **10,** 231-243.

Choi, S., Cho, Y.H., Kim, K., Matsui, M., Son, S.H., Kim, S.K., Fujioka, S., and Hwang, I. (2013). BAT1, a putative acyltransferase, modulates brassinosteroid levels in Arabidopsis. Plant Journal **73,** 380-391.

Chong, J., Baltz, R., Schmitt, C., Beffa, R., Fritig, B., and Saindrenan, P. (2002). Downregulation of a pathogen-responsive tobacco UDP-Glc:phenylpropanoid glucosyltransferase reduces scopoletin glucoside accumulation, enhances oxidative stress, and weakens virus resistance. Plant Cell **14,** 1093-1107.

Clouse, S.D. (2011a). Brassinosteroid signal transduction: from receptor kinase activation to transcriptional networks regulating plant development. Plant Cell **23,** 1219-1230.

Clouse, S.D. (2011b). Brassinosteroids. The Arabidopsis Book **9.**

Clouse, S.D., Langford, M., and McMorris, T.C. (1996). A brassinosteroid-insensitive mutant in *Arabidopsis thaliana* exhibits multiple defects in growth and development. Plant Physiology **111,** 671-678.

Clouse, S.D., Hall, A.F., Langford, M., Mcmorris, T.C., and Baker, M.E. (1993). Physiological and molecular effects of brassinosteroids on *Arabidopsis thaliana*. J Plant Growth Regul **12,** 61-66.

D'Auria, J.C. (2006). Acyltransferases in plants: a good time to be BAHD. Curr Opin Plant Biol **9,** 331-340.

D'Auria, J.C., Pichersky, E., Schaub, A., Hansel, A., and Gershenzon, J. (2007a). Characterization of a BAHD acyltransferase responsible for producing the green leaf volatile (*Z*)-3-hexen-1-yl acetate in *Arabidopsis thaliana*. Plant Journal **49,** 194-207.

D'Auria, J.C., Reichelt, M., Luck, K., Svatos, A., and Gershenzon, J. (2007b). Identification and characterization of the BAHD acyltransferase malonyl CoA: anthocyanidin 5-*O*-glucoside-6''-*O*-malonyltransferase (At5MAT) in *Arabidopsis thaliana*. FEBS letters **581,** 872-878.

Dudareva, N., Pichersky, E., and Gershenzon, J. (2004). Biochemistry of plant volatiles. Plant Physiology **135,** 1893-1902.

Dudareva, N., D'Auria, J.C., Nam, K.H., Raguso, R.A., and Pichersky, E. (1998). Acetyl-CoA:benzylalcohol acetyltransferase-an enzyme involved in floral scent production in *Clarkia breweri*. Plant Journal **14,** 297-304.

Einhellig, F.A., and Kuan, L.-Y. (1971). Effects of Scopoletin and Chlorogenic Acid on Stomatal Aperture in Tobacco and Sunflower. Bulletin of the Torrey Botanical Club **98,** 155-162.

Fan, M., Bai, M.Y., Kim, J.G., Wang, T., Oh, E., Chen, L., Park, C.H., Son, S.H., Kim, S.K., Mudgett, M.B., and Wang, Z.Y. (2014). The bHLH transcription factor HBI1 mediates the trade-off between growth and pathogen-associated molecular pattern-triggered immunity in Arabidopsis. Plant Cell **26,** 828-841.

Fraser, C.M., Thompson, M.G., Shirley, A.M., Ralph, J., Schoenherr, J.A., Sinlapadech, T., Hall, M.C., and Chapple, C. (2007). Related Arabidopsis serine carboxypeptidase-like sinapoylglucose acyltransferases display distinct but overlapping substrate specificities. Plant Physiology **144,** 1986-1999.

Fujioka, S. (1999). Natural occurrence of brassinosteroids in the plant kingdom. In Brassinosteroid: Steroidal Plant Hormones**,** 21-45.

Fujioka, S., and Yokota, T. (2003). Biosynthesis and metabolism of brassinosteroids. Annual review of plant biology **54,** 137-164.

Fujiwara, H., Tanaka, Y., Fukui, Y., Nakao, M., Ashikari, T., and Kusumi, T. (1997). Anthocyanin 5-aromatic acyltransferase from *Gentiana triflora*. Purification, characterization and its role in anthocyanin biosynthesis. European Journal of Biochemistry **249,** 45-51.

Fujiwara, H., Tanaka, Y., Fukui, Y., Ashikari, T., Yamaguchi, M., and Kusumi, T. (1998a). Purification and characterization of anthocyanin 3-aromatic acyltransferase from *Perilla frutescens*. Plant Sci **137,** 87-94.

Fujiwara, H., Tanaka, Y., Yonekura-Sakakibara, K., Fukuchi-Mizutani, M., Nakao, M., Fukui, Y., Yamaguchi, M., Ashikari, T., and Kusumi, T. (1998b). cDNA cloning, gene expression and subcellular localization of anthocyanin 5-aromatic acyltransferase from *Gentiana triflora*. Plant Journal **16,** 421-431.

Gachon, C., Baltz, R., and Saindrenan, P. (2004). Over-expression of a scopoletin glucosyltransferase in *Nicotiana tabacum* leads to precocious lesion formation during the hypersensitive response to tobacco mosaic virus but does not affect virus resistance. Plant Molecular Biology **54,** 137-146.

Gampala, S.S., Kim, T.W., He, J.X., Tang, W.Q., Deng, Z.P., Bai, M.Y., Guan, S.H., Lalonde, S., Sun, Y., Gendron, J.M., Chen, H.J., Shibagaki, N., Ferl, R.J., Ehrhardt, D., Chong, K., Burlingame, A.L., and Wang, Z.Y. (2007). An essential role for 14-3-3 proteins in brassinosteroid signal transduction in *Arabidopsis*. Dev Cell **13,** 177-189.

Gomez, C., Terrier, N., Torregrosa, L., Vialet, S., Fournier-Level, A., Verries, C., Souquet, J.M., Mazauric, J.P., Klein, M., Cheynier, V., and Ageorges, A. (2009). Grapevine MATE-type proteins act as vacuolar H^+-dependent acylated anthocyanin transporters. Plant Physiology **150,** 402-415.

Gou, J.Y., Yu, X.H., and Liu, C.J. (2009). A hydroxycinnamoyltransferase responsible for synthesizing suberin aromatics in *Arabidopsis*. P Natl Acad Sci USA **106,** 18855-18860.

Grana, E., Costas-Gil, A., Longueira, S., Celeiro, M., Teijeira, M., Reigosa, M.J., and Sanchez-Moreiras, A.M. (2017). Auxin-like effects of the natural coumarin scopoletin on *Arabidopsis* cell structure and morphology. J Plant Physiol **218,** 45-55.

Grienenberger, E., Besseau, S., Geoffroy, P., Debayle, D., Heintz, D., Lapierre, C., Pollet, B., Heitz, T., and Legrand, M. (2009). A BAHD acyltransferase is expressed in the tapetum of Arabidopsis anthers and is involved in the synthesis of hydroxycinnamoyl spermidines. Plant Journal **58,** 246-259.

Grillet, L., and Schmidt, W. (2019). Iron acquisition strategies in land plants: not so different after all. New Phytologist **224,** 11-18.

Grove, M.D., Spencer, G.F., Rohwedder, W.K., Mandava, N., Worley, J.F., Warthen, J.D., Steffens, G.L., Flippenanderson, J.L., and Cook, J.C. (1979). Brassinolide, a plant growth promoting steroid isolated from *Brassica napus* pollen. Nature **281,** 216-217.

Guo, H., Li, L., Aluru, M., Aluru, S., and Yin, Y. (2013). Mechanisms and networks for brassinosteroid regulated gene expression. Curr Opin Plant Biol **16,** 545-553.

Guo, Z.X., Fujioka, S., Blancaflor, E.B., Miao, S., Gou, X.P., and Li, J. (2010). TCP1 modulates brassinosteroid biosynthesis by regulating the expression of the key biosynthetic gene *DWARF4* in *Arabidopsis thaliana*. Plant Cell **22,** 1161-1173.

Hao, Y., Wang, H., Qiao, S., Leng, L., and Wang, X. (2016). Histone deacetylase HDA6 enhances brassinosteroid signaling by inhibiting the BIN2 kinase. P Natl Acad Sci USA **113,** 10418-10423.

Harborne, J.B., and Williams, C.A. (2000). Advances in flavonoid research since 1992. Phytochemistry **55,** 481-504.

He, J.X., Gendron, J.M., Yang, Y.L., Li, J.M., and Wang, Z.Y. (2002). The GSK3-like kinase BIN2 phosphorylates and destabilizes BZR1, a positive regulator of the brassinosteroid signaling pathway in *Arabidopsis*. P Natl Acad Sci USA **99,** 10185-10190.

He, J.X., Gendron, J.M., Sun, Y., Gampala, S.S.L., Gendron, N., Sun, C.Q., and Wang, Z.Y. (2005). BZR1 is a transcriptional repressor with dual roles in brassinosteroid homeostasis and growth responses. Science **307,** 1634-1638.

He, K., Gou, X.P., Yuan, T., Lin, H.H., Asami, T., Yoshida, S., Russell, S.D., and Li, J. (2007). BAK1 and BKK1 regulate brassinosteroid-dependent growth and brassinosteroid independent cell-death pathways. Curr Biol **17,** 1109-1115.

Heiling, S., Schuman, M.C., Schoettner, M., Mukerjee, P., Berger, B., Schneider, B., Jassbi, A.R., and Baldwin, I.T. (2010). Jasmonate and ppHsystemin regulate key malonylation steps in the biosynthesis of 17-hydroxygeranyllinalool diterpene glycosides, an abundant and effective direct defense against herbivores in *Nicotiana attenuata*. Plant Cell **22,** 273-292.

Hillier, S.G., and Lathe, R. (2019). Terpenes, hormones and life: isoprene rule revisited. J Endocrinol **242,** R9-R22.

Hoffmann, L., Besseau, S., Geoffroy, P., Ritzenthaler, C., Meyer, D., Lapierre, C., Pollet, B., and Legrand, M. (2005). Acyltransferase-catalysed *p*-coumarate ester formation is a committed step of lignin biosynthesis. Plant Biosyst **139,** 50-53.

Hothorn, M., Belkhadir, Y., Dreux, M., Dabi, T., Noel, J.P., Wilson, I.A., and Chory, J. (2011). Structural basis of steroid hormone perception by the receptor kinase BRI1. Nature **474,** 467-U490.

Houbaert, A., Zhang, C., Tiwari, M., Wang, K., de Marcos Serrano, A., Savatin, D.V., Urs, M.J., Zhiponova, M.K., Gudesblat, G.E., Vanhoutte, I., Eeckhout, D., Boeren, S., Karimi, M., Betti, C., Jacobs, T., Fenoll, C., Mena, M., de Vries, S., De Jaeger, G., and Russinova, E. (2018). POLAR-guided signalling complex assembly and localization drive asymmetric cell division. Nature **563,** 574-578.

Husar, S., Berthiller, F., Fujioka, S., Rozhon, W., Khan, M., Kalaivanan, F., Elias, L., Higgins, G.S., Li, Y., Schuhmacher, R., Krska, R., Seto, H., Vaistij, F.E., Bowles, D., and Poppenberger, B. (2011).

Overexpression of the *UGT73C6* alters brassinosteroid glucoside formation in *Arabidopsis thaliana*. BMC plant biology **11,** 51.

Initiative, A.G. (2000). Analysis of the genome sequence of the flowering plant *Arabidopsis thaliana*. Nature **408,** 796-815.

Irmisch, S., Jo, S., Roach, C.R., Jancsik, S., Man Saint Yuen, M., Madilao, L.L., O'Neil-Johnson, M., Williams, R., Withers, S.G., and Bohlmann, J. (2018). Discovery of UDP-Glycosyltransferases and BAHD-Acyltransferases Involved in the Biosynthesis of the Antidiabetic Plant Metabolite Montbretin A. Plant Cell **30,** 1864-1886.

Jaillais, Y., Hothorn, M., Belkhadir, Y., Dabi, T., Nimchuk, Z.L., Meyerowitz, E.M., and Chory, J. (2011). Tyrosine phosphorylation controls brassinosteroid receptor activation by triggering membrane release of its kinase inhibitor. Gene Dev **25,** 232-237.

Kai, K., Shimizu, B., Mizutani, M., Watanabe, K., and Sakata, K. (2006). Accumulation of coumarins in *Arabidopsis thaliana*. Phytochemistry **67,** 379-386.

Kai, K., Mizutani, M., Kawamura, N., Yamamoto, R., Tamai, M., Yamaguchi, H., Sakata, K., and Shimizu, B.I. (2008). Scopoletin is biosynthesized via *ortho*-hydroxylation of feruloyl CoA by a 2-oxoglutarate-dependent dioxygenase in *Arabidopsis thaliana*. Plant Journal **55,** 989-999.

Kang, J.G., Yun, J., Kim, D.H., Chung, K.S., Fujioka, S., Kim, J.I., Dae, H.W., Yoshida, S., Takatsuto, S., Song, P.S., and Park, C.M. (2001). Light and brassinosteroid signals are integrated via a dark-induced small G protein in etiolated seedling growth. Cell **105,** 625-636.

Karlova, R., Boeren, S., Russinova, E., Aker, J., Vervoort, J., and de Vries, S. (2006). The *Arabidopsis* SOMATIC EMBRYOGENESIS RECEPTOR-LIKE KINASE1 protein complex includes BRASSINOSTEROID-INSENSITIVE1. Plant Cell **18,** 626-638.

Kessler, A., and Kalske, A. (2018). Plant secondary metabolite diversity and species interactions. Annual Review of Ecology, Evolution, and Systematics **49,** 115-138.

Khan, B.R., Wherritt, D.J., Huhman, D., Sumner, L.W., Chapman, K.D., and Blancaflor, E.B. (2016). Malonylation of glucosylated N-lauroylethanolamine: a new pathway that determines N-acylethanolamine metabolic fate in plants. Journal of Biological Chemistry **291,** 27112-27121.

Kim, T.W., and Wang, Z.Y. (2010). Brassinosteroid signal transduction from receptor kinases to transcription factors. Annual review of plant biology **61,** 681-704.

Kim, T.W., Guan, S.H., Burlingame, A.L., and Wang, Z.Y. (2011). The CDG1 kinase mediates brassinosteroid signal transduction from BRI1 receptor kinase to BSU1 phosphatase and GSK3-like kinase BIN2. Mol Cell **43,** 561-571.

Kim, T.W., Hwang, J.Y., Kim, Y.S., Joo, S.H., Chang, S.C., Lee, J.S., Takatsuto, S., and Kim, S.K. (2005). Arabidopsis CYP85A2, a cytochrome P450, mediates the Baeyer-Villiger oxidation of castasterone to brassinolide in brassinosteroid biosynthesis. Plant Cell **17,** 2397-2412.

Kinoshita, T., Cano-Delgado, A.C., Seto, H., Hiranuma, S., Fujioka, S., Yoshida, S., and Chory, J. (2005). Binding of brassinosteroids to the extracellular domain of plant receptor kinase BRI1. Nature **433,** 167-171.

Kolbe, A., Schneider, B., Porzel, A., and Adam, G. (1996). Metabolism of 24-epi-castasterone and 24-epi-brassinolide in cell suspension cultures of *Ornithopus sativus*. Phytochemistry **41,** 163-167.

Kolbe, A., Schneider, B., Porzel, A., Schmidt, J., and Adam, G. (1995). Acyl-conjugated metabolites of brassinosteroids in cell suspension cultures of *Ornithopus sativus*. Phytochemistry **38,** 633-636.

Kosma, D.K., Molina, I., Ohlrogge, J.B., and Pollard, M. (2012). Identification of an Arabidopsis fatty alcohol: caffeoyl-coenzyme a acyltransferase required for the synthesis of alkyl hydroxycinnamates in root waxes. Plant Physiology **160,** 237-248.

Lehfeldt, C., Shirley, A.M., Meyer, K., Ruegger, M.O., Cusumano, J.C., Viitanen, P.V., Strack, D., and Chapple, C. (2000). Cloning of the *SNG1* gene of Arabidopsis reveals a role for a serine carboxypeptidase-like protein as an acyltransferase in secondary metabolism. Plant Cell **12,** 1295-1306.

Li, J., and Wu, J. (2016). Scopolin, a glycoside form of the phytoalexin scopoletin, is likely involved in the resistance of *Nicotiana attenuata* against *Alternaria alternata*. J Plant Pathol **98,** 641-644.

Li, J., Wen, J.Q., Lease, K.A., Doke, J.T., Tax, F.E., and Walker, J.C. (2002). BAK1, an *Arabidopsis* LRR receptor-like protein kinase, interacts with BRI1 and modulates brassinosteroid signaling. Cell **110,** 213-222.

Li, J., Schuman, M.C., Halitschke, R., Li, X., Guo, H., Grabe, V., Hammer, A., and Baldwin, I.T. (2018). The decoration of specialized metabolites influences stylar development. Elife **7.**

Li, J.M., and Chory, J. (1997). A putative leucine-rich repeat receptor kinase involved in brassinosteroid signal transduction. Cell **90,** 929-938.

Li, J.M., and Nam, K.H. (2002). Regulation of brassinosteroid signaling by a GSK3/SHAGGY-like kinase. Science **295,** 1299-1301.

Lim, E.K., Baldauf, S., Li, Y., Elias, L., Worrall, D., Spencer, S.P., Jackson, R.G., Taguchi, G., Ross, J., and Bowles, D.J. (2003). Evolution of substrate recognition across a multigene family of glycosyltransferases in *Arabidopsis*. Glycobiology **13,** 139-145.

Lin, D.R., Xiao, M.S., Zhao, J.J., Li, Z.H., Xing, B.S., Li, X.D., Kong, M.Z., Li, L.Y., Zhang, Q., Liu, Y.W., Chen, H., Qin, W., Wu, H.J., and Chen, S.Y. (2016). An overview of plant phenolic compounds and their importance in human nutrition and management of Type 2 diabetes. Molecules **21.**

Lozano-Elena, F., and Cano-Delgado, A.I. (2019). Emerging roles of vascular brassinosteroid receptors of the BRI1-like family. Curr Opin Plant Biol **51,** 105-113.

Luo, J., Nishiyama, Y., Fuell, C., Taguchi, G., Elliott, K., Hill, L., Tanaka, Y., Kitayama, M., Yamazaki, M., Bailey, P., Parr, A., Michael, A.J., Saito, K., and Martin, C. (2007). Convergent evolution in the BAHD family of acyl transferases: identification and characterization of anthocyanin acyl transferases from *Arabidopsis thaliana*. Plant Journal **50,** 678-695.

Ma, X., Koepke, J., Panjikar, S., Fritzsch, G., and Stockigt, J. (2005). Crystal structure of vinorine synthase, the first representative of the BAHD superfamily. Journal of Biological Chemistry **280,** 13576-13583.

Mandava, N.B. (1988). Plant growth promoting brassinosteroids. Annu Rev Plant Phys **39,** 23-52.

Marsolais, F., Boyd, J., Paredes, Y., Schinas, A.M., Garcia, M., Elzein, S., and Varin, L. (2007). Molecular and biochemical characterization of two brassinosteroid sulfotransferases from *Arabidopsis*, AtST4a (At2g14920) and AtST1 (At2g03760). Planta **225,** 1233-1244.

Matern, U., Heller, W., and Himmelspach, K. (1983). Conformational changes of apigenin 7-*O*-(6-*O*-malonylglucoside), a vacuolar pigment from parsley, with solvent composition and proton concentration. European Journal of Biochemistry **133,** 439-448.

Matern, U., Reichenbach, C., and Heller, W. (1986). Efficient uptake of flavonoids into parsley (*Petroselinum hortense*) vacuoles requires acylated glycosides. Planta **167,** 183-189.

Mathur, J., Molnar, G., Fujioka, S., Takatsuto, S., Sakurai, A., Yokota, T., Adam, G., Voigt, B., Nagy, F., Maas, C., Schell, J., Koncz, C., and Szekeres, M. (1998). Transcription of the *Arabidopsis CPD* gene, encoding a steroidogenic cytochrome P450, is negatively controlled by brassinosteroids. Plant Journal **14,** 593-602.

Matsuda, F., Hirai, M.Y., Sasaki, E., Akiyama, K., Yonekura-Sakakibara, K., Provart, N.J., Sakurai, T., Shimada, Y., and Saito, K. (2010). AtMetExpress development: a phytochemical atlas of *Arabidopsis* development. Plant Physiology **152,** 566-578.

Milkowski, C., and Strack, D. (2004). Serine carboxypeptidase-like acyltransferases. Phytochemistry **65,** 517-524.

Mitchell, J.W., Mandava, N., Worley, J.F., Plimmer, J.R., and Smith, M.V. (1970). Brassins: a new family of plant hormones from rape pollen. Nature **225,** 1065-1066.

Mora-Garcia, S., Vert, G., Yin, Y.H., Cano-Delgado, A., Cheong, H., and Chory, J. (2004). Nuclear protein phosphatases with Kelch-repeat domains modulate the response to brassino steroids in *Arabidopsis*. Gene Dev **18,** 448-460.

Mueller, L.A., Zhang, P., and Rhee, S.Y. (2003). AraCyc: a biochemical pathway database for *Arabidopsis*. Plant Physiology **132,** 453-460.

Mugford, S.T., Louveau, T., Melton, R., Qi, X., Bakht, S., Hill, L., Tsurushima, T., Honkanen, S., Rosser, S.J., Lomonossoff, G.P., and Osbourn, A. (2013). Modularity of plant metabolic gene clusters: a trio of linked genes that are collectively required for acylation of triterpenes in oat. Plant Cell **25,** 1078-1092.

Mugford, S.T., Qi, X.Q., Bakht, S., Hill, L., Wegel, E., Hughes, R.K., Papadopoulou, K., Melton, R., Philo, M., Sainsbury, F., Lomonossoff, G.P., Roy, A.D., Goss, R.J.M., and Osbourn, A. (2009). A serine carboxypeptidase-like acyltransferase is required for synthesis of antimicrobial compounds and disease resistance in oats. Plant Cell **21,** 2473-2484.

Nakamura, M., Satoh, T., Tanaka, S., Mochizuki, N., Yokota, T., and Nagatani, A. (2005). Activation of the cytochrome P450 gene, *CYP72C1*, reduces the levels of active brassinosteroids *in vivo*. J Exp Bot **56,** 833-840.

Nakayama, T., Suzuki, H., and Nishino, T. (2003a). Anthocyanin acyltransferases: specificities, mechanism, phylogenetics, and applications. J Mol Catal B-Enzym **23,** 117-132.

Nakayama, T., Suzuki, H., and Nishino, T. (2003b). Anthocyanin acyltransferases: specificities, mechanism, phylogenetics, and applications. Journal of Molecular Catalysis B: Enzymatic **23,** 117-132.

Nam, K.H., and Li, J.M. (2002). BRI1/BAK1, a receptor kinase pair mediating brassinosteroid signaling. Cell **110,** 203-212.

Neff, M.M., Nguyen, S.M., Malancharuvil, E.J., Fujioka, S., Noguchi, T., Seto, H., Tsubuki, M., Honda, T., Takatsuto, S., Yoshida, S., and Chory, J. (1999). *BAS1*: A gene regulating brassinosteroid levels and light responsiveness in *Arabidopsis*. P Natl Acad Sci USA **96,** 15316-15323.

Negre, F., Kish, C.M., Boatright, J., Underwood, B., Shibuya, K., Wagner, C., Clark, D.G., and Dudareva, N. (2003). Regulation of methylbenzoate emission after pollination in snapdragon and petunia flowers. Plant Cell **15,** 2992-3006.

Nolan, T., Vukasinovic, N., Liu, D., Russinova, E., and Yin, Y. (2019). Brassinosteroids: multi-dimensional regulators of plant growth, development, and stress responses. Plant Cell.

Nomura, T., Kushiro, T., Yokota, T., Kamiya, Y., Bishop, G.J., and Yamaguchi, S. (2005). The last reaction producing brassinolide is catalyzed by cytochrome P-450s, CYP85A3 in tomato and CYP85A2 in *Arabidopsis*. Journal of Biological Chemistry **280,** 17873-17879.

Oh, E., Zhu, J.Y., and Wang, Z.Y. (2012). Interaction between BZR1 and PIF4 integrates brassinosteroid and environmental responses. Nature Cell Biology **14,** 802-U864.

Ohnishi, T., Godza, B., Watanabe, B., Fujioka, S., Hategan, L., Ide, K., Shibata, K., Yokota, T., Szekeres, M., and Mizutani, M. (2012). CYP90A1/CPD, a brassinosteroid biosynthetic cytochrome P450 of *Arabidopsis*, catalyzes C-3 oxidation. Journal of Biological Chemistry **287,** 31551-31560.

Ohnishi, T., Szatmari, A.M., Watanabe, B., Fujita, S., Bancos, S., Koncz, C., Lafos, M., Shibata, K., Yokota, T., Sakata, K., Szekeres, M., and Mizutani, M. (2006). C-23 hydroxylation by *Arabidopsis* CYP90C1 and CYP90D1 reveals a novel shortcut in brassinosteroid biosynthesis. Plant Cell **18,** 3275-3288.

Panikashvili, D., Shi, J.X., Schreiber, L., and Aharoni, A. (2009). The *Arabidopsis DCR* encoding a soluble BAHD acyltransferase is required for cutin polyester formation and seed hydration properties. Plant Physiology **151,** 1773-1789.

Poppenberger, B., Rozhon, W., Khan, M., Husar, S., Adam, G., Luschnig, C., Fujioka, S., and Sieberer, T. (2011). CESTA, a positive regulator of brassinosteroid biosynthesis. EMBO Journal **30,** 1149-1161.

Poppenberger, B., Fujioka, S., Soeno, K., George, G.L., Vaistij, F.E., Hiranuma, S., Seto, H., Takatsuto, S., Adam, G., Yoshida, S., and Bowles, D. (2005). The UGT73C5 of *Arabidopsis thaliana* glucosylates brassinosteroids. P Natl Acad Sci USA **102,** 15253-15258.

Pyne, M.E., Narcross, L., and Martin, V.J.J. (2019). Engineering plant secondary metabolism in microbial systems. Plant Physiology **179,** 844-861.

Rajniak, J., Giehl, R.F.H., Chang, E., Murgia, I., von Wiren, N., and Sattely, E.S. (2018). Biosynthesis of redox-active metabolites in response to iron deficiency in plants. Nature Chemical Biology **14,** 442-450.

Roh, H., Jeong, C.W., Fujioka, S., Kim, Y.K., Lee, S., Ahn, J.H., Choi, Y.D., and Lee, J.S. (2012). Genetic evidence for the reduction of brassinosteroid levels by a BAHD acyltransferase-like protein in *Arabidopsis*. Plant Physiology **159,** 696-709.

Rouleau, M., Marsolais, F., Richard, M., Nicolle, L., Voigt, B., Adam, G., and Varin, L. (1999). Inactivation of brassinosteroid biological activity by a salicylate-inducible steroid sulfotransferase from *Brassica napus*. Journal of Biological Chemistry **274,** 20925-20930.

Rozhon, W., Akter, S., Fernandez, A., and Poppenberger, B. (2019). Inhibitors of brassinosteroid biosynthesis and signal transduction. Molecules **24**.

Rozhon, W., Mayerhofer, J., Petutschnig, E., Fujioka, S., and Jonak, C. (2010). ASKθ, a group-III Arabidopsis GSK3, functions in the brassinosteroid signalling pathway. Plant Journal **62,** 215-223.

Ryu, H., Kim, K., Cho, H., Park, J., Choe, S., and Hwang, I. (2007). Nucleocytoplasmic shuttling of BZR1 mediated by phosphorylation is essential in *Arabidopsis* brassinosteroid signaling. Plant Cell **19,** 2749-2762.

Sandermann, H., Schmitt, R., Eckey, H., and Bauknecht, T. (1991). Plant biochemistry of xenobiotics: Isolation and properties of soybean *O*-glucosyl and *N*-glucosyl and *O*-malonyltransferases and *N*-malonyltransferases for chlorinated phenols and anilines. Archives of Biochemistry and Biophysics **287,** 341-350.

Sasse, J.M. (2003). Physiological actions of brassinosteroids: An update. J Plant Growth Regul **22,** 276-288.

Schmid, N.B., Giehl, R.F., Doll, S., Mock, H.P., Strehmel, N., Scheel, D., Kong, X., Hider, R.C., and von Wiren, N. (2014). Feruloyl-CoA 6'-Hydroxylase1-dependent coumarins mediate iron acquisition from alkaline substrates in *Arabidopsis*. Plant Physiology **164,** 160-172.

Schmidt, W. (2019). The Yin and Yang of Iron in Plants and Beyond: 19th International Symposium on Iron Nutrition and Interactions in Plants (ISINIP) in Taiwan. Plant Cell Physiol **60,** 1401-1404.

Schmitt, R., and Sandermann, H. (1982). Specific localization of β-D-Glucoside conjugates of 2,4-Dichlorophenoxyacetic acid in soybean vacuoles. Zeitschrift für Naturforschung C-A Journal of Biosciences **37,** 772-777.

Schneider, K., Breuer, C., Kawamura, A., Jikumaru, Y., Hanada, A., Fujioka, S., Ichikawa, T., Kondou, Y., Matsui, M., Kamiya, Y., Yamaguchi, S., and Sugimoto, K. (2012). Arabidopsis PIZZA has the capacity to acylate brassinosteroids. PLoS One **7,** e46805.

Schoch, G., Goepfert, S., Morant, M., Hehn, A., Meyer, D., Ullmann, P., and Werck-Reichhart, D. (2001). CYP98A3 from *Arabidopsis thaliana* is a 3'-hydroxylase of phenolic esters, a missing link in the phenylpropanoid pathway. Journal of Biological Chemistry **276,** 36566-36574.

She, J., Han, Z.F., Kim, T.W., Wang, J.J., Cheng, W., Chang, J.B., Shi, S.A., Wang, J.W., Yang, M.J., Wang, Z.Y., and Chai, J.J. (2011). Structural insight into brassinosteroid perception by BRI1. Nature **474,** 472-U496.

Shimada, Y., Fujioka, S., Miyauchi, N., Kushiro, M., Takatsuto, S., Nomura, T., Yokota, T., Kamiya, Y., Bishop, G.J., and Yoshida, S. (2001). Brassinosteroid-6-oxidases from Arabidopsis and tomato catalyze multiple C-6 oxidations in brassinosteroid biosynthesis. Plant Physiology **126,** 770-779.

Shirley, A.M., McMichael, C.M., and Chapple, C. (2001). The *sng2* mutant of *Arabidopsis* is defective in the gene encoding the serine carboxypeptidase-like protein sinapoylglucose: choline sinapoyltransferase. Plant Journal **28,** 83-94.

Siwinska, J., Kadzinski, L., Banasiuk, R., Gwizdek-Wisniewska, A., Olry, A., Banecki, B., Lojkowska, E., and Ihnatowicz, A. (2014). Identification of QTLs affecting scopolin and scopoletin biosynthesis in *Arabidopsis thaliana*. BMC plant biology **14,** 280.

Siwinska, J., Siatkowska, K., Olry, A., Grosjean, J., Hehn, A., Bourgaud, F., Meharg, A.A., Carey, M., Lojkowska, E., and Ihnatowicz, A. (2018). Scopoletin 8-hydroxylase: a novel enzyme involved in coumarin biosynthesis and iron-deficiency responses in *Arabidopsis*. J Exp Bot **69,** 1735-1748.

Soeno, K., Asakawa, S., Natsume, M., and Abe, H. (2000). Reversible conversion between teasterone and its ester conjugates in lily cell cultures. J Pestic Sci **25,** 117-122.

Song, S., Wang, H., Sun, M., Tang, J., Zheng, B., Wang, X., and Tan, Y.W. (2019). Reactive oxygen species-mediated BIN2 activity revealed by single-molecule analysis. New Phytologist **223,** 692-704.

Sreeramulu, S., Mostizky, Y., Sunitha, S., Shani, E., Nahum, H., Salomon, D., Ben Hayun, L., Gruetter, C., Rauh, D., Ori, N., and Sessa, G. (2013). BSKs are partially redundant positive regulators of brassinosteroid signaling in *Arabidopsis*. Plant Journal **74,** 905-919.

St-Pierre, B., and De Luca, V. (2000). Origin and diversification of the BAHD superfamily of acyltransferases involved in secondary metabolism. Recent Adv. Phytochem **34,** 285-315.

St-Pierre, B., Laflamme, P., Alarco, A.M., and De Luca, V. (1998). The terminal *O*-acetyltransferase involved in vindoline biosynthesis defines a new class of proteins responsible for coenzyme A-dependent acyl transfer. Plant Journal **14,** 703-713.

Steffens, G.L. (1991). U.S. Department of Agriculture Brassins Project: 1970—1980. In Brassinosteroids (American Chemical Society), pp. 2-17.

Stringlis, I.A., de Jonge, R., and Pieterse, C.M.J. (2019). The age of coumarins in plant-microbe interactions. Plant Cell Physiology **60,** 1405-1419.

Stringlis, I.A., Yu, K., Feussner, K., de Jonge, R., Van Bentum, S., Van Verk, M.C., Berendsen, R.L., Bakker, P., Feussner, I., and Pieterse, C.M.J. (2018). MYB72-dependent coumarin exudation shapes root microbiome assembly to promote plant health. P Natl Acad Sci USA **115,** E5213-E5222.

Sun, H.H., Wang, L., Zhang, B.Q., Ma, J.H., Hettenhausen, C., Cao, G.Y., Sun, G.L., Wu, J.Q., and Wu, J.S. (2014). Scopoletin is a phytoalexin against *Alternaria alternata* in wild tobacco dependent on jasmonate signalling. J Exp Bot **65,** 4305-4315.

Sun, Y., Fan, X.Y., Cao, D.M., Tang, W., He, K., Zhu, J.Y., He, J.X., Bai, M.Y., Zhu, S., Oh, E., Patil, S., Kim, T.W., Ji, H., Wong, W.H., Rhee, S.Y., and Wang, Z.Y. (2010). Integration of brassinosteroid signal transduction with the transcription network for plant growth regulation in *Arabidopsis*. Dev Cell **19,** 765-777.

Suzuki, H., Nakayama, T., Yamaguchi, M.A., and Nishino, T. (2004a). cDNA cloning and characterization of two *Dendranthema* x *morifolium* anthocyanin malonyltransferases with different functional activities. Plant Sci **166,** 89-96.

Suzuki, H., Sawada, S., Watanabe, K., Nagae, S., Yamaguchi, M.A., Nakayama, T., and Nishino, T. (2004b). Identification and characterization of a novel anthocyanin malonyltransferase from scarlet sage (*Salvia splendens*) flowers: an enzyme that is phylogenetically separated from other anthocyanin acyltransferases. Plant Journal **38,** 994-1003.

Suzuki, H., Nakayama, T., Yonekura-Sakakibara, K., Fukui, Y., Nakamura, N., Yamaguchi, M.A., Tanaka, Y., Kusumi, T., and Nishino, T. (2002). cDNA cloning, heterologous expressions, and functional characterization of malonyl-coenzyme A: anthocyanidin 3-*O*-glucoside-6"-*O*-malonyltransferase from dahlia flowers. Plant Physiology **130,** 2142-2151.

Suzuki, H., Nakayama, T., Yonekura-Sakakibara, K., Fukui, Y., Nakamura, N., Nakao, M., Tanaka, Y., Yamaguchi, M.A., Kusumi, T., and Nishino, T. (2001). Malonyl-CoA: anthocyanin 5-*O*-glucoside-6'''-*O*-malonyltransferase from scarlet sage (*Salvia splendens*) flowers. Journal of Biological Chemistry **276,** 49013-49019.

Taguchi, G., Shitchi, Y., Shirasawa, S., Yamamoto, H., and Hayashida, N. (2005). Molecular cloning, characterization, and downregulation of an acyltransferase that catalyzes the malonylation of flavonoid and naphthol glucosides in tobacco cells. Plant Journal **42,** 481-491.

Taguchi, G., Fujikawa, S., Yazawa, T., Kodaira, R., Hayashida, N., Shimosaka, M., and Okazaki, M. (2000). Scopoletin uptake from culture medium and accumulation in the vacuoles after conversion to scopolin in 2,4-D treated tobacco cells. Plant Sci **151,** 153-161.

Taguchi, G., Ubukata, T., Nozue, H., Kobayashi, Y., Takahi, M., Yamamoto, H., and Hayashida, N. (2010). Malonylation is a key reaction in the metabolism of xenobiotic phenolic glucosides in *Arabidopsis* and tobacco. Plant Journal **63,** 1031-1041.

Takahashi, N., Nakazawa, M., Shibata, K., Yokota, T., Ishikawa, A., Suzuki, K., Kawashima, M., Ichikawa, T., Shimada, H., and Matsui, M. (2005). *shk1-D*, a dwarf *Arabidopsis* mutant caused by activation of the *CYP72C1* gene, has altered brassinosteroid levels. Plant Journal **42,** 13-22.

Tal, B., and Robeson, D.J. (1986). The metabolism of sunflower phytoalexins ayapin and scopoletin: plant-fungus interactions. Plant Physiol **82,** 167-172.

Tanaka, K., Asami, T., Yoshida, S., Nakamura, Y., Matsuo, T., and Okamoto, S. (2005). Brassinosteroid homeostasis in *Arabidopsis* is ensured by feedback expressions of multiple genes involved in its metabolism. Plant Physiology **138,** 1117-1125.

Tang, W., Yuan, M., Wang, R., Yang, Y., Wang, C., Oses-Prieto, J.A., Kim, T.W., Zhou, H.W., Deng, Z., Gampala, S.S., Gendron, J.M., Jonassen, E.M., Lillo, C., DeLong, A., Burlingame, A.L., Sun, Y., and Wang, Z.Y. (2011). PP2A activates brassinosteroid-responsive gene expression and plant growth by dephosphorylating BZR1. Nat Cell Biology **13,** 124-131.

Tang, W.Q., Kim, T.W., Oses-Prieto, J.A., Sun, Y., Deng, Z.P., Zhu, S.W., Wang, R.J., Burlingame, A.L., and Wang, Z.Y. (2008). BSKs mediate signal transduction from the receptor kinase BRI1 in *Arabidopsis*. Science **321,** 557-560.

Tholl, D., Chen, F., Petri, J., Gershenzon, J., and Pichersky, E. (2005). Two sesquiterpene synthases are responsible for the complex mixture of sesquiterpenes emitted from *Arabidopsis* flowers. Plant Journal **42,** 757-771.

Thompson, M.J., Meudt, W.J., Mandava, N.B., Dutky, S.R., Lusby, W.R., and Spaulding, D.W. (1982). Synthesis of brassinosteroids and relationship of structure to plant growth promoting effects. Steroids **39,** 89-105.

Thompson, M.J., Mandava, N., Flippenanderson, J.L., Worley, J.F., Dutky, S.R., Robbins, W.E., and Lusby, W. (1979). Synthesis of brassino steroids: new plant growth promoting steroids. J Org Chem **44,** 5002-5004.

Thornton, L.E., Rupasinghe, S.G., Peng, H., Schuler, M.A., and Neff, M.M. (2010). *Arabidopsis* CYP72C1 is an atypical cytochrome P450 that inactivates brassinosteroids. Plant Molecular Biology **74,** 167-181.

Tong, W.-Y. (2013). Biotransformation of Terpenoids and Steroids. In Natural Products: Phytochemistry, Botany and Metabolism of Alkaloids, Phenolics and Terpenes (Berlin, Heidelberg: Springer Berlin Heidelberg), pp. 2733-2759.

Truernit, E., Bauby, H., Belcram, K., Barthelemy, J., and Palauqui, J.C. (2012). OCTOPUS, a polarly localised membrane-associated protein, regulates phloem differentiation entry in *Arabidopsis thaliana*. Development **139,** 1306-1315.

Tsai, H.H., Rodriguez-Celma, J., Lan, P., Wu, Y.C., Velez-Bermudez, I.C., and Schmidt, W. (2018). Scopoletin 8-hydroxylase-mediated fraxetin production is crucial for iron mobilization. Plant Physiology **177,** 194-207.

Tuominen, L.K., Johnson, V.E., and Tsai, C.J. (2011). Differential phylogenetic expansions in BAHD acyltransferases across five angiosperm taxa and evidence of divergent expression among Populus paralogues. BMC Genomics **12,** 236.

Turk, E.M., Fujioka, S., Seto, H., Shimada, Y., Takatsuto, S., Yoshida, S., Denzel, M.A., Torres, Q.I., and Neff, M.M. (2003). CYP72B1 inactivates brassinosteroid hormones: an intersection between photomorphogenesis and plant steroid signal transduction. Plant Physiology **133,** 1643-1653.

Turk, E.M., Fujioka, S., Seto, H., Shimada, Y., Takatsuto, S., Yoshida, S., Wang, H., Torres, Q.I., Ward, J.M., Murthy, G., Zhang, J., Walker, J.C., and Neff, M.M. (2005). BAS1 and SOB7 act redundantly to modulate *Arabidopsis* photomorphogenesis via unique brassinosteroid inactivation mechanisms. Plant Journal **42,** 23-34.

Unno, H., Ichimaida, F., Suzuki, H., Takahashi, S., Tanaka, Y., Saito, A., Nishino, T., Kusunoki, M., and Nakayama, T. (2007). Structural and mutational studies of anthocyanin malonyltransferases establish the features of BAHD enzyme catalysis. Journal of Biological Chemistry **282,** 15812-15822.

Unterholzner, S.J., Rozhon, W., and Poppenberger, B. (2017). Analysis of *In Vitro* DNA interactions of brassinosteroid-controlled transcription factors using electrophoretic mobility shift assay. Methods Mol Biol **1564,** 133-144.

Valle, T., Lopez, J.L., Hernandez, J.M., and Corchete, P. (1997). Antifungal activity of scopoletin and its differential accumulation in *Ulmus pumila* and *Ulmus campestris* cell suspension cultures infected with *Ophiostoma ulmi* spores. Plant Sci **125,** 97-101.

Vanholme, R., Sundin, L., Seetso, K.C., Kim, H., Liu, X., Li, J., De Meester, B., Hoengenaert, L., Goeminne, G., Morreel, K., Haustraete, J., Tsai, H.H., Schmidt, W., Vanholme, B., Ralph, J., and Boerjan, W. (2019). COSY catalyses trans-cis isomerization and lactonization in the biosynthesis of coumarins. Nature Plants **5,** 1066-1075.

Vert, G., and Chory, J. (2006). Downstream nuclear events in brassinosteroid signalling. Nature **441,** 96-100.

Voges, M.J.E.E.E., Bai, Y., Schulze-Lefert, P., and Sattely, E.S. (2019). Plant-derived coumarins shape the composition of an *Arabidopsis* synthetic root microbiome. P Natl Acad Sci USA **116,** 12558-12565.

Wang, M.J., Liu, X.Y., Wang, R., Li, W.C., Rodermel, S., and Yu, F. (2012). Overexpression of a putative *Arabidopsis* BAHD acyltransferase causes dwarfism that can be rescued by brassinosteroid. J Exp Bot **63,** 5787-5801.

Wang, S., Alseekh, S., Fernie, A.R., and Luo, J. (2019). The structure and function of major plant metabolite modifications. Mol Plant **12,** 899-919.

Wang, X.F., Kota, U., He, K., Blackburn, K., Li, J., Goshe, M.B., Huber, S.C., and Clouse, S.D. (2008). Sequential transphosphorylation of the BRI1/BAK1 receptor kinase complex impacts early events in brassinosteroid signaling. Dev Cell **15,** 220-235.

Wang, X.F., Goshe, M.B., Soderblom, E.J., Phinney, B.S., Kuchar, J.A., Li, J., Asami, T., Yoshida, S., Huber, S.C., and Clouse, S.D. (2005). Identification and functional analysis of *in vivo* phosphorylation sites of the *Arabidopsis* BRASSINOSTEROID-INSENSITIVE1 receptor kinase. Plant Cell **17,** 1685-1703.

Wang, X.L., and Chory, J. (2006). Brassinosteroids regulate dissociation of BKI1, a negative regulator of BRI1 signaling, from the plasma membrane. Science **313,** 1118-1122.

Wang, Z.Y., Seto, H., Fujioka, S., Yoshida, S., and Chory, J. (2001). BRI1 is a critical component of a plasma-membrane receptor for plant steroids. Nature **411,** 219-219.

Wang, Z.Y., Nakano, T., Gendron, J., He, J.X., Chen, M., Vafeados, D., Yang, Y.L., Fujioka, S., Yoshida, S., Asami, T., and Chory, J. (2002). Nuclear-localized BZR1 mediates brassinosteroid-induced growth and feedback suppression of brassinosteroid biosynthesis. Dev Cell **2,** 505-513.

Wei, Z.Y., Yuan, T., Tarkowska, D., Kim, J., Nam, H.G., Novak, O., He, K., Gou, X.P., and Li, J. (2017). Brassinosteroid biosynthesis is modulated via a transcription factor cascade of COG1, PIF4, and PIF5. Plant Physiology **174,** 1260-1273.

Winter, J., Schneider, B., Meyenburg, S., Strack, D., and Adam, G. (1999). Monitoring brassinosteroid biosynthetic enzymes by fluorescent tagging and HPLC analysis of their substrates and products. Phytochemistry **51,** 237-242.

Wurtzel, E.T., and Kutchan, T.M. (2016). Plant metabolism, the diverse chemistry set of the future. Science **353,** 1232-1236.

Yan, Z.Y., Zhao, J., Peng, P., Chihara, R.K., and Li, J.M. (2009). BIN2 functions redundantly with other *Arabidopsis* GSK3-like kinases to regulate brassinosteroid signaling. Plant Physiology **150,** 710-721.

Yang, Q., Reinhard, K., Schiltz, E., and Matern, U. (1997). Characterization and heterologous expression of hydroxycinnamoyl/benzoyl-CoA: anthranilate N-hydroxycinnamoyl/benzoyltransferase from elicited cell cultures of carnation, *Dianthus caryophyllus* L. Plant Molecular Biology **35,** 777-789.

Yin, Y.H., Vafeados, D., Tao, Y., Yoshida, S., Asami, T., and Chory, J. (2005). A new class of transcription factors mediates brassinosteroid-regulated gene expression in *Arabidopsis*. Cell **120,** 249-259.

Yin, Y.H., Wang, Z.Y., Mora-Garcia, S., Li, J.M., Yoshida, S., Asami, T., and Chory, J. (2002). BES1 accumulates in the nucleus in response to brassinosteroids to regulate gene expression and promote stem elongation. Cell **109,** 181-191.

Youn, J.H., Kim, T.W., Joo, S.H., Son, S.H., Roh, J., Kim, S., Kim, T.W., and Kim, S.K. (2018). Function and molecular regulation of DWARF1 as a C-24 reductase in brassinosteroid biosynthesis in *Arabidopsis*. J Exp Bot **69,** 1873-1886.

Yu, X., Li, L., Zola, J., Aluru, M., Ye, H., Foudree, A., Guo, H., Anderson, S., Aluru, S., Liu, P., Rodermel, S., and Yin, Y. (2011). A brassinosteroid transcriptional network revealed by genome-wide identification of BES1 target genes in *Arabidopsis thaliana*. Plant Journal **65,** 634-646.

Yu, X.H., Gou, J.Y., and Liu, C.J. (2009). BAHD superfamily of acyl-CoA dependent acyltransferases in *Populus* and *Arabidopsis*: bioinformatics and gene expression. Plant Molecular Biology **70,** 421-442.

Zhang, Z.Q., and Xu, L.P. (2018). Arabidopsis BRASSINOSTEROID INACTIVATOR2 is a typical BAHD acyltransferase involved in brassinosteroid homeostasis. J Exp Bot **69,** 1925–1941.

Zhao, B.L., and Li, J. (2012). Regulation of Brassinosteroid Biosynthesis and Inactivation. J Integr Plant Biol **54,** 746-759.

Zhao, J., and Dixon, R.A. (2010). The 'ins' and 'outs' of flavonoid transport. Trends Plant Sci **15,** 72-80.

Zhao, J., Huhman, D., Shadle, G., He, X.Z., Sumner, L.W., Tang, Y., and Dixon, R.A. (2011). MATE2 mediates vacuolar sequestration of flavonoid glycosides and glycoside malonates in *Medicago truncatula*. Plant Cell **23,** 1536-1555.

Zhou, A., Wang, H.C., Walker, J.C., and Li, J. (2004). BRL1, a leucine-rich repeat receptor-like protein kinase, is functionally redundant with BRI1 in regulating *Arabidopsis* brassinosteroid signaling. Plant Journal **40,** 399-409.

Zhu, J.Y., Li, Y., Cao, D.M., Yang, H., Oh, E., Bi, Y., Zhu, S., and Wang, Z.Y. (2017). The F-box protein KIB1 mediates brassinosteroid-induced inactivation and degradation of GSK3-like kinases in *Arabidopsis*. Mol Cell **66,** 648-657 e644.

Zhu, W., Wang, H., Fujioka, S., Zhou, T., Tian, H., Tian, W., and Wang, X. (2013). Homeostasis of brassinosteroids regulated by DRL1, a putative acyltransferase in *Arabidopsis*. Mol Plant **6,** 546-558.

Acknowledgements

I would like to thank my supervisor Prof. Dr. Brigitte Poppenberger for giving me the chance to conduct my research in her group. I would like to sincerely thank her for her professional guidance, continuous support and discussions throughout my study.

Most special thanks go to Dr. Wilfried Rozhon for the valuable assistance, regular discussion, as well as for data interpretation and sharing lab skills.

Special thanks to Dr. Tobias Sieberer for his valuable discussion and scientific advice about the results of my research.

Special thanks to Christina Duffner for her assistance in my working.

Many thanks to Irene Ziegler for the great technical support in my lab work.

I gratefully thank Prof. Dr. Wilfried Schwab for examining the thesis and Prof. Dr. Wolfgang Liebl for chairing the thesis committee.

I want to thank all my former and present colleagues at the Biotechnology of horticultural crops, Dr. Saiqi Yang, Dr. Pablo Albertos, Konstantin Wagner, Tanja Wlk, Sebastian Schramm, Veronica Ramirez, Haiwei Shuai, Adebimpe ADEDEJI-BADMUS for a great friendly working environment and support.

Special thanks to the China Scholarship Council (CSC) for providing me the opportunity to study abroad and the financial support.

Finally, I would like to express my sincere thanks to my beloved girlfriend Jin Mijing and to my parents for their support and understanding.

Curriculum Vitae

PERSONAL INFORMATION

Name:	Gan Sufu
Date of birth:	25.01.1991
Nationality:	Chinese

EDUCATION

10/2016 - present	PhD candidate
	Biotechnology of horticultural crops
	Technical University of Munich
	Freising, Germany
10/2013 – 07/2016	Master
	College of Horticulture
	Northwest A&F University
	Yangling, Shaanxi, China
09/2009 – 07/2013	Bachelor
	Northwest A&F University
	Yangling, Shaanxi, China